

# Multi-media geochemical and Pb isotopic evaluation of modern drainages on Vancouver Island



Alexei S. Rukhlov<sup>1, a</sup>, Gabe Fortin<sup>1</sup>, Gennady N. Kaplenkov<sup>2</sup>, Ray E. Lett<sup>3</sup>,  
Vivian W.-M. Lai<sup>4</sup>, and Dominique Weis<sup>4</sup>

<sup>1</sup>British Columbia Geological Survey, Ministry of Energy, Mines and Petroleum Resources, Victoria, BC, V8W 9N3

<sup>2</sup>2874 Eton Street, Vancouver, BC, Canada, V5K 1K5

<sup>3</sup>3936 Ashford Road, Victoria, BC, Canada, V8P 3S5

<sup>4</sup>Pacific Centre for Isotopic and Geochemical Research, Department of Earth, Ocean and Atmospheric Sciences,  
University of British Columbia, Vancouver, BC, Canada, V6T 1Z4

<sup>a</sup>corresponding author: Alexei.Rukhlov@gov.bc.ca

Recommended citation: Rukhlov, A.S., Fortin, G., Kaplenkov, G.N., Lett, R.E., Lai, V. W.-M., and Weis, D., 2020. Multi-media geochemical and Pb isotopic evaluation of modern drainages on Vancouver Island. In: Geological Fieldwork 2019, British Columbia Ministry of Energy, Mines and Petroleum Resources, British Columbia Geological Survey Paper 2020-01, pp. 133-167.

## Abstract

Prognostic geochemistry attempts to identify prospective areas for economic deposits of a wide range of commodities, including non-traditional deposit-types. Although the geochemistry of panned heavy mineral concentrates (HMC) from stream sediments has been used elsewhere to discover economic metal deposits that were missed by conventional stream-sediment surveys, the method has not been used extensively for regional geochemical surveys (RGS) in British Columbia. Instead, such surveys tend to use elaborate laboratory processing of bulk samples to recover HMC and indicator minerals, which although robust, are at a cost that is prohibitive for most prospectors. With the objective of developing geochemical exploration methods that are both effective and inexpensive, herein we use the <1 mm fraction of HMC samples (200-400 g) recovered by sluicing and panning of 11-16 kg of the <2 mm fraction of bulk alluvium in the field. We analyzed these heavy mineral concentrates, stream waters, and conventional stream and moss-captured sediments (<0.18 mm fraction) from several Vancouver Island drainages for a wide range of elements using different analytical methods. Analysis of the field-processed HMC samples greatly enhanced the geochemical anomaly contrast and confidently identified visually confirmed mineralization even at the mouths of third- to fifth-order streams, many km downstream from known mineralization. In contrast, analysis of the conventional stream and moss-captured sediments commonly failed to detect even proximal mineralization. In addition, for the first time, we measured Pb isotopic compositions of stream waters and 2.5N HCl leachates of the sediments and HMC by economic ICP-MS. These Pb isotopic compositions fingerprint mineralization isotopically distinct from country rocks. Strongly acidic (sulphuric) waters of Hushamu Creek drain blind porphyry Cu-Mo-Au and epithermal Au-Ag-Cu deposits hosted by volcanic rocks of the Bonanza magmatic arc (Late Triassic to Middle Jurassic) on northern Vancouver Island. The geochemistry of HMC and water samples reveals strong lithochemical (mechanical) Au-Ag-Se-Bi-Te-Mo-Pb-Re-Hg-Ba-Sn-Co-Tl-In-Cu and hydrochemical Co-Mn-Al-Sn-Fe-Zn-Cu-Cd-Y-Ni-La-Ba dispersion in the Hushamu watershed. Above-background productivities (tonnes per 1 m depth) of Au (315), Ag (24), Ba (22350), V (4964), Zr (4584), P (4050), Zn (1146), Pb (247), B (228), Se (569), Sn (75), Co (52), Bi (49), Te (34), Cs (27), Li (17), Sb (16), Hg (9), Tl (8), and In (2) reflect epithermal Au-Ag-Cu and the uppermost primary dispersion halo of the blind porphyry Cu-Mo-Au system under the extensive leached cap in the Hushamu basin. Multiplicative ratios of highly mobile to less mobile ore and indicator elements such as (Cu·Pb·Zn)/(Sn·Co·Mo) or (Ag·Hg·Sb)/(W·Sn·Bi) also indicate shallow level of erosion or blind mineralization. Strong LREE-Y-V-Ba-Sr-P-Zr-Hf-Nb-Ta-U-Th dispersion in some drainages on northern Vancouver Island may indicate undiscovered peralkaline granite- or carbonatite-hosted, rare-metal mineralization possibly related to Neogene extension in the Queen Charlotte basin and similar to deposits in Alaska. HMC samples at Loss Creek on southern Vancouver Island yield (tonnes/m): 833 Au, 78 Ag, 2568 W, plus 3066533 Mn, 86132 Y, 41516  $\Sigma$ HREE (Gd+Tb+Dy+Ho+Er+Tm+Yb+Lu), 38542 Cr, 28724 Zn, 14377 Li, 5553 Sc, 3511 Ba, 2873  $\Sigma$ LREE (La+Ce+Pr+Nd+Sm+Eu), 2182 Ni, 1640 Ga, 1532 Se, 871 Co, 753 Ge, 661 B, 621 Pb, 613 Cd, 594 Nb, 235 Hf, 207 Th, and 76 Ta. The prognostic geochemical resources not only confirm placer gold and its orogenic Au-type source in the Loss Creek basin, but also indicate a large, unconventional type of a placer garnet-hosted HREE-Y-Sc-Mn deposit and other 'critical' commodities. Water chemistry provides an important control on hydrochemical dispersion and constrains ore mineral assemblages. We propose a three-stage method for drainage geochemical surveys that is rapid, inexpensive, and effective.

**Keywords:** Drainage geochemical survey, mineral exploration, stream sediment, moss-mat sediment, heavy mineral concentrate (HMC), sluice, pan, dispersion streams, geochemical anomaly, basin productivity, geochemical resources, lithochemistry, hydrochemistry, Pb isotopic data, northern Vancouver Island, Hushamu, porphyry Cu-Mo-Au, epithermal Au-Ag-Cu, unconventional garnet-hosted HREE-Y-Sc deposit, peralkaline intrusion- or carbonatite-hosted LREE and rare-metal mineralization, indicator mineral

## 1. Introduction

Regional geochemical surveys support the societal resource base by identifying prospective areas for large-tonnage

economic deposits in undeveloped and underexplored regions. Such surveys are based on pioneering studies of the migration, dispersion, and concentration of elements by V.I. Vernadsky,

V.M. Goldschmidt, and A.E. Fersman, along with studies of ore deposits and dispersion of indicator elements (Safronov, 1971). The first ‘metallometric surveys’ carried out in several mining regions by N.I. Safronov and A.P. Solovov in 1931-1932 demonstrated the effectiveness of the new ‘physico-chemical exploration method’ based on the theory of geochemical field and anomaly, analogous to geophysical methods. At the same time, V.A. Sokolov developed geochemical methods for oil and gas exploration (Grigoryan et al., 1983; Solovov, 1985; Solovov et al., 1990; Matveev, 2003). In 1956, V.I. Krasnikov outlined the theory and practice of modern lithochemical, hydrochemical, atmochemical, and biochemical exploration methods. These methods have since been widely applied, leading to the discovery of hundreds of ore deposits, including very large ones such as Escondida Cu, Chile; Salobo Cu, Brazil; Cerro Colorado Cu-Mo, Panama; Carlin Au in Nevada, USA; McArthur River and Woodlawn Pb-Zn-Ag±Cu, Australia; Husky Ag-Pb-Zn and Casino Cu-Au-Mo-Ag in Yukon, Canada (Hawkes, 1976; Rose et al., 1979; Matveev, 2003).

In British Columbia, stream, lake, and moss-mat sediments, and waters have been analyzed in regional drainage geochemical survey (RGS) programs carried out by mining companies since 1950s and later managed by the Geological Survey of Canada, the British Columbia Geological Survey, and Geoscience BC. Interpretation of these data has led to the discovery of many precious and base metal deposits in the province such as Highland Valley Copper, Northair Gold, Galore Creek, Berg, Huckleberry, Equity Silver, and Island Copper on northern Vancouver Island (Lett and Rukhlov, 2017).

Most ore deposits have been found by prospectors. Proven by centuries of prospecting, panning of stream sediment is effective for finding economic deposits of placer gold, diamonds, tin, tungsten, and other commodities. Although the geochemistry of heavy mineral concentrates (HMC) samples from stream sediments was used in eastern Chukotka to discover several large base and precious metal deposits that were missed by conventional, stream-sediment surveys (Kukanov et al., 1983; Petrenko et al., 1986; Kaplenkov, 2003, 2006, 2008), this method has not been widely used in regional geochemical survey programs in British Columbia (see Rukhlov and Gorham, 2007 for an exception). Instead, stream-sediment and till geochemical surveys in the province tend to use elaborate laboratory processing of bulk samples to recover HMC and indicator minerals (see Lett and Rukhlov, 2017 for review). Although indicator minerals are robust tools, the cost of such processing is prohibitive for most prospectors.

In this study we evaluate a new drainage geochemical survey method using the <1 mm fraction of HMC samples (200-400 g) recovered by sluicing and panning of 11-16 kg of the <2 mm fraction of bulk alluvium in the field. We also consider other sample media such as conventional stream and moss-mat sediments (<0.18 mm fraction), stream water geochemistry, and, for the first time, Pb isotopes. We begin by testing different preparation and analytical methods on samples from a placer gold occurrence near the mouth of Loss Creek on southern

Vancouver Island. Next, we present the results of an orientation survey on northern Vancouver Island using samples from streams draining prospective rocks of the Bonanza arc (Triassic to Middle Jurassic) with porphyry Cu-Mo-Au, epithermal Au-Ag-Cu, and other styles of mineralization (Northcote and Muller, 1972; Muller et al., 1974; Panteleyev, 1992; Panteleyev and Koyanagi, 1993, 1994; Panteleyev et al., 1995; Perelló et al., 1995; Tahija et al., 2017). We conclude by proposing a revised, three-stage method for regional geochemical surveys to identify prospective areas for large, economic deposits of a wide range of commodities, including non-traditional deposit-types. The new method is rapid, economic, and effective, and thus we recommend it to prospectors. The raw data upon which this study is based are provided in Rukhlov et al. (2019).

## 2. Previous geochemical studies on Vancouver Island

The first RGS programs that used conventional stream and moss-captured sediment samples (<0.18 mm-fraction) were carried out on northern Vancouver Island by Matysek and Day (1988), Gravel and Matysek (1989), and Matysek et al. (1989). Kerr et al. (1992) and Bobrowsky and Sibbick (1996) carried out regional till geochemical surveys. Koyanagi and Panteleyev (1993, 1994), Sibbick and Laurus (1995a), and Panteleyev et al. (1996b) carried out detailed hydrochemical surveys of several natural acid drainages. Sibbick (1994), Sibbick and Laurus (1995b), and Arne and Brown (2015) performed statistical catchment analysis of the historical RGS data on northern Vancouver Island, and Lett (2008) summarized historical drainage geochemical surveys and discussed the results of multi-media orientation studies. More recently, Jackaman (2011, 2013a, b, 2014) reanalyzed archived RGS stream-sediment and till samples and carried out new infill regional drainage moss-mat sediment and till geochemical work.

## 3. Geology, mineralization, and physiography

Vancouver Island is mainly underlain by Late Paleozoic to Early Mesozoic rocks of Wrangell terrane, with slivers of Pacific Rim and Crescent terranes along the west coast and southern tip of the Island (Fig. 1; Muller, 1977; Nelson et al., 2013). Amalgamated with Alexander terrane by the Late Carboniferous, Wrangellia, now part of the Insular superterrane, accreted to inboard terranes of the Coast and Intermontane belts between Middle Jurassic and mid-Cretaceous (Nelson et al., 2013; Monger, 2014).

Lithologic units at Loss Creek site (Fig. 2) consist of staurolite-garnet schists and argillites of the Leech River complex (Jurassic to Cretaceous), juxtaposed against basalts and gabbro of the Metchosin Igneous complex (Paleocene to Eocene) along the Leech River fault. Along the coast, these older rocks are overlain by a narrow fringe of siliciclastic rocks of the Carmanah Group (Late Eocene to Oligocene). Intermediate intrusions of the Mount Washington plutonic suite (Eocene to Oligocene) intrude the metamorphic rocks of the Leech River complex (Muller, 1977, 1980, 1982). Orogenic Au veins such as the Ox and Sombrio 2 showings (MINFILE

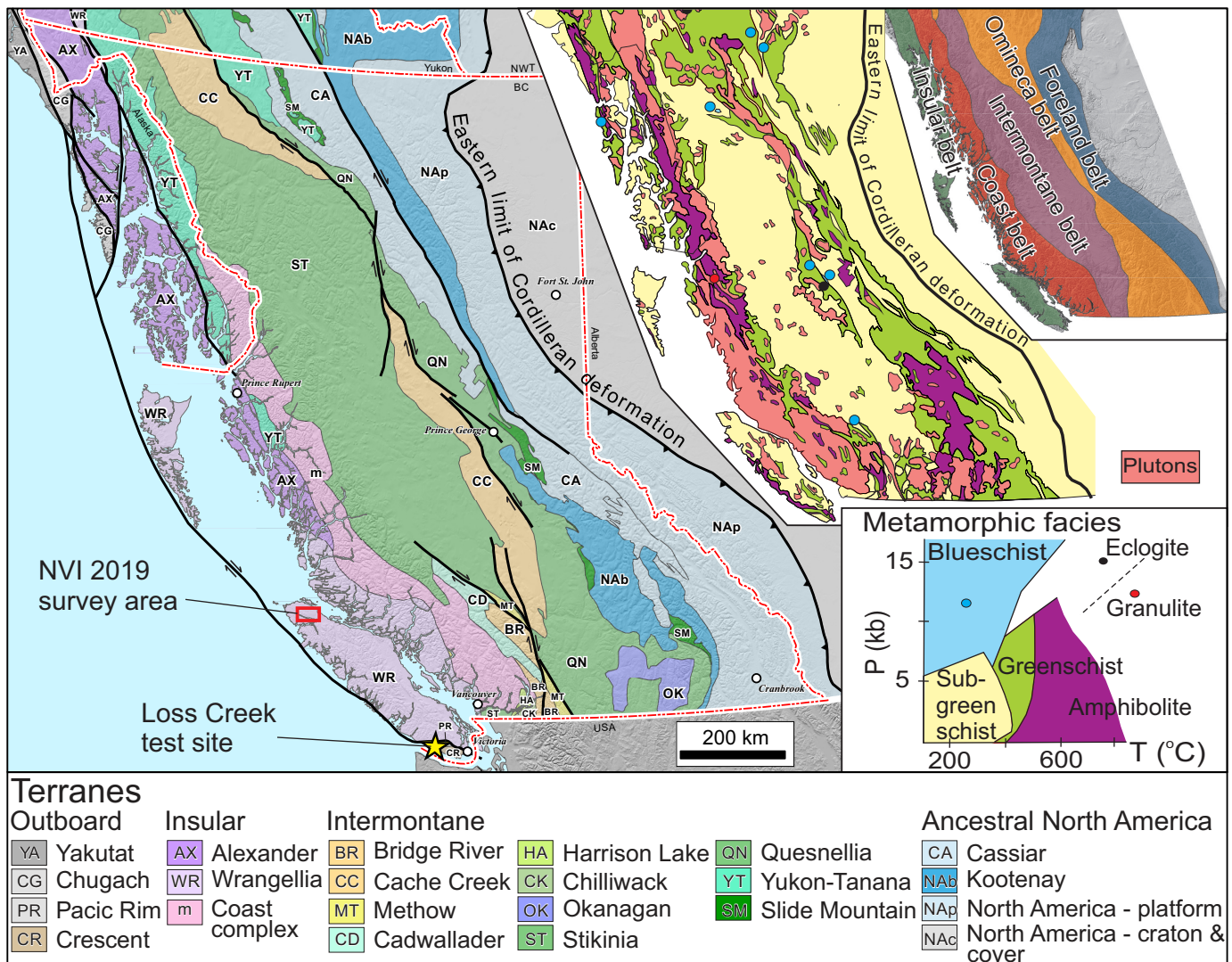


**Fig. 1.** Location of Loss Creek sampling site and northern Vancouver Island survey area. Terrane geology after Nelson et al. (2013). Metamorphic and plutonic rocks after Monger and Hutchison (1971), Read et al. (1991), and Monger (2014). Cordilleran morphogeological belts after Gabrielse et al. (1991).

092C 059 and 214) are possible sources of placer gold in Loss Creek (MINFILE 092C 236 and 235) and at Sombrio beach (MINFILE 092C 044). Mafic rock-hosted, shear-related and felsic intrusion-related  $\text{Cu}\pm\text{Ag}\pm\text{Au}$  mineralization also occurs in the area (MINFILE 092C 137, 138, 171, and 218).

Dawson (1887a, b) made the first geological investigation of northern Vancouver Island. Subsequent bedrock mapping and studies of the stratigraphy, magmatism, and mineralization of the area (Fig. 3) were carried out by Jeffrey (1962), Northcote (1969, 1971), Northcote and Muller (1972), Muller et al. (1974), Muller and Roddick (1983), Massey and Melville (1991), Panteleyev (1992), Panteleyev and Koyanagi (1993, 1994), Hammack et al. (1994, 1995), Nixon et al. (1994, 1995, 1997, 2000, 2006a, b, 2011a, b), Archibald and Nixon (1995), Panteleyev et al. (1995, 1996a), Perelló et al. (1995), DeBari et al. (1999), Nixon and Orr (2007), and Nixon et al. (2008). Northern Vancouver Island is mainly underlain by the

Vancouver and Bonanza groups (Nixon and Orr, 2007). The Vancouver Group (Late Triassic) consists of flood basalts of the Karmutsen Formation overlain by limestone of the Quatsino Formation. The older rocks are unconformably overlain by the Bonanza Group (Late Triassic to Middle Jurassic), which includes a basal carbonate-siliciclastic-volcanic succession, the Parson Bay Formation (Norian to Rhaetian) that is overlain by volcano-sedimentary strata and the main volcanic phases of the Nahwitti River, Pegattem Creek, LeMare Lake, Hathaway Creek, and Holberg units (Late Triassic to Middle Jurassic). The stratigraphy of the Bonanza magmatic arc reflects basaltic to andesitic volcanism in the Late Triassic (Parson Bay Formation), followed by basaltic to rhyolitic volcanism of the main phase in the earliest Jurassic (LeMare Lake volcanics), and basaltic to rhyolitic arc of the final phase in the early Middle Jurassic (Holberg volcanics). The largely subaerial volcanism of the main and final phases was accompanied by

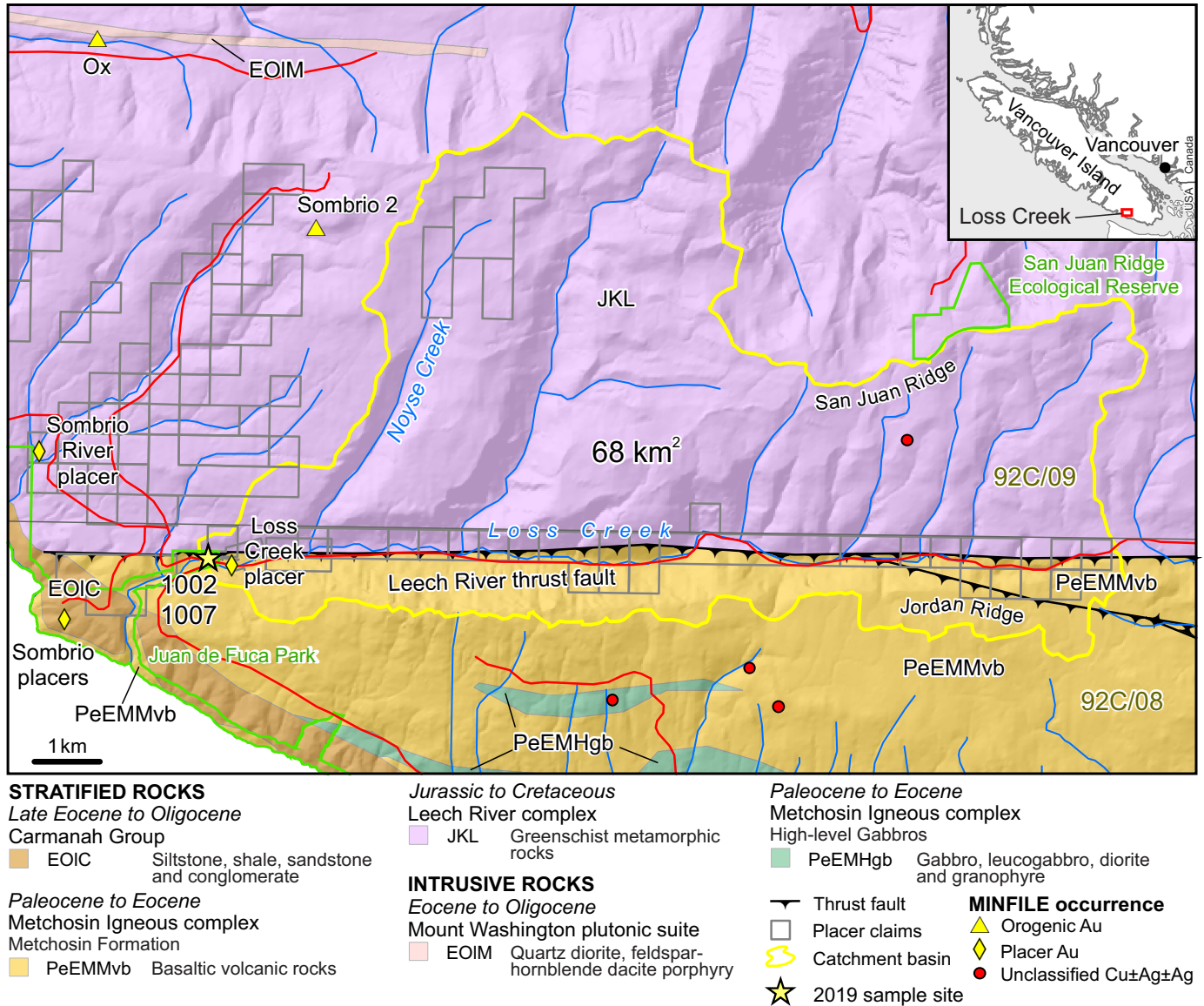


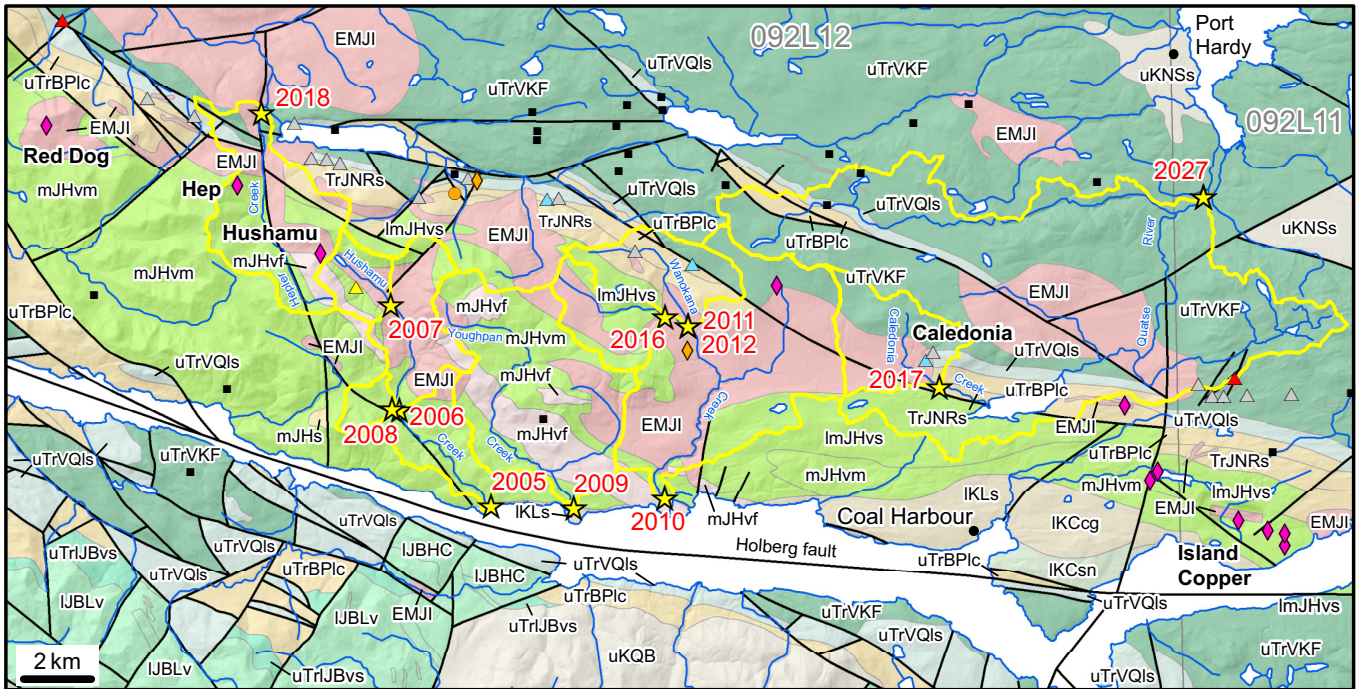
Fig. 2. Loss Creek sampling site and catchment area. Geology after Muller et al. (1977, 1980, 1982).

the emplacement of coeval granitoids of the Island Plutonic suite (Northcote and Muller, 1972; DeBari et al., 1999; Nixon and Orr, 2007). Cyclical marine and continental sedimentary sequences containing coal beds of the Coal Harbour (Early Cretaceous), and Queen Charlotte and Nanaimo (Late Cretaceous) groups mark deposition in fault bounded basins along the northern (Queen Charlotte Group) and eastern (Nanaimo Group) margins of the island (Muller, 1977; Lewis et al., 1997).

The evolution of the Bonanza magmatic arc brought about major porphyry Cu-Mo±Au deposits such as Island Copper (past producer - MINFILE 092L 158), Hushamu (MINFILE 092L 240), Hep (MINFILE 092L 078), Red Dog (MINFILE 092L 200), and related epithermal Au-Ag-Cu (Hushamu), base metal skarn (e.g., Caledonia; MINFILE 092L 061), polymetallic vein (MINFILE 092L 131), and other styles of

mineralization (Northcote and Muller, 1972; Muller et al., 1974; Panteleyev, 1992; Panteleyev and Koyanagi, 1993, 1994; Panteleyev et al., 1995; Perelló et al., 1995; Tahija et al., 2017). The Klaskish Plutonic Suite (Late Neogene) also carries porphyry Cu-Mo±Au mineralization immediately to the south of Holberg fault, marking another metallogenic event associated with extension in the Queen Charlotte basin (Lewis et al., 1997; Nixon et al., 2020). In addition, high-Mg basalts of the Karmutsen Formation raise the possibility of magmatic Ni-Cu-PGE deposits (Nixon et al., 2008).

The Insular Mountains, forming the backbone of Vancouver Island, display U-shaped valleys with steep slopes and summits up to 2200 m above sea level (Holland, 1976; Muller, 1977). The Nahwitti lowland of the Coastal trough characterizes the physiography of northern Vancouver Island, with low hills (up to 600 m above sea level) and low-lying coastal plains (Holland,



**STRATIFIED ROCKS**

**LATE CRETACEOUS**

Nanaimo Group equivalents (in part)

Suquash Formation

uKNSs Wacke, siltstone, conglomerate, minor shale and coal

Queen Charlotte Group equivalents (in part)

Blumberg Formation

uKQB Coarse siliciclastic sedimentary rocks and conglomerate

**EARLY CRETACEOUS**

Coal Harbour Group

IKCsn Upper sandstone unit: wacke, siltstone, minor conglomerate and coal

IKCcg Lower conglomerate unit: conglomerate and minor wacke

Longarm Formation

IKLs Sandstone, siltstone, mudstone, conglomerate and minor coal

**LATE TRIASSIC TO MIDDLE JURASSIC**

Bonanza Group - north of Holberg fault

Early? to Middle Jurassic

Holberg volcanic unit

mJHvm Mafic volcanic rocks and minor wacke, siltstone and shale

mJHvf Felsic volcanic rocks

mJHs Wacke, sandstone, shale, mudstone and siltstone

ImJHvs Mafic volcanic rocks, wacke, minor siltstone and mudstone

Late Triassic to Early Jurassic

Nahwitti River siltstone-wacke

TrJNRs Siltstone, mudstone and wacke

Bonanza Group - south of Holberg fault

Early Jurassic

Hathaway Creek volcanic-sedimentary unit

IJBHC Undivided mafic volcanic and siliciclastic sedimentary rocks

LeMare Lake volcanic unit

IJBLv Undivided mafic to felsic volcanic rocks and minor marine to non-marine sedimentary rocks

Pegattem Creek siltstone

IJBPCsf Siltstone and mudstone

Late Triassic

Volcaniclastic-sedimentary unit

uTrIJBvs Volcaniclastic rocks, siltstone and mudstone

Bonanza Group

Late Triassic

Parson Bay Formation

uTrBPlc Limestone, mudstone, siltstone, shale, wacke, sandstone, conglomerate and volcanic rocks

**LATE TRIASSIC**

Vancouver Group

Quatsino Formation

uTrVQls Limestone, minor chert and oolitic layers

Karmutsen Formation: Flow Member

uTrVKF Undivided mafic volcanic rocks and minor limestone

**INTRUSIVE ROCKS**

EARLY TO MIDDLE JURASSIC

Island Plutonic Suite

EMJI Undivided granitoid rocks and porphyry

— Faults

— Catchment basins

**MINFILE occurrences**

◆ Porphyry Cu-Au±Mo

▲ High-sulphidation epithermal Au-Ag-Cu

● Manto Ag-Pb-Zn

▲ Cu skarn

▲ Pb-Zn skarn

▲ Undefined skarn

◆ Vein Ag-Pb-Zn

■ Undefined type

★ Sample sites

**Fig. 3.** Sampling sites and catchment basins in the northern Vancouver Island area. Geology based on Jeffrey (1962), Northcote (1969, 1971), Muller et al. (1974), Muller and Roddick (1983), Hammack et al. (1994, 1995), Nixon et al. (1994, 1997, 2000, 2006a, b, 2011a, b), and Nixon and Orr (2007).

1976). Most of the surficial deposits on Vancouver Island formed during or after the Fraser Glaciation (see Lett, 2008 for an overview). Surficial mapping of northern Vancouver Island was carried out by Clague et al. (1982), Kerr (1992), Bobrowsky and Meldrum (1994a, b), Meldrum and Bobrowsky (1994), Bobrowsky et al. (1995), and Bobrowsky (1997).

## 4. Methods

### 4.1. Sample collection

To test different sample media and analytical methods, we collected stream and moss-captured sediment, HMC, and water samples from Loss Creek, southern Vancouver Island (Fig. 2) in April and June, 2019. In August, we sampled stream water, sediment, and HMC, and stream boulders representing a local Cu-Zn-Pb mineralization on northern Vancouver Island (Fig. 3). Field duplicates of water, stream sediment, and HMC were collected at random sites. Field observations regarding local terrain, sample site, and sample type, including lithological and shape counting of pebbles, were captured into a MS Access form based on a modified GSC sediment sampling card (Martin McCurdy, personal communication). The field data are listed in Appendix 1 of Rukhlov et al. (2019).

#### 4.1.1. Stream and moss-mat sediment, and heavy mineral concentrate

Stream sediment samples weighing 1.2 to 3.2 kg consisted of mainly the <2 mm sieved fraction or bulk (if wet) alluvium, collected from active stream channels, 10-15 cm above the water level. In addition to stream sediment, moss-mat sediment (0.9 kg) was sampled at Loss Creek.

More representative HMC samples were recovered from the wet-sieved <2 mm fraction of alluvium (11-16 kg) collected from gravel bars immediately downstream of boulders or logs, which serve as natural traps of heavy particles (Fig. 4). We used 12 mm- and 2 mm-size opening stainless-steel sieves stacked on a bucket to process bulk alluvium samples (110-150 L or



**Fig. 4.** Typical stream sediment and HMC sampling site on a gravelly stream.

4-5 buckets). A portable, gas-powered, 2.5 cm-diameter water pump with a 100- $\mu$ m nylon foot valve sock and a garden hose permitted most samples being processed far enough from an active stream to prevent silt-laden water entering the stream.

To test HMC recovered by different methods, a 15 kg sample of the <2 mm fraction of bulk stream sediment collected from Loss Creek in April was dried in an oven at 36°C and split by a Jones splitter into two sub-samples. One 7.5 kg sub-sample was panned, and the other 7.5 kg sub-sample was concentrated on a Wilfley shaking table at the British Columbia Geological Survey. We collected two additional duplicate bulk alluvium samples (11 kg each) from the same site in June. One duplicate was concentrated by sluicing on site as described below and the other was archived for testing a spiral Morfee concentrator at the British Columbia Geological Survey.

For recovering HMC from the bulk alluvium in the field, we used a Keene Engineering A-51 mini-sluice box (25.5 x 91.4 x 11.4 cm), lined with a grooved rubber matting and coupled with a shower feeder assembly fitting a garden hose (Fig. 5). Based on the experience (Gene Dodd, personal communication), the sluice was levelled on a frame and operated at a consistent forward slope of 10-11° and water flow of 33-35 L/min, supplied by a 2.5 cm-diameter pump. The rate of sample



**Fig. 5.** A sluice box (25.5 cm wide) coupled with shower sample feeder set up on a stream bank.

feeding was adjusted to achieve even sediment flow across the sluice box, which avoided clogging of the sluice ladders and metal mesh above the rubber matting. Typical processing time was 20-30 minutes per 11-15 kg sample. Sluice concentrate was then transferred into a clean bucket and further refined by quick panning to wash off coarse mica, feldspar, and other low-density minerals, yielding 200-500 g (wet mass) HMC samples. The samples were transferred into Hubco® bags, which in turn were placed in zip-lock plastic bags, drained, and weighed. Plastic bags were removed and samples were let dry on racks. Cleaned with a nylon brush and visually examined, the sluice box and hopper were transported in plastic bags.

#### 4.1.2. Water

We adopted a modified GSC water sampling procedure, collecting water midstream with a high-density polyethylene (HDPE) bottle attached to a Nasco extendable-pole swing sampler. Pre-cleaned with nitric acid by the manufacturer, a new 250 mL sampling bottle was used for each sample, which was rinsed a few times with stream water. Water temperature, pH, conductivity, and total dissolved solids (TDS) were measured with an Oakton PCTSTestr 50 combination-electrode meter in the field. For the measurements, a new 50 mL polypropylene beaker was rinsed first with deionized (18.2 MΩ·cm) water and then with stream water. We calibrated the meter daily, using pH (4.01, 7.01, and 10.01) and conductivity/TDS (23, 84, 447, and 1413 μS/cm) reference solutions. The same conductivity solutions were used for TDS calibration, applying factor 0.5. The meter electrodes were rinsed with deionized water and stream water before the measurements, and with 95% ethanol and deionized water after the measurements. A piece of wet wipe paper was placed in the cap protecting the electrodes during the day; the electrodes were soaked in tap water overnight.

ALS Canada (Environmental) Ltd., Vancouver, British Columbia (ALS-Environmental) supplied pre-cleaned sample containers with preserving acids in individual vials for laboratory analysis. For Pb isotopic analysis, we used Falcon 50 mL polypropylene tubes, which were cleaned and pre-charged with 0.5 mL of 50% HNO<sub>3</sub> in a clean laboratory at the Pacific Centre for Isotopic and Geochemical Research, University of British Columbia (PCIGR) two weeks before collecting the samples. Earlier tests showed that after storing 0.5 mL 50% HNO<sub>3</sub> in the tubes for up to 26 days, the acid blanks were 0.7-3.6 pg Pb (n = 4), which is a typical acid blank level at PCIGR. All sample containers were placed along with the corresponding acid vials in individual zip-lock plastic bags in a Class 100 clean zone before transporting to the field.

For anion analysis, a 0.5 L HDPE bottle was filled with untreated stream water, whereas water samples for cation and Pb isotopic analysis were filtered and immediately acidified in the field. We used a Sterivex-HV polyvinylidene fluoride (PVDF) 0.45 μm filter units and all-plastic HSW Norm-Ject™ 50 mL syringes; a new syringe was used for each sample. After removing the plunger and attaching the filter unit, the syringe was filled with deionized water while not touching

the plunger or tips of the syringe and filter unit. The plunger was rinsed with deionized water and inserted into the syringe, discarding the deionized water through the filter. The syringe and filter were rinsed again with stream water before filtering the water sample into a 20 mL glass bottle for dissolved Hg analysis, a 50 mL HDPE bottle for other cations, and a 50 mL polypropylene tube for Pb isotopic analysis. Filtered water samples were immediately preserved with 0.3 mL 1:1 hydrochloric acid (for Hg) and with about 1 mL 18% nitric acid (for other cations). The sample containers for Pb isotopic analysis were already pre-charged with 0.5 mL 50% nitric acid. Filled water sample containers were placed back into their plastic bags and immediately stored in a cooler with ice packs. All water samples were kept refrigerated at about 4°C until shipped in coolers with ice to ALS-Environmental and PCIGR for analysis.

We monitored three types of water blanks. The acid blank is the unfiltered, deionized water drawn directly from the water purification system and acidified in a Class 100 clean zone at BCGS; acid blanks did not travel to the field. The travel blank is the unfiltered, deionized water drawn directly from the water purification system in a Class 100 clean zone at BCGS and acidified in the field. The filtration blank is the deionized water from a clean HDPE container transported to the field and filtered and acidified in the field the same way as routine samples. To evaluate seasonal variations in water chemistry, we sampled water from Loss Creek during spring runoff in April and at lower discharge in June. We also collected four water samples at the same site from the Quatse River, northern Vancouver Island every third day during the survey in August to monitor short-term variations.

#### 4.2. Sample preparation

Rock samples were crushed in a jaw crusher and screened on a 10-mesh stainless-steel sieve. After manually removing fragments with surface oxidation, a split of the >2 mm material (about 60 g) was pulverized to >90% passing <75 μm particle size in a Cr-steel bowl. All sediment and HMC samples were oven dried at 36°C, sieved through stainless-steel sieves, and then split using a Jones splitter at BCGS. Blind quality controls, including analytical (pulp) duplicates, preparation blanks (Aldrich 99.995% SiO<sub>2</sub>), and reference materials were inserted in each sample batch of 12-23 samples. Consistent with the provincial RGS programs, the <0.18 mm, sieved fraction of stream and moss-mat sediment samples was used for analysis. The whole 1-2 mm and 1/8<sup>th</sup> split of 0.5-1.0 mm-size, sieved fractions of HMC samples were kept for mineralogical examination. Splits of the <1 mm-size, sieved fraction were pulverized for elemental and Pb isotopic analyses. Panned and Wilfley table HMC samples, rocks, and the corresponding preparation silica blanks were milled in a Cr-steel bowl at BCGS. Sluice HMC samples and the corresponding preparation silica blanks were milled in a ceramic bowl at Bureau Veritas Commodities (Minerals) Canada Ltd., Vancouver, B.C. (BVM), or by using an agate pestle and mortar at Activation

Laboratories Ltd., Ancaster, Ontario (Actlabs).

For Pb isotopic analysis, splits of the sluice HMC samples and the corresponding preparation silica blanks were pulverized at BCGS. One HMC sample (number 2005) was milled using a low-Cr steel pestle and mortar. Because the equipment partially magnetized the sample, a duplicate HMC sample number 2005 and the rest of the HMC samples were pulverized using an agate pestle and mortar. All grinding equipment was cleaned by pulverizing silica sand between samples. BVM used an extra cleaning sand cycle to minimize potential carry-over contamination. Both commercial laboratories analyzed random samples of their cleaning sand. Blind preparation silica blanks were sieved, split, and pulverized the same way as routine samples. Stream and moss-mat sediment, HMC, rock samples, and blind quality controls are listed in Appendix 2 in Rukhlov et al. (2019).

### 4.3. Sample analysis

#### 4.3.1. Lithochemistry

Stream sediment, moss-mat sediment and HMC samples from Loss Creek were analyzed by several standard analytical methods in commercial laboratories. Three different digestions, combined with inductively coupled plasma emission spectrometry (ICP-ES), inductively coupled plasma mass spectrometry (ICP-MS), and X-ray fluorescence (XRF) analysis were performed at BVM.

A split of the <0.18 mm material (30 g) was digested in a H<sub>2</sub>O-HCl-HNO<sub>3</sub> (1:1:1 v/v) mixture (modified aqua regia) at 95°C. The supernatant solution was diluted and analyzed by ICP-ES for major elements and by ICP-MS for trace elements, determining a total of 65 analytes with the lowest detection limits. Although the H<sub>2</sub>O-HCl-HNO<sub>3</sub> digestion can dissolve gold, carbonates, and sulphides, it does not fully dissolve silicates, oxides and other refractory minerals such as barite. Therefore, concentrations of elements determined by aqua regia digestion should be treated as ‘partial’ rather than ‘total’.

A more aggressive digestion in a HF-HClO<sub>4</sub>-HNO<sub>3</sub> mixture heated to fuming, followed by dissolution of the dried residue using HCl breaks down most minerals. After digesting a 0.25 g sample in HF-HClO<sub>4</sub>-HNO<sub>3</sub> and HCl, combined ICP-ES and ICP-MS analysis determines 59 elements. The four-acid digestion is considered ‘near-total’, because some refractory minerals such as barite, zircon, titanite, and oxides of Al, Fe, Mn, Nb, Sn, REE, Ta, Ti, and W may not be fully dissolved or stable in solution. Furthermore, fuming of HF-HClO<sub>4</sub>-HNO<sub>3</sub> results in erratic volatilization of some elements, including As, Cr, S, Sb, Se and U. Hence, these elements plus Au and Hg cannot be accurately determined with the four-acid digestion.

Fusion of the sample (0.7 g) with Li<sub>2</sub>B<sub>4</sub>O<sub>7</sub>-LiBO<sub>2</sub> combined with XRF and laser ablation ICP-MS (LA-ICP-MS) analysis on the fused glass disk results in the determination of ‘total’ concentrations for 65 elements with the lowest detection limits compared to those of other ‘total’ methods. In addition, loss on ignition (LOI) at 1000°C is determined gravimetrically. Combining LA-ICP-MS and XRF extends the dynamic range

for some analytes such as Sn from sub-ppm to percent level thus eliminating over-limit results. This method requires pulverizing samples to <75 µm to ensure complete fusion of resistate minerals, but strong oxidizing agents are required to fully digest sulphide-rich samples. Some elements such as As, Sb, and Se are partially volatilized by the fusion, and Au is not analyzed by this method.

Splits of the samples were also analyzed at Actlabs by different methods. Thermal instrumental neutron activation analysis (INAA) was performed on 10-51 g samples irradiated for 30 minutes in a neutron flux of 7·10<sup>12</sup> neutrons·cm<sup>-2</sup>·s<sup>-1</sup>. After a period of 7 days to allow <sup>24</sup>Na to decay, characteristic gamma-ray emissions for 34 elements were measured using a gamma-ray spectrometer with a high-resolution, coaxial Ge detector. Counting time is about 15 minutes per sample. INAA determines ‘total’ element concentrations and irradiating with thermal neutrons avoids inaccurate (low) Au values due to the self-shielding effect resulting from irradiation with epithermal neutrons. Although INAA is non-destructive, activated material is radioactive and thus not immediately available for analysis by other methods. Another major limitation is poor sensitivity for Ag, Ba, Br, Ca, Cs, Hg, Ir, Mo, Nd, Ni, Rb, Se, Sr, and Zn, resulting in most determinations being below detection limit or having poor precision. Furthermore, INAA cannot measure a number of elements, including key commodity metals such as Pb and Cu. These elements were determined on a separate split of the sample (0.5 g) digested in a hot HCl-H<sub>2</sub>O-HNO<sub>3</sub> mixture. The supernatant solution was analyzed for Hg by cold vapour atomic absorption spectrophotometry (CVAAS) and for Ag, Cd, Cu, Mn, Mo, Ni, Pb, S, and Zn by ICP-ES.

A split of the sample (0.8 g), pulverized to <75 µm particle size, was sintered with Na<sub>2</sub>O<sub>2</sub> in a zirconium crucible at 560°C in a muffle furnace. The fused sample was dissolved in deionized water and acidified with concentrated HNO<sub>3</sub> and HCl. The resulting solution was diluted and analyzed on a Varian 735 ICP-ES and on an Agilent 7900 ICP-MS for a total of 55 elements. In addition, rhenium was analyzed in some HMC samples, with all results being below the detection limit. Phosphorus and zirconium were also determined on a Panalytical Axios Advanced wavelength dispersive XRF on a fused glass disk prepared from a separate split (0.8 g) fused with Li<sub>2</sub>B<sub>4</sub>O<sub>7</sub>-LiBO<sub>2</sub> in a Pt crucible. The sodium peroxide fusion is strongly oxidizing and thus is effective for decomposing sulphides and most refractory minerals. The relatively low temperature of the sintering minimizes the loss of volatile elements. Hence, element concentrations determined by this method are considered ‘total’. Although Na and some of the key commodity elements such as Ag and Au are not determined, the advantage of the method is that determinations for B and Li, which cannot be analyzed by Li<sub>2</sub>B<sub>4</sub>O<sub>7</sub>-LiBO<sub>2</sub> fusion are ‘total’.

Splits (30 g) of stream sediment, HMC, and rock samples from northern Vancouver Island were analyzed by the H<sub>2</sub>O-HCl-HNO<sub>3</sub> digestion - ICP-ES/MS at BVM. In addition, splits of the HMC and rock samples were analyzed by the Li<sub>2</sub>B<sub>4</sub>O<sub>7</sub>-LiBO<sub>2</sub> fusion - LA-ICP-MS combined with XRF on fused glass

disk at the same laboratory, and by Na<sub>2</sub>O<sub>2</sub> sintering - ICP-MS/ES on solution at Actlabs. Lithochemical analyses are listed in Appendix 3 of Rukhlov et al. (2019).

#### 4.3.2. Hydrochemistry

Water samples were analyzed for elemental compositions at ALS-Environmental. Concentrations of Br<sup>-</sup>, Cl<sup>-</sup>, F<sup>-</sup>, NO<sub>3</sub><sup>-</sup>, NO<sub>2</sub><sup>-</sup>, and SO<sub>4</sub><sup>2-</sup> anions in untreated water were determined by ion chromatography after the United States Environmental Protection Agency (USEPA) method reference 300.1. Filtered (0.45 µm) and preserved with hydrochloric acid, water samples underwent cold-oxidation with bromine monochloride, followed by reduction with stannous chloride. Dissolved Hg was then analyzed by CVAAS or cold vapour atomic fluorescence spectroscopy (CVAFS) after the American Public Health Association (APHA) method reference 3030B and USEPA method reference 1631EB. Filtered (0.45 µm) and preserved with nitric acid water samples were analyzed for a total of 45 dissolved metals by collision-reaction cell ICP-MS (CRC-ICP-MS) after USEPA method reference 6020B. Water field measurements and laboratory analyses are listed in Appendix 4 of Rukhlov et al. (2019).

#### 4.3.3. Lead isotopic analysis

Lead isotopic ratios were measured in water and leachates of stream sediment, moss-mat sediment, HMC, and rock samples using a direct solution analysis on ICP-MS. Lead isotopic analysis of water samples that were filtered (0.45 µm) and acidified with nitric acid was performed at PCIGR. Water samples were concentrated approximately 20 times in two steps and then diluted with 2% HNO<sub>3</sub> to about 0.2 ppb Pb level. All blanks and sample number 2018 (with low-Pb) were brought up to a minimum volume to run the samples. Lead isotopic ratios in water were measured on a Nu AttoM double-focusing, high-resolution magnetic sector ICP-MS (HR-ICP-MS), using sample-standard bracketing correction for instrumental mass bias.

During the test part of this study at Loss Creek, we analyzed Pb isotopic ratios in leachates of stream sediment, moss-mat sediment, and HMC samples using different digestions in two laboratories. A split (0.5 g) was digested in aqua regia, and Pb isotopic ratios were measured in the supernatant solution by ICP-MS at ALS Canada (Geochemistry) Ltd., Vancouver, British Columbia (ALS-Geochemistry). A second split (0.4 g) was leached in 2.5N HCl as described below and Pb isotopic ratios were measured in the supernatant solution on the Nu AttoM HR-ICP-MS at PCIGR. We preferred this method for subsequent Pb isotopic analysis of samples from northern Vancouver Island. Samples were mixed with 8-10 mL of 2.5N HCl and the mixtures were shaken on a bench shaker at room temperature for 2 hours. The samples were then centrifuged at 2500 rpm for 30 minutes, or at 4000 rpm for 15 minutes. The supernatants were transferred to Savillex vials and evaporated to dryness. Concentrated nitric acid (1-2 mL)

was added to the dry residues and evaporated to dryness. The final residues were re-dissolved in 2% HNO<sub>3</sub> and the solutions were centrifuged at 14,500 rpm for 6 minutes to preclude any suspended particles from entering the ICP-MS sample introduction system. The solutions were then diluted with 2% HNO<sub>3</sub> to about 0.5 ppb Pb and measured for Pb isotopic ratios on the AttoM HR-ICP-MS, using sample-standard bracketing correction for instrumental mass bias. The Pb isotopic data are listed in Appendix 5 of Rukhlov et al. (2019).

#### 4.3.4. Modal mineralogy

Sieved, 1-2 mm and 0.5-1.0 mm-size fractions of HMC samples were examined under the binocular microscope, with ambiguous mineral grains identified by a portable XRF (Rukhlov et al., 2018) at BCGS. Automated bulk mineralogical analysis (BMA) on the 0.5-1.0 mm fraction of selected HMC samples was performed at Actlabs. Representative splits (2 g) were embedded in the epoxy resin for preparing round polished sections. The modal mineralogy was determined by a FEI QEMSCAN 650F field emission gun-scanning electron microscope (FEG-SEM), equipped with high-resolution back-scattered electron (BSE) and two Bruker 5030D energy dispersive spectrometers (EDS), using an accelerating voltage of 25 kV, a spot size of 5.8 µm, and a working distance of 13 mm. A custom mineral reference library was built for the samples. The BMA results are listed in Appendix 6 of Rukhlov et al. (2019).

#### 4.4. Quality control

To evaluate the variability introduced by the sampling and analytical methods, we analyzed field duplicate samples, along with blind analytical duplicates (i.e., splits of recovered sieved fraction or pulverized material), matrix matching in-house and certified reference materials, and preparation blanks such as splits of pure silica sand processed the same way as routine samples (see Appendix 2 in Rukhlov et al., 2019). An average coefficient of variation,  $CV_{avr}$  (%), estimates the relative precision of the analytical results per analyte based on the field and analytical duplicates:

$$CV_{avr}(\%) = 100 \cdot \sqrt{\frac{2}{N} \sum_{i=1}^N \left( \frac{(a_i - b_i)^2}{(a_i + b_i)^2} \right)} \quad (\text{Eq. 1})$$

where  $a_i$  and  $b_i$  are duplicate results, and  $N$  is the number of duplicate pairs (after Abzalov, 2008). Appendices 3d, 4b, and 5a in Rukhlov et al. (2019) list the calculated  $CV_{avr}$  (%) values per analyte in different sample media. Values below an arbitrary 30% threshold indicate generally acceptable reproducibility of the analytical data, although those greater than 30% may also reflect sample media heterogeneity such as size fraction and nugget effect. Analysis of reference materials monitors accuracy or systematic bias of the analytical data. Blanks monitor contamination introduced by preparation and analytical methods.

#### 4.4.1. Stream and moss mat-sediment, heavy mineral concentrate, and rock analysis

Lithochemical analyses using different digestions combined with ICP-MS/ES and XRF instrumentation have acceptable precision for most analytes (Appendix 3d in Rukhlov et al., 2019). Aqua regia digestion–ICP-MS/ES analysis on a 30 g split of <0.18 mm material has marginal to poor precision for Ag, Au, B, Hg, In, Re, and Na. Repeated analysis of reference materials (Appendix 3b in Rukhlov et al., 2019) indicates good precision and accuracy for these analytes, except Na, which is ‘partial’ by aqua regia digestion. Hence, site-specific sample heterogeneity is clearly contributing the variability of these elements.  $CV_{avr}$  (%) values for ‘total’ concentrations analyzed by lithium borate fusion - combined LA-ICP-MS and XRF on fused glass disk indicate similar marginal to poor precision for Ag, Bi, and Re, but Au, B and Hg are not determined by this method. In the case of sodium peroxide fusion–ICP-MS/ES analysis, poor precision for ‘total’ concentrations of B, Cd, Hf, Ho, Mo, Pb, Se, Sn, and W can be attributed to higher detection limits (10-100 times) for some of the analytes or erratic, elevated blanks compared to those of other analytical methods (Appendices 3b and c in Rukhlov et al., 2019). Precision of thermal INAA, combined with CVAAS and ICP-ES on a separate split of the sample digested in aqua regia, and of multi-acid digestion–ICP-MS/ES cannot be adequately assessed here, because these analytical methods were used only to test a few splits of HMC samples early in this study. Thermal INAA has poor precision for ‘total’ concentrations of Eu, Tb, U, and W, based on one duplicate pair. Multi-acid digestion–ICP-ES/MS also has poor precision for ‘near total’ values of Ag, Bi, and Re, based on two pairs of duplicates.

Repeated analysis of reference materials estimates both precision and accuracy of the analytical data. Appendix 3b of Rukhlov et al. (2019) lists analytical results of blind reference materials,  $2\sigma$  ranges ( $\pm 2$  times standard deviation) of their expected mean ‘total’ and ‘partial’ values, blind preparation blanks, and blanks inserted by the commercial laboratories. Randomly inserted silica blanks (Aldrich 99.995% SiO<sub>2</sub> material) are generally below detection limits for most elements. Silica blanks pulverized in Cr-steel bowl at BCGS indicate 4-200 ppb Ag, 4-19 ppb Au, 36-430 ppm Cr, 0.09-0.36 wt.% Fe, 20-116 ppm Mn, 2-20 ppm Ni, 0.3-2.4 ppm Y, and 1-40 ppm Zn (n = 10), reflecting both carry-over contamination (e.g., gold lamination) and contribution from the grinding equipment. Sieved (<0.18 mm fraction) silica blanks and those pulverized in a ceramic bowl in a batch of HMC samples with an extra cycle of silica sand cleaning at BVM all indicate near-detection level of Au (0.4-1.6 ppb) and negligible or below detection limit values of other elements (Appendix 3b in Rukhlov et al., 2019).

Appendix 3c in Rukhlov et al. (2019) lists minimum detection limits (MDL) and sensitivity of the analytical methods in terms of percentage of results above the detection limit per analyte. Owing to generally low MDLs, acid digestion–ICP-ES/MS and lithium borate fusion–combined LA-ICP-MS and XRF on

fused glass have good sensitivity for 95% analytes (total 59 to 66), based on 8 to 45 analyses. Mostly undetected analytes include Pd, Pt, and Ta by aqua regia digestion–ICP-ES/MS; Be, Re, and S by four-acid digestion–ICP-ES/MS; and Se, Te, and Tl by lithium borate fusion–LA-ICP-MS. Generally higher MDLs of sodium peroxide fusion–ICP-ES/MS method result in poor sensitivity (i.e., >50% results per element below MDL) for 17% analytes (total 59), including B, Be, Bi, Cd, Hf, In, Re, Sb, Te, and W, based on 25 analyses. Thermal INAA combined with aqua regia digestion–CVAAS and ICP-ES on a separate split have poor sensitivity for 50% analytes (total 44), based on 7 analyses (Appendix 3c in Rukhlov et al., 2019).

#### 4.4.2. Water analysis

Precision of water data is estimated based on one field duplicate pair and replicate analyses of National Research Council of Canada (NRC) SLRS-6 river water certified reference material. Parameters measured in the field by a combination-electrode meter (T, pH, conductivity, and TDS) have  $CV_{avr}$  values of <1% indicating good reproducibility. Concentrations of anions in untreated water and dissolved metals in filtered (0.45  $\mu\text{m}$ ), acidified water all have acceptable precision, except Se, which has a  $CV_{avr}$  value of 43% (Appendix 4a in Rukhlov et al., 2019). Reported concentrations of NO<sub>3</sub><sup>-</sup> and NO<sub>2</sub><sup>-</sup> anions determined by ion chromatography should be treated with caution because most samples exceeded the recommended holding time of 3 days before analysis (4-18 days). Nitrite and bromide anions were not detected in water samples analyzed in this study. Only 29% (total 17) showed detectable F<sup>-</sup>. Dissolved Hg in filtered (0.45  $\mu\text{m}$ ) and acidified with hydrochloric acid water by CVAAS/ CVAFS was detected in one of 18 analyzed samples. CRC-ICP-MS analysis of other dissolved metals in filtered (0.45  $\mu\text{m}$ ) and acidified with nitric acid water has good sensitivity (i.e., <50% results per element below MDL) for 67% analytes (total 45). Bismuth, gallium, niobium, phosphorus, silver, tantalum, tellurium, and tungsten cations were not detected in water samples analyzed in this study.

Results of replicate analyses of NRC SLRS-6 river water standard are within uncertainties of the certified values, indicating good accuracy of the data (Appendix 4b in Rukhlov et al., 2019). Concentrations of anions were not analyzed in water blanks. Concentrations of dissolved metals measured in water blanks were generally below the MDLs, except erratic positive values for Ba, Ca, Cu, Fe, Pb, and Zn, thus ruling out significant contamination introduced by the sampling method. Water data are listed in Appendix 4 of Rukhlov et al. (2019).

#### 4.4.3. Lead isotopic analysis

Based on 22 duplicate pairs, Pb isotopic ratios measured in 2.5N HCl leachates of stream and moss-mat sediment, HMC, and rock samples on the AttoM HR-ICP-MS at PCIGR have  $CV_{avr}$  values of 0.15% for <sup>208</sup>Pb/<sup>206</sup>Pb ratio, 0.28% for <sup>206</sup>Pb/<sup>207</sup>Pb, 0.42% for <sup>208</sup>Pb/<sup>204</sup>Pb, 0.43% for <sup>206</sup>Pb/<sup>204</sup>Pb, and 0.49% for <sup>207</sup>Pb/<sup>204</sup>Pb. Precision of Pb isotopic ratios measured

in water samples on the same instrumentation at PCIGR is about 1.3-2.0 times the above  $CV_{avr}$  (%) values, based on 6 duplicate pairs. Lead isotopic ratios measured in aqua regia leachates of stream and moss-mat sediment, and HMC samples by ICP-MS at ALS-Geochemistry have larger  $CV_{avr}$  values of 0.55% for  $^{208}\text{Pb}/^{206}\text{Pb}$  ratio, 0.46% for  $^{206}\text{Pb}/^{207}\text{Pb}$ , 0.96% for  $^{208}\text{Pb}/^{204}\text{Pb}$ , 0.72% for  $^{206}\text{Pb}/^{204}\text{Pb}$ , and 0.78% for  $^{207}\text{Pb}/^{204}\text{Pb}$ , based on eight duplicate pairs. Hence, precision of the analysis by ICP-MS is enough to resolve natural Pb isotopic variability between the analyzed samples, showing maximum contrast of 1.5-2.7% for  $^{208}\text{Pb}/^{206}\text{Pb}$  ratio, 1.4-2.7% for  $^{206}\text{Pb}/^{207}\text{Pb}$ , 2.4-4.8% for  $^{208}\text{Pb}/^{204}\text{Pb}$ , 2.3-5.2% for  $^{206}\text{Pb}/^{204}\text{Pb}$ , and 2.5-4.2% for  $^{207}\text{Pb}/^{204}\text{Pb}$ . Replicate analyses of USGS BCR-2 reference material are consistent within the uncertainties with the published values by multi-collector ICP-MS and thermal ionization mass spectrometry, thus validating accuracy of the data reported here. Lead isotopic data, including reference materials and preparation and laboratory procedural blanks, are listed in Appendix 5 of Rukhlov et al. (2019).

## 5. Results

### 5.1. Loss Creek

#### 5.1.1. Lithochemistry

Analytical results for stream and moss mat-sediment (<0.18 mm sieved fraction) and HMC (milled, <1 mm sieved fraction) samples are listed in Appendix 3a of Rukhlov et al. (2019). Ranked element contrast (REC) plots (Fig. 6) are log plots of sorted (maximum to minimum) analytical results normalized to survey minimum values, specific for HMC and stream and moss-mat sediment samples. Normalizing to minimum sets the Y-axis origin to unity and thus simplifies the plot by avoiding fractions; normalizing to the median does not change the REC pattern. REC plots reveal associations of elements showing the maximum contrast to minimum or background (ranked leaders) and the magnitude of the contrast (geochemical anomaly), which reflects dispersion in a stream system. Contrast leaders (maximum/minimum) of the HMC samples at Loss Creek are Au (36752), Ag (121), W (107), Mn (59), heavy rare earth elements (HREE) such as Yb (58), Tm (54), Er (46), Ho (45), Lu (43), Dy (30), and Tb (15), plus Y (41). The magnitude of contrast for Au ( $n \cdot 10^4$ ) and HREE+Y ( $n \cdot 10^1$ ) are impressive. The anomalous element association reflects the occurrence of placer Au and abundant garnet (host of Mn, Y and HREE) at Loss Creek (Fig. 7). Anomalous Au-Ag-W is a signature of orogenic Au veins in the catchment area (Fig. 2). Notably, both the low-volume, bulk stream and moss-mat sediment materials, which are conventionally sampled in RGS surveys, missed the Au-Ag-W-HREE-Y anomaly and yielded only background levels. In contrast, HMC samples greatly enhanced the anomaly contrast and are thus much more effective. Furthermore, panning or sluicing in the field is inexpensive and rapid relative to costly and time-consuming processing of bulk samples in a laboratory and is well-suited for prospectors. As many elements as possible should be analyzed to minimize missing anomalous elements and keeping an open

mind for non-traditional types of ore deposits. At a minimum, we recommend aqua regia digestion–ultra-trace ICP-MS/ES analysis of a full suite of elements (currently 65). Ideally, this method should be supplemented with fusion–combined LA-ICP-MS and XRF on the fused glass, which determine ‘total’ concentrations of 65 elements plus LOI, including constituents of refractory minerals, which aqua regia digestion cannot break down.

#### 5.1.2. Hydrochemistry

Complete analytical results for stream water are listed in Appendix 4a of Rukhlov et al. (2019). Loss Creek water sampled in April was Na-Cl type with 3.6 mg/L  $\text{HCO}_3^-$  estimated by ion charge imbalance. The stream water became Ca- $\text{HCO}_3$  type with 11.66 mg/L  $\text{HCO}_3^-$  estimated by ion charge imbalance in June. Both April and June water samples had similar pH (6.8-7.2), conductivity (36  $\mu\text{S}/\text{cm}$ ), ionic strength (0.20-0.41 mmol/L), and major ion compositions (Fig. 8), but distinct abundances of dissolved trace metals (Fig. 9). A REC plot for Loss Creek water (Fig. 10) highlights the subtle differences in Loss Creek water chemistry between the spring runoff and lower discharges later in the summer. Ranked contrast (result/survey minimum) leaders in water sampled in April are Ti (19), Al (5), V (4), and Rb (4), whereas contrast leaders in water sampled in June are Mn (12), Rb (11), V (9), K (6), and Co (5). Note that  $\text{Rb}^+$  and anion-forming  $\text{V}^{3+}$ , soluble in neutral water, are invariable contrast leaders, reflecting the chemistry of country rocks, including staurolite-garnet schists of Leech River complex and basalts of Metchosin Formation. Although the subtle differences in dissolved metal contents reflect seasonal variability, water chemistry is an objective indicator of hydrochemical dispersion as will be discussed below.

#### 5.1.3. Lead isotopes

Analytical results on water and leachates of stream and moss-mat sediment and HMC samples are listed in Appendix 5a of Rukhlov et al. (2019). Lead isotopic ratios in leachates range from 18.52 to 19.30 for  $^{206}\text{Pb}/^{204}\text{Pb}$ , 15.41 to 16.11 for  $^{207}\text{Pb}/^{204}\text{Pb}$ , 37.51 to 39.71 for  $^{208}\text{Pb}/^{204}\text{Pb}$ , 1.187 to 1.211 for  $^{206}\text{Pb}/^{207}\text{Pb}$ , and 2.026 to 2.083 for  $^{208}\text{Pb}/^{206}\text{Pb}$ . Data for aqua regia leachates show more scattering in the Pb isotopic ratio plots than are those for 2.5N HCl leachates, which define linear trends in all diagrams (Figs. 10b-g). Although the larger uncertainties of the aqua regia leachates can partly explain the discrepancy, 2.5N HCl leachates of panned HMC samples have more radiogenic Pb isotopic ratios than are aqua regia leachates on splits of the same samples. The isotopic composition of water extends the linear data arrays of leachates in both  $^{206}\text{Pb}/^{204}\text{Pb}$  vs.  $^{207}\text{Pb}/^{204}\text{Pb}$  and  $^{206}\text{Pb}/^{204}\text{Pb}$  vs.  $^{208}\text{Pb}/^{204}\text{Pb}$  diagrams and falls in the middle of the linear trend in  $^{206}\text{Pb}/^{207}\text{Pb}$  vs.  $^{208}\text{Pb}/^{206}\text{Pb}$  diagram (Figs. 10e-g). Linear trends in the Pb isotopic ratio correlation diagrams could reflect mixing of two isotopically distinct end members or a secondary isochron (Gulson, 1986; Bell and Franklin, 1993; Bell and Murton, 1995; Simonetti et

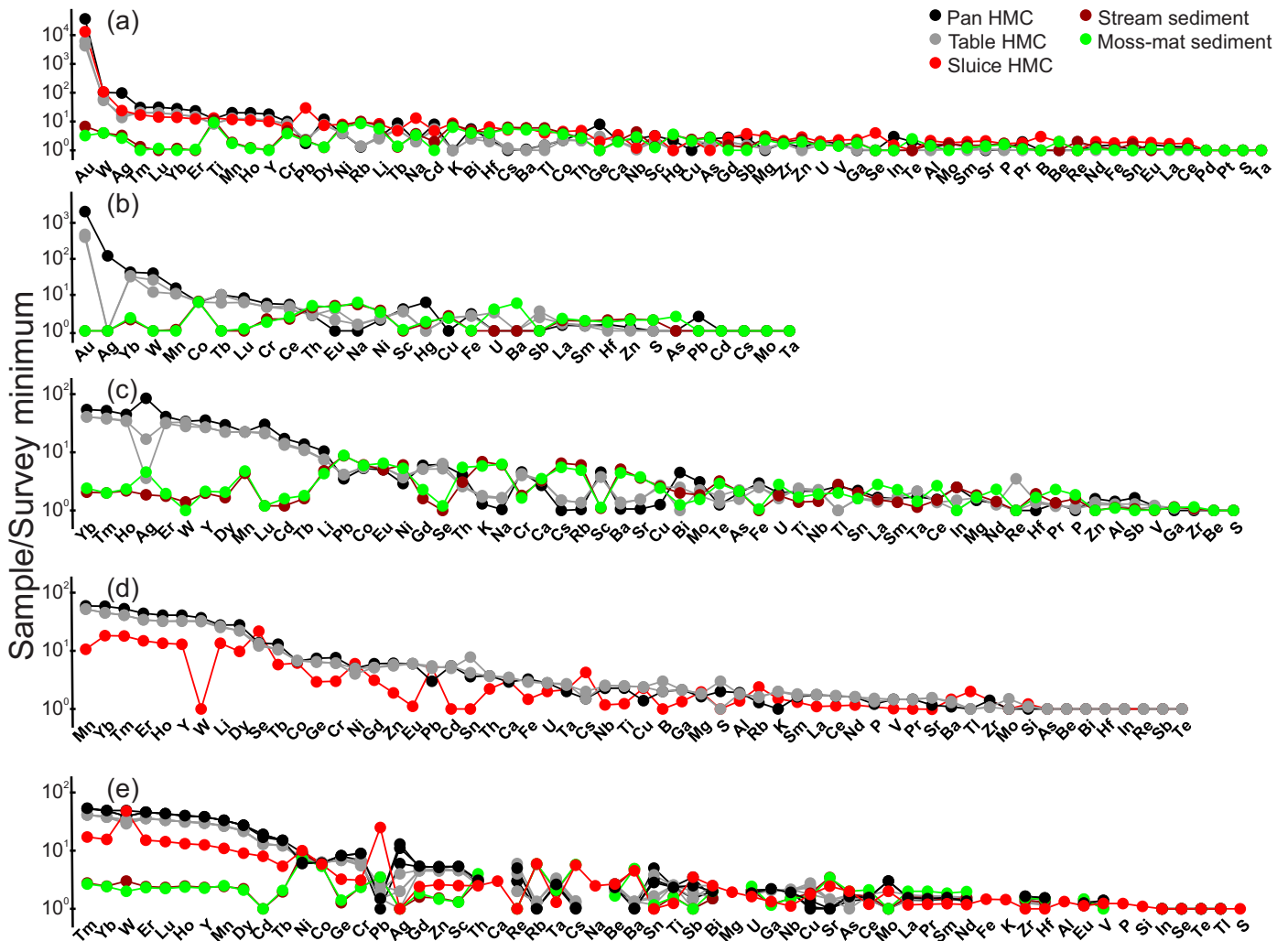


**Fig. 6.** Loss Creek ranked element contrast plots relative to survey minimum for stream sediment, moss-mat sediment, and heavy mineral concentrates by different analytical methods. **a)** H<sub>2</sub>O-HCl-HNO<sub>3</sub> digestion of <0.18 mm fraction or milled material (30 g) combined with inductively coupled plasma emission spectrometry (ICP-ES) and inductively coupled plasma mass spectrometry (ICP-MS) on the solution, determining ‘partial’ concentrations of 65 elements. **b)** Thermal instrumental neutron activation analysis (INAA) on <0.18 mm fraction or milled material (10-51 g), determining ‘total’ concentrations of 34 elements, combined with Hg by cold vapour atomic absorption spectrophotometry (CVAAS) and Ag, Cd, Cu, Mn, Mo, Ni, Pb, S, and Zn by ICP-ES on a separate split (0.5 g) digested in aqua regia. **c)** HF-HClO<sub>4</sub>-HNO<sub>3</sub>-HCl digestion of <0.18 mm fraction or milled material (0.25 g) combined with ICP-ES/MS on the solution, determining ‘near-total’ concentrations of 59 elements. **d)** Na<sub>2</sub>O<sub>2</sub> digestion of <75 μm milled material (0.8 g), followed by ICP-ES/MS on the solution, combined with Li<sub>2</sub>B<sub>4</sub>O<sub>7</sub>-LiBO<sub>2</sub> fusion of a separate split (0.8 g), followed by P and Zr analysis by X-ray fluorescence (XRF) on the fused glass disk, determining ‘total’ concentrations of 58 elements. **e)** Li<sub>2</sub>B<sub>4</sub>O<sub>7</sub>-LiBO<sub>2</sub> fusion of <75 μm milled material (0.7 g) combined with XRF and laser ablation ICP-MS (LA-ICP-MS) analysis on the fused glass disk, determining ‘total’ concentrations of 65 elements plus loss on ignition (LOI) at 1000°C gravimetrically.

al., 1996; Hussein et al., 2003; Rukhlov and Ferbey, 2015). In case of binary mixing, data points define hyperbolic curves in terms of Pb concentration versus Pb isotopic ratio (Figs. 11a-c). In these diagrams, the 2.5N HCl leachates of stream and moss-mat sediment and HMC samples partly overlap a binary mixing trend defined by MC-ICP-MS data for 2.5N HCl leachates of till matrix (<64 μm-size fraction), massive sulphide ore, and country diorite in southwestern British Columbia (Rukhlov and Ferbey, 2015).

Lead isotopic signature diagrams for Loss Creek leachates of stream and moss mat-sediment, HMC, and water samples,

(Figs. 11d-f) are linear plots of Pb isotopic ratios recast as δ values (in %) relative to survey minimum values

(Eq. 2)

$$\delta^{201\text{Pb}/201\text{Pb}} (\%) = 10^2 \cdot \frac{(^{201\text{Pb}}/^{201\text{Pb}})_{\text{sample}} - ^{201\text{Pb}}/^{201\text{Pb}}_{\text{minimum}}}{^{201\text{Pb}}/^{201\text{Pb}}_{\text{minimum}}}$$

where  $^{201\text{Pb}}/^{201\text{Pb}}_{\text{sample}}$  is measured Pb isotopic ratio in a sample and  $^{201\text{Pb}}/^{201\text{Pb}}_{\text{minimum}}$  is the survey minimum value of the ratio. δPb (%) values define Pb isotopic signature of a sample, which fingerprints the distinct Pb sources such as Pb-rich ore and host crustal rocks. The δPb (%) signature plots highlight the

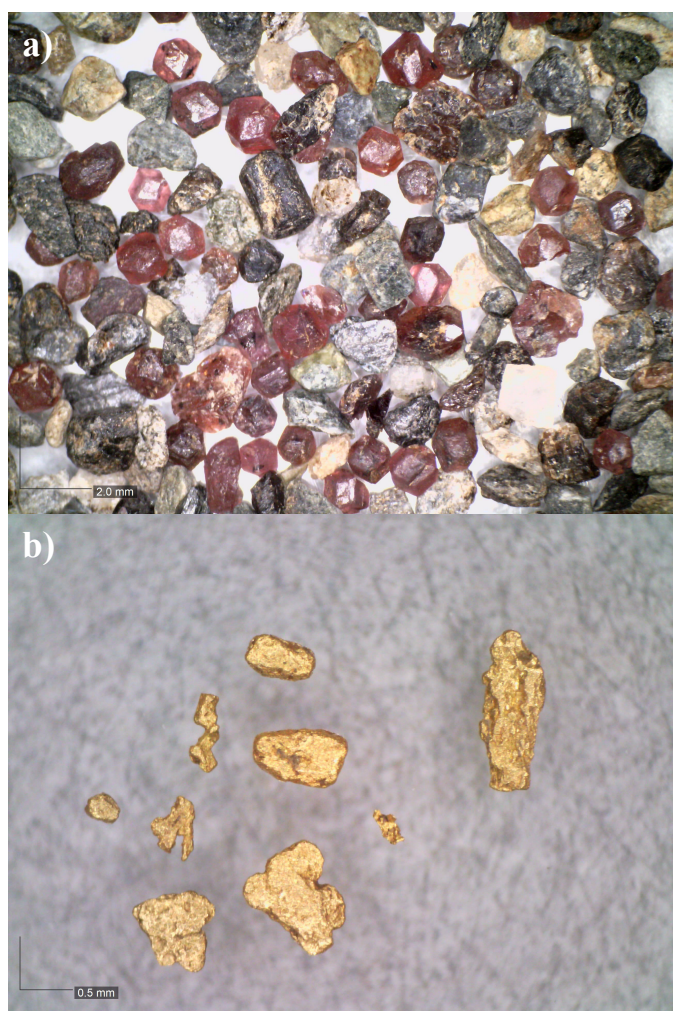


**Fig. 7.** Photomicrographs of panned sluice heavy mineral concentrate at Loss Creek (sample 1002). **a)** Abundant pink euhedral Mn-rich almandine,  $(\text{Fe}^{2+}, \text{Mn}^{2+})_3(\text{Al}, \text{Fe}^{3+})_2(\text{SiO}_4)_3$  in 1-2 mm fraction. **b)** Gold grains.

Pb isotopic contrast between the aqua regia and 2.5N HCl leachates of the HMC samples discussed above. Water and aqua regia leachate of stream sediment (<0.18 mm fraction) samples have the lowest  $\delta\text{Pb}$  (‰) values, whereas leachates of HMC samples (<1 mm-size) have more radiogenic Pb isotopic compositions with  $\delta\text{Pb}$  values up to 6‰ in  $^{208}\text{Pb}/^{204}\text{Pb}$ .

## 5.2. Northern Vancouver Island

Please see Rukhlov et al. (2019) for complete lithochemical analyses of 14 stream-sediment (<0.18 mm fraction), 14 panned sluice HMC (<1 mm fraction), and 2 rock samples collected at 13 sites from 6 major watersheds and their tributaries on northern Vancouver Island (Appendix 3a), water pH, conductivity, TDS, and concentrations of anions and dissolved metals in 15 samples from these streams (Appendix 4a), and Pb isotopic compositions of water (21) and 2.5N HCl leachates of HMC (17) and rock (2) (Appendix 5a).  $\delta\text{Pb}$  (‰) values for the northern Vancouver Island data are relative to the composition

of 2.5N HCl leachate of galena-bearing sample 19ARU001 from Caledonia Pb-Zn skarn occurrence (MINFILE 092L 061):  $^{206}\text{Pb}/^{204}\text{Pb} = 18.427$ ,  $^{207}\text{Pb}/^{204}\text{Pb} = 15.478$ ,  $^{208}\text{Pb}/^{204}\text{Pb} = 37.901$ ,  $^{206}\text{Pb}/^{207}\text{Pb} = 1.1905$ , and  $^{208}\text{Pb}/^{206}\text{Pb} = 2.0568$ .

### 5.2.1. Geochemistry and Pb isotopic composition of water

Analyzed stream waters range from Na-Cl and Ca-HCO<sub>3</sub> types (ionic strength 0.29-0.57 mmol/L) to Ca-SO<sub>4</sub> type (ionic strength 1.11-1.70 mmol/L). Significant ranges of pH (3.81-7.02), conductivity (27.5-138.2  $\mu\text{S}/\text{cm}$ ), and TDS (12.8-66.5 ppm) values, and major and trace ion compositions (Figs. 8, 9) are consistent with the historical drainage geochemical data (Matysek and Day, 1988; Gravel and Matysek, 1989; Matysek et al., 1989; Koyanagi and Panteleyev, 1993, 1994; Sibbick and Laurus, 1995a; Panteleyev et al., 1996b; Jackaman, 2011, 2013a). Lead isotopic ratios of the waters range from 18.17 to 18.63 for  $^{206}\text{Pb}/^{204}\text{Pb}$ , 15.32 to 15.71 for  $^{207}\text{Pb}/^{204}\text{Pb}$ , 37.46 to 38.36 for  $^{208}\text{Pb}/^{204}\text{Pb}$ , 1.173 to 1.196 for  $^{206}\text{Pb}/^{207}\text{Pb}$ , and 2.049 to 2.079 for  $^{208}\text{Pb}/^{206}\text{Pb}$ . The acidic (pH 3.81-4.30), Ca-SO<sub>4</sub> waters of Hushamu and Youghpan creeks have high conductivity (108.4-138.2  $\mu\text{S}/\text{cm}$ ), TDS (52.4-66.5 ppm), F<sup>-</sup>, Mg<sup>2+</sup>, Fe<sup>3+</sup>, Al<sup>3+</sup>, Mn<sup>2+</sup>, Ba<sup>2+</sup>, Zn<sup>2+</sup>, Cu<sup>2+</sup>, Co<sup>3+</sup>, Ni<sup>2+</sup>, Sn<sup>2+</sup>, and Pb<sup>2+</sup> cations compared with other streams. The Ca-SO<sub>4</sub> water of Hepler Creek has higher pH (6.8), lower conductivity (81.5  $\mu\text{S}/\text{cm}$ ), TDS (39.5 ppm), F<sup>-</sup>, Fe<sup>3+</sup>, and Al<sup>3+</sup>, but similar concentrations of Mg<sup>2+</sup> and most trace dissolved metals. In contrast, Na-Cl and Ca-HCO<sub>3</sub> waters from other streams have higher concentrations of NO<sub>3</sub><sup>-</sup>, V<sup>3+</sup>, and Cr<sup>3+</sup>, but generally lower abundances of other ions (Figs. 8, 9). Quatse River water was sampled every third day in August to monitor variability of water chemistry. Following a heavy rainfall the previous day, on August 2 the river had a much higher discharge than during the rainless period between August 3 and August 11. Concentrations of Cl<sup>-</sup>, B(OH)<sub>3</sub>, K<sup>+</sup>, and Rb<sup>+</sup> increased slightly, whereas NO<sub>3</sub><sup>-</sup>, Al<sup>3+</sup>, Fe<sup>3+</sup>, Mn<sup>2+</sup>, Ni<sup>2+</sup>, and Zn<sup>2+</sup> decreased slightly between August 2 to August 11. Water pH and concentrations of other ions remained generally consistent (Fig. 12).

Element contrast leaders (result/survey minimum) in stream water samples highlight anomalous element associations, which reflect variable solubility of metals depending on water pH and primary and secondary halos of hydrothermal ore systems drained by the streams (Figs. 13-17). Element contrast leaders in waters of Hushamu, Youghpan, and Hepler creeks are Co (91-243), Mn (52-123), Al (1-54), SO<sub>4</sub> (25-46), Fe (5-46), Zn (13-31), and Cu (5-26), which reflect soluble species in acidic waters draining argillic-altered volcanic rocks of the Bonanza Group, which host sulphide mineralization in the stream catchments (Northcote and Muller, 1972; Panteleyev, 1992; Panteleyev and Koyanagi, 1993, 1994; Panteleyev et al., 1995; Perelló et al., 1995; Tahija et al., 2017). In contrast, REC leaders in waters of a Hushamu Creek tributary, Wanokana and Caledonia creeks, and Quatse River are Ti-V-Zr±NO<sub>3</sub>±U±Al±Mo±Mn±Sn, reflecting hydrochemical dispersion of anion-forming and carbonate complexes of these metals soluble in neutral waters draining mainly mafic volcanic rocks. Waters of Hushamu and

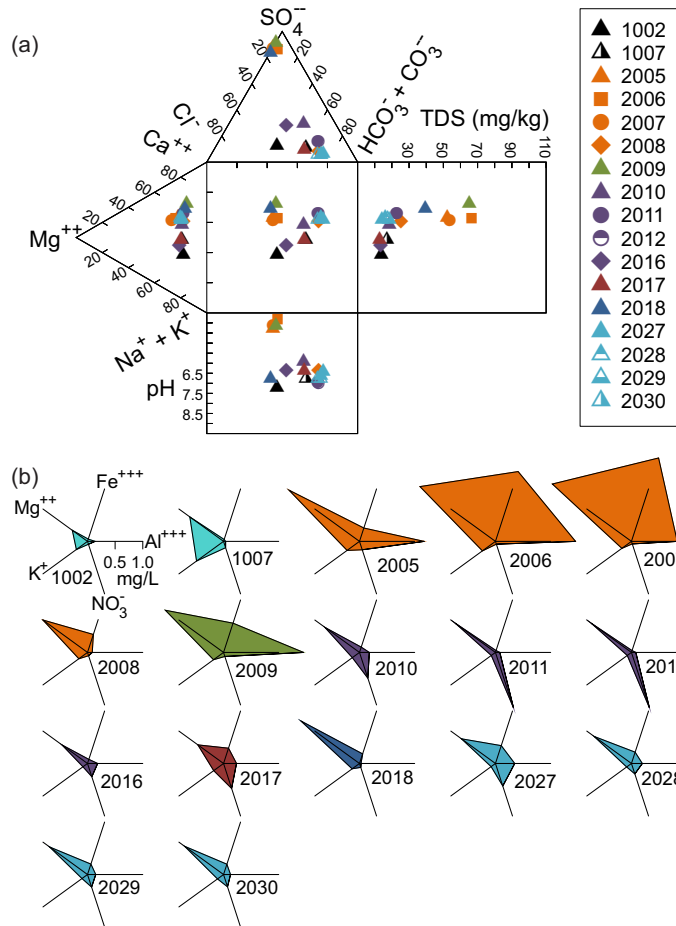


**Fig. 8.** Composition of Loss Creek and northern Vancouver Island stream water. **a)** Durov diagram, representing major ions ( $SO_4^{2-}$ ,  $HCO_3^- + CO_3^{2-}$ ,  $Ca^{2+}$ ,  $Mg^{2+}$ , and  $Na^+ + K^+$ ), total dissolved solids (TDS), and pH; and **b)** Radial plots in terms of  $K^+ - Mg^{2+} - Fe^{3+} - Al^{3+} - NO_3^-$  ions (in mg/L). See Appendix 4 in Rukhlov et al. (2019) for details.

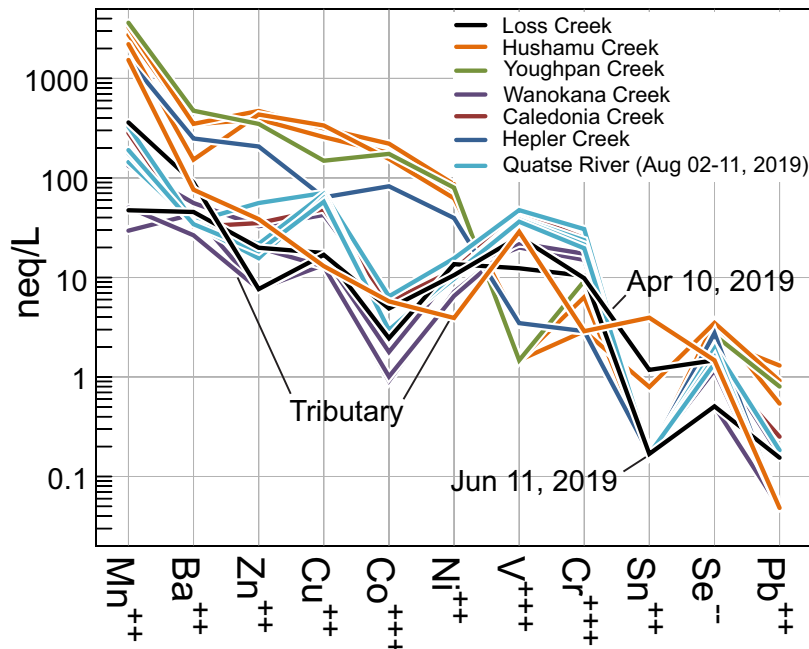


**Fig. 9.** Schoeller diagram for Vancouver Island streams showing patterns of minor ions in nanoequivalent concentration (neq/L).

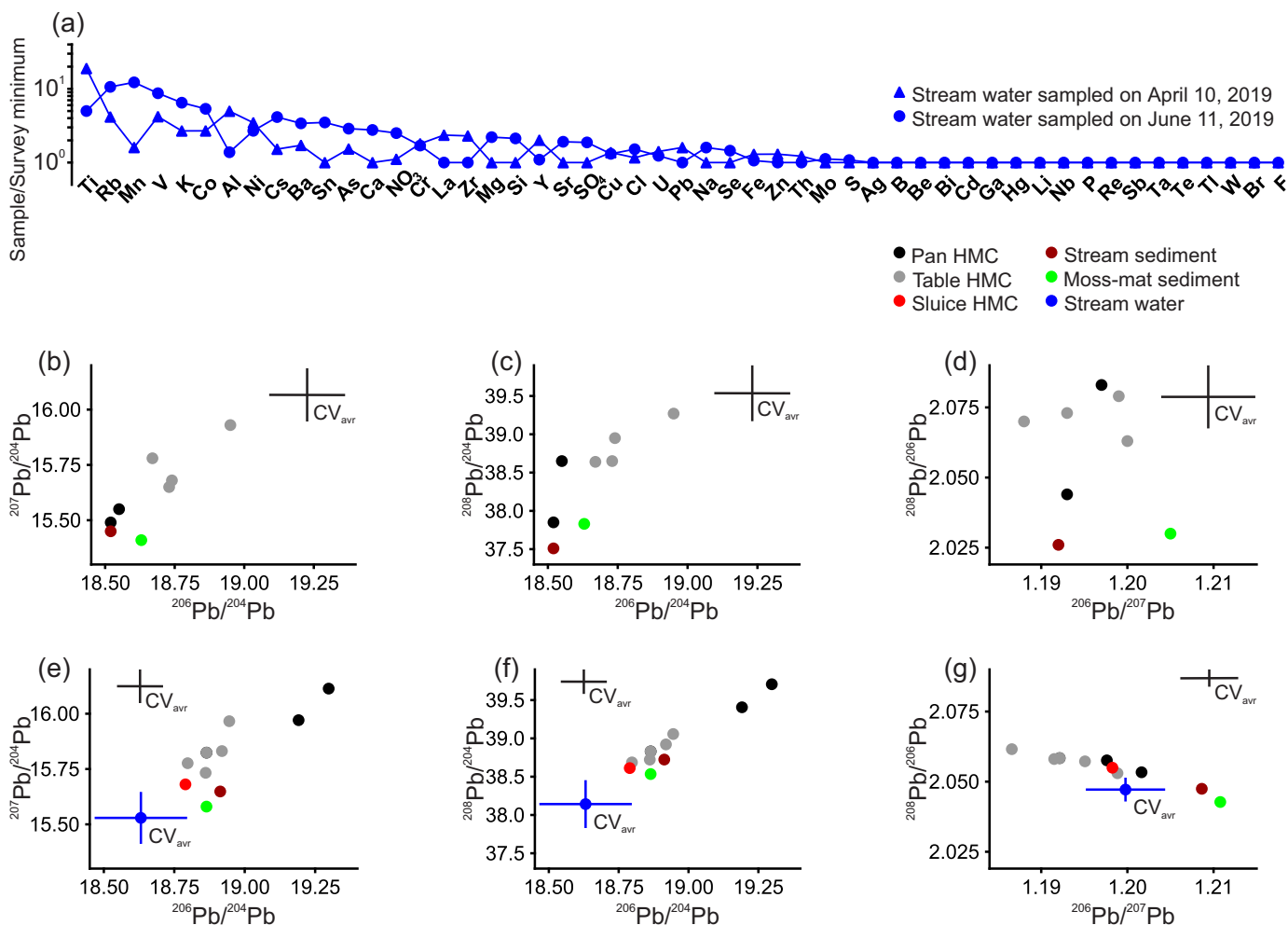


**Fig. 10.** **(a)** Ranked element contrast plot relative to survey minimum for water samples collected at Loss Creek in April and June, 2019. Concentrations of bromide, chloride, fluoride, nitrate, and sulphate anions in untreated water by ion chromatography; dissolved Hg in filtered (0.45  $\mu\text{m}$ ) and acidified with hydrochloric acid water by cold vapour atomic absorption spectrophotometry (CVAAS) or cold vapour atomic fluorescence spectroscopy (CVAFS); dissolved 45 other metals in filtered (0.45  $\mu\text{m}$ ) and acidified with nitric acid water by collision-reaction cell inductively coupled plasma mass spectrometry (CRC-ICP-MS). **(b-d)** Lead isotopic ratio plots for aqua regia leachates of stream sediment, moss-mat-sediment, and heavy mineral concentrate samples (0.5 g) from Loss Creek analyzed on ICP-MS at ALS Canada (Geochemistry) Ltd., Vancouver, British Columbia. **(e-g)** Lead isotopic ratio plots for filtered (0.45  $\mu\text{m}$ ), acidified with nitric acid, water samples (50 mL) and for 2.5N HCl leachates of stream sediment, moss-mat-sediment, and heavy mineral concentrate samples (0.3-0.5 g) from Loss Creek analyzed on a Nu AttoM double-focusing, high-resolution magnetic sector ICP-MS (HR-ICP-MS) at the Pacific Centre for Isotopic and Geochemical Research, University of British Columbia (PCIGR), Vancouver, British Columbia. **(b, e)**  $^{206}\text{Pb}/^{204}\text{Pb}$  vs.  $^{207}\text{Pb}/^{204}\text{Pb}$ . **(c, f)**  $^{206}\text{Pb}/^{204}\text{Pb}$  vs.  $^{208}\text{Pb}/^{204}\text{Pb}$ . **(d, g)**  $^{206}\text{Pb}/^{207}\text{Pb}$  vs.  $^{208}\text{Pb}/^{206}\text{Pb}$ . Uncertainties in terms of average coefficient of variation ( $CV_{avr}$ ) based on at least 6 duplicate pairs (after Abzalov, 2008).

Youghan creeks also have distinct  $\delta\text{Pb}$  (%) patterns with low  $\delta\text{Pb}$  (%) values, which reflect sources having unradiogenic Pb isotopic compositions such as galena-bearing Caledonia Pb-Zn skarn (MINFILE 092L 061; Figs. 13, 15). Different  $\delta\text{Pb}$  (%) patterns of stream waters indicate isotopically heterogeneous sources.

### 5.2.2. Geochemistry and Pb isotopic composition of stream sediment and heavy mineral concentrate

Geochemistry of stream sediment (<0.18 mm fraction) and HMC (<1 mm fraction) samples reveals different REC leaders, which are Au, Bi, Se, Te, Mo, Pb, Re, S, Sn, Tl, In, and Cu at

the headwaters of Hushamu Creek (Fig. 13). The anomalous element association confirms not only epithermal Au-Ag-Cu (MINFILE 092L 185) and porphyry Cu-Mo±Au (MINFILE 092L 240) mineralization immediately upstream, but also suggests shallow erosion of the mineralization (Panteleyev, 1992; Panteleyev and Koyanagi, 1993, 1994; Panteleyev et al., 1995; Perelló et al., 1995; Tahija et al., 2017). HMC samples collected farther downstream and near the mouth of Hushamu Creek (catchment, 20.5 km<sup>2</sup>) also show maximum element contrast for Au (30709 times background), S, Se, Ag, Bi, Te, Mo, Re, and Pb. Subdued contrast and distinct element association (Se-Mo-Bi-Co-Te-S-Li-Cs) in an HMC sample

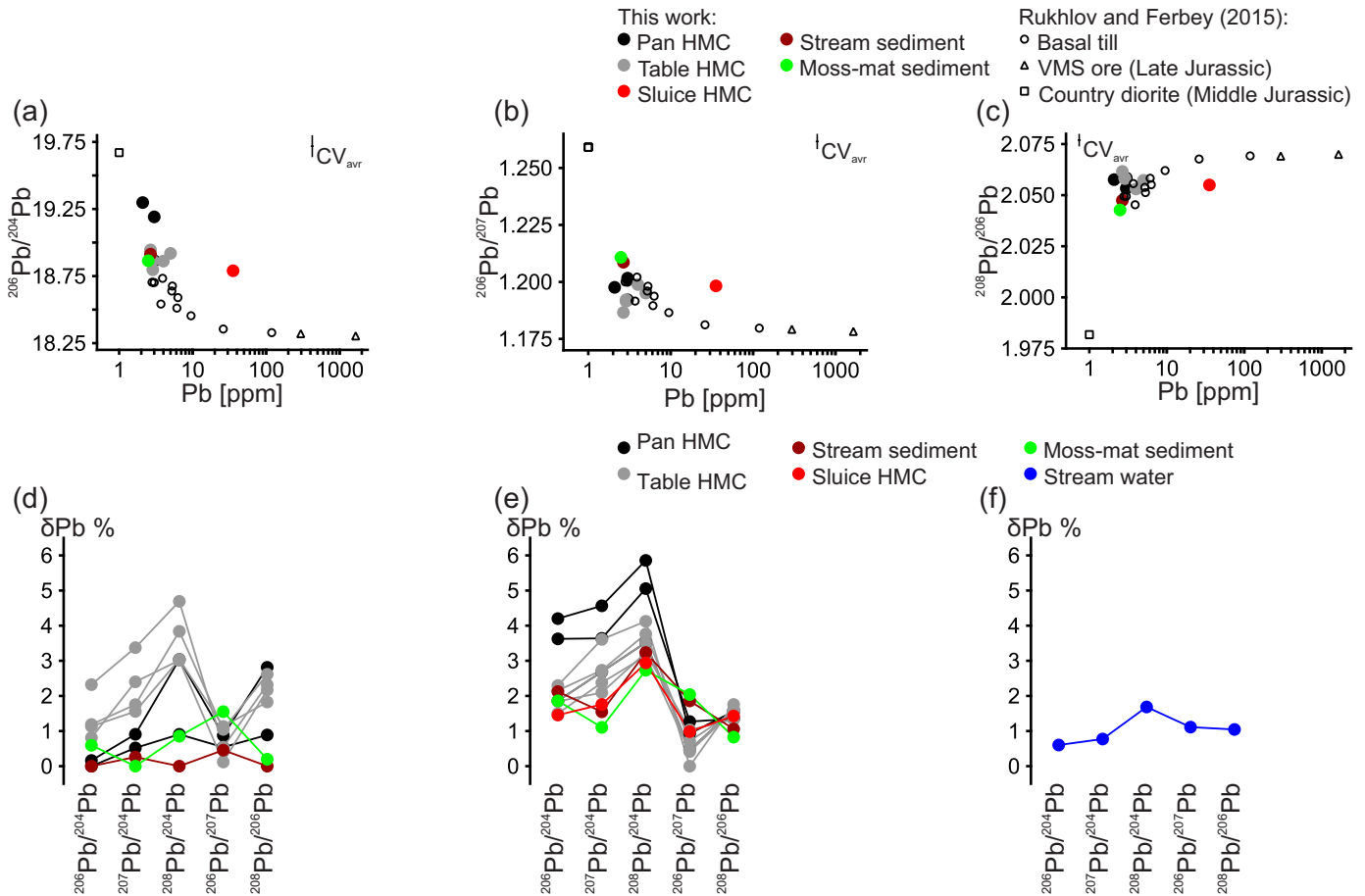


**Fig. 11. (a-c)** Mixing plots for stream sediment, moss mat-sediment, and heavy mineral concentrate samples from Loss Creek in terms of Pb concentration by aqua regia digestion–inductively coupled plasma mass spectrometry (ICP-MS) vs. Pb isotopic ratio in 2.5N HCl leachates of the samples analyzed on a Nu AttoM double-focusing, high-resolution magnetic sector ICP-MS (HR-ICP-MS). **a)** Pb [ppm] vs.  $^{206}\text{Pb}/^{204}\text{Pb}$ . **b)** Pb [ppm] vs.  $^{206}\text{Pb}/^{207}\text{Pb}$ . **c)** Pb [ppm] vs.  $^{208}\text{Pb}/^{206}\text{Pb}$ . Multi-collector ICP-MS (MC-ICP-MS) data for 2.5N HCl leachates of <63  $\mu\text{m}$ -size, sieved fraction of basal till matrix, massive sulphide ore, and country diorite from southern British Columbia after Rukhlov and Ferbey (2015). Uncertainties in terms of average coefficient of variation ( $CV_{avr}$ ) based on 22 duplicate pairs (after Abzalov, 2008). **(d-f)** Lead isotopic signature plots for stream sediment, moss mat-sediment, heavy mineral concentrate, and water samples from Loss Creek in terms of Pb isotopic ratios recast as  $\delta$  values (in %) relative to the survey minimum values as follows:  $\delta^{20i}\text{Pb}/^{20j}\text{Pb}$  (%) =  $100 \cdot \left( \frac{^{20i}\text{Pb}/^{20j}\text{Pb}_{\text{sample}}}{^{20i}\text{Pb}/^{20j}\text{Pb}_{\text{minimum}}} - 1 \right)$ . **d)**  $\delta\text{Pb}$  (%) plots for  $^{206}\text{Pb}/^{204}\text{Pb}$ ,  $^{207}\text{Pb}/^{204}\text{Pb}$ ,  $^{208}\text{Pb}/^{204}\text{Pb}$ ,  $^{206}\text{Pb}/^{207}\text{Pb}$ , and  $^{208}\text{Pb}/^{206}\text{Pb}$  values in aqua regia leachates of stream sediment, moss mat-sediment, and heavy mineral concentrate samples analyzed on ICP-MS at ALS Canada (Geochemistry) Ltd., Vancouver, British Columbia. **e)**  $\delta\text{Pb}$  (%) plots for  $^{206}\text{Pb}/^{204}\text{Pb}$ ,  $^{207}\text{Pb}/^{204}\text{Pb}$ ,  $^{208}\text{Pb}/^{204}\text{Pb}$ ,  $^{206}\text{Pb}/^{207}\text{Pb}$ , and  $^{208}\text{Pb}/^{206}\text{Pb}$  values in 2.5N HCl leachates of stream sediment, moss mat-sediment, and heavy mineral concentrate samples analyzed on a Nu AttoM double-focusing, high-resolution magnetic sector ICP-MS (HR-ICP-MS) at the Pacific Centre for Isotopic and Geochemical Research, University of British Columbia (PCIGR), Vancouver, British Columbia. **f)**  $\delta\text{Pb}$  (%) plots for  $^{206}\text{Pb}/^{204}\text{Pb}$ ,  $^{207}\text{Pb}/^{204}\text{Pb}$ ,  $^{208}\text{Pb}/^{204}\text{Pb}$ ,  $^{206}\text{Pb}/^{207}\text{Pb}$ , and  $^{208}\text{Pb}/^{206}\text{Pb}$  values in filtered (0.45  $\mu\text{m}$ ), acidified with nitric acid, water sample analyzed on the AttoM HR-ICP-MS at PCIGR.

collected near the mouth of a Hushamu Creek tributary rule out significant mineralization in that basin (Fig. 13).

HMC samples collected near mouths of Youghpan (catchment, 25.0  $\text{km}^2$ ) and Wanokana (catchment, 43.5  $\text{km}^2$ ) creeks show maximum contrast for Au (1779–22328 times background), S, Ag, Bi, Se, Te, Mo, Co, Ba, Re, Tl, Hg, and Pb, indicating significant epithermal Au–Ag–Cu and blind porphyry Cu–Mo–Au mineralization (Figs. 15, 16). HMC samples collected at the headwaters of Wanokana Creek and near the mouth of Quatse River (catchment, 89.4  $\text{km}^2$ ) have a distinct geochemical signature with anomalous  $\text{Hg} \pm \text{Au} \pm \text{Ag}$  and elevated background for Ti, Ni, Co, and Ca, reflecting

mafic rock types (Figs. 16, 17). HMC sample from Caledonia Creek (catchment, 9.35  $\text{km}^2$ ), downstream of a Pb–Zn skarn occurrence (MINFILE 092L 061), shows a weak contrast and elevated background for W, Mo, Co, Ti, Ca, Bi, Na, Ni, Mn, Au, Pb, and Cd, which rule out significant mineralization in that basin (Fig. 17). Lead isotopic compositions also discriminate between the two groups of HMC samples. Smoother  $\delta\text{Pb}$  (%) patterns with values about zero characterize 2.5N leachates of HMC samples from Hushamu and Youghpan creeks, whereas others have more variable  $\delta\text{Pb}$  (%) patterns indicating Pb isotopic heterogeneity in the catchment basins (Figs. 13, 15–17).

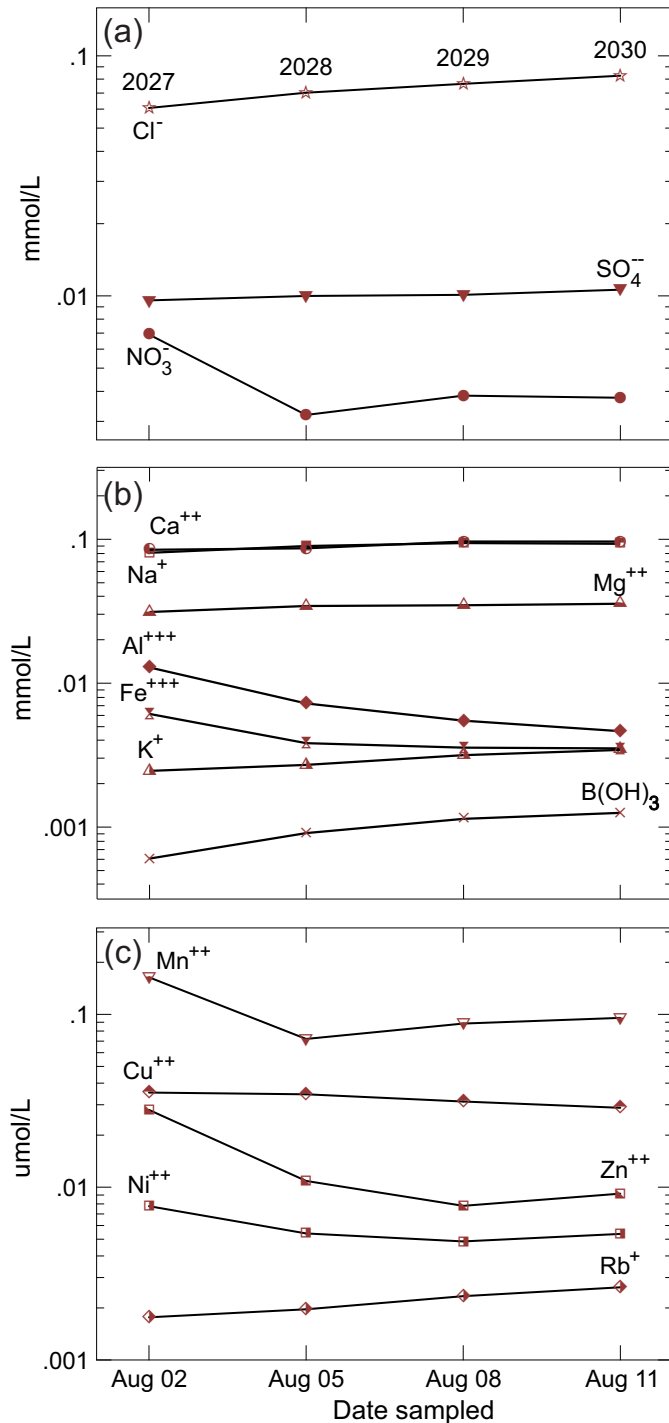


**Fig. 12.** Sampling date versus composition of Quatse River water at monitor site, northern Vancouver Island. **a)**  $\text{Cl}^-$ ,  $\text{SO}_4^{2-}$ , and  $\text{NO}_3^-$  anions (mmol/L). **b)**  $\text{Na}^+$ ,  $\text{K}^+$ ,  $\text{Ca}^{2+}$ ,  $\text{Mg}^{2+}$ ,  $\text{Al}^{3+}$ , and  $\text{Fe}^{3+}$  cations, and  $\text{B(OH)}_3$  component (mmol/L). **c)**  $\text{Rb}^+$ ,  $\text{Cu}^{2+}$ ,  $\text{Mn}^{2+}$ ,  $\text{Ni}^{2+}$ , and  $\text{Zn}^{2+}$  cations ( $\mu\text{mol/L}$ ).

In summary, near-mouth HMC samples (<1 mm fraction) confidently identify epithermal Au-Ag-Cu and blind porphyry Cu-Mo±Au mineralization in the Hushamu, Youghpan, and Wanokana watersheds (20.5-43.5 km<sup>2</sup>). In contrast, all stream-sediment samples (<0.18 mm fraction) collected near

mouths of these basins have background concentrations of Au and Ag, consistent with previous moss-mat sediment RGS data (Figs. 13, 15, 16; Matysek and Day, 1988; Gravel and Matysek, 1989; Matysek et al., 1989; Jackaman, 2011, 2013a, 2014). Conventional RGS sample media contrast ore metals only immediately downstream of known mineralization such as the Hushamu deposit, whereas HMC samples greatly enhance the geochemical anomaly contrast for a much larger catchment area. For regional geochemical drainage surveys, we recommend collecting one near-mouth HMC sample (200-400 g), recovered from 10-15 kg of bulk alluvium (<2 mm fraction). Geochemistry of the 'grey' HMC (<1 mm fraction), which retains sulphides, garnet, and other indicator minerals (i.e., not 'black sand' with specific gravity >5 g·cm<sup>-3</sup>), is more representative of element dispersion in a stream system and thus basin metallogeny than are low-volume, bulk stream and moss-mat sediment samples.

### 5.3. Mineralogy of heavy mineral concentrate

Microscopic examination of 1-2 mm and 0.5-1.0 mm fractions of HMC samples, coupled with pXRF identification on single grains of ambiguous minerals, provides information on ore minerals such as gold and diamonds and indicators of hydrothermal alteration and ore systems. Appendix 6 in Rukhlov et al. (2019) lists BMA results on selected HMC samples (0.5-1.0 mm fraction) by QEMSCAN. Panned sluice HMC recovered from alluvium at Loss Creek has abundant Mn-rich almandine (25%), staurolite, and amphibole derived from staurolite-garnet schists (Fig. 7a). The delicate shape of detrital gold grains (wires and leaves; Fig. 7b) indicates a nearby bedrock source, such as the orogenic Au veins in the area (MINFILE 092C 214, 213, 217, and 059). In contrast, alluvial HMC samples from northern Vancouver Island have 1-2% garnet, including brown-red spessartine and pink almandine (Fig. 18). Glacial dispersion of spessartine garnet in tills has been successfully used in exploring for epithermal Au-Ag-Cu deposits of the Interior Plateau (Lett and Rukhlov, 2017 and references therein). Other porphyry Cu-Mo-Au and epithermal Au-Ag-Cu indicator minerals in alluvial HMC samples from Hushamu Creek include pyrite, magnetite, goethite, rutile, ardealite, alunite, anhydrite, böhmite, titanite, epidote, muscovite, illite, chlorite, Si-Al clays, siderite, and apatite (Appendix 6 in Rukhlov et al., 2019). A near-mouth HMC sample from Wanokana Creek contains abundant plagioclase, K-feldspar, amphibole, and epidote, and elevated counts of hematite, ilmenite, titanite, and apatite relative to other HMC samples (Appendix 6 in Rukhlov et al., 2019).

## 6. Discussion

### 6.1. Basic principles

Weathering of an in situ ore body and its primary dispersion halo results in hypogene enrichment of nearby surficial materials in ore and related elements, forming a secondary dispersion halo. This secondary geochemical anomaly generally mimics the shape of the primary bedrock anomaly in plan view but has

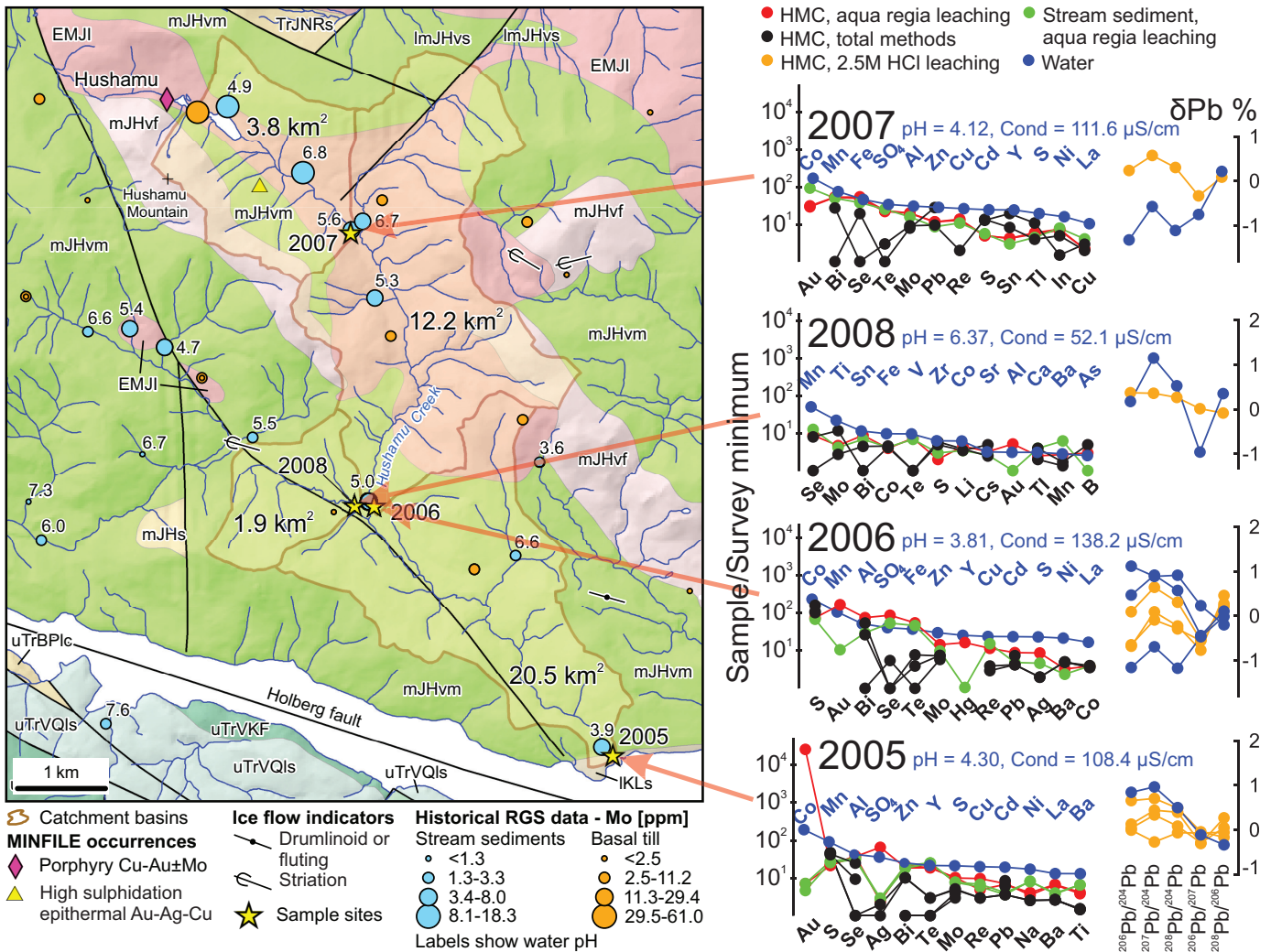


**Fig. 13.** Hushamu Creek catchment, northern Vancouver Island. Leaders of ranked element contrast relative to survey minimum and  $\delta^{206}\text{Pb}/^{204}\text{Pb}$ ,  $\delta^{207}\text{Pb}/^{204}\text{Pb}$ ,  $\delta^{208}\text{Pb}/^{204}\text{Pb}$ ,  $\delta^{206}\text{Pb}/^{207}\text{Pb}$ , and  $\delta^{208}\text{Pb}/^{206}\text{Pb}$  patterns (in %) for stream sediment, heavy mineral concentrate, and water samples. Water pH, conductivity, and analyte labels shown above patterns.  $\delta\text{Pb}$  (%) values calculated as follows:  $\delta^{206}\text{Pb}/^{204}\text{Pb}$  (%) =  $100 \cdot \left( \frac{^{206}\text{Pb}/^{204}\text{Pb}_{\text{sample}}}{^{206}\text{Pb}/^{204}\text{Pb}_{\text{galena}}} - 1 \right)$ , where  $^{206}\text{Pb}/^{204}\text{Pb}_{\text{galena}}$  is the Pb isotopic composition of 2.5N HCl leachate of galena-bearing mineralization (sample 19ARU001; MINFILE 092L 061). Ice-flow indicators from Clague et al. (1982), Kerr (1992), Meldrum and Bobrowsky (1994), Bobrowsky et al. (1995), Bobrowsky (1997), and Bobrowsky and Meldrum (1994a, b). Regional geochemical survey (RGS) data after Matysek and Day (1988), Gravel and Matysek (1989), Matysek et al. (1989), Kerr et al. (1992), Bobrowsky and Sibbick (1996), and Jackaman (2011, 2013a, b, 2014). Bedrock legend as in Figure 3.

a much larger footprint. The mechanical, hydrous, and gaseous dispersion of a primary bedrock anomaly or its secondary dispersion halo in a drainage system further generates a geochemically anomalous dispersion stream. Concentrations of elements in dispersion streams are intermediate between local background and the higher values of secondary and primary geochemical anomalies near-ore sources. Extending for many km from these sources, these dispersion streams eventually become diluted and approach background levels. However, high concentrations of Cu (REC leader) in alluvial HMC samples from the Fraser River delta (Kaplenkov, unpublished data) reflect a prominent dispersion stream from large porphyry

copper deposits even 100s of km upstream in a catchment basin of 220,000 km<sup>2</sup>! Secondary dispersion halos and dispersion streams develop in all geospheres, encompassing bedrock, its weathered products and soils, surficial and underground waters, air, and living organisms. According to Vernadsky’s law, lithochemical, hydrochemical, atmochemical, and biochemical secondary dispersion halos and streams are closely related due to the universal dispersion and migration of elements and constant interaction between all geospheres (Safronov, 1971; Hawkes, 1976; Rose et al., 1979; Grigoryan et al., 1983; Solovov, 1985; Solovov et al., 1990; Matveev, 2003).

Geochemical anomalies are deviations from the local

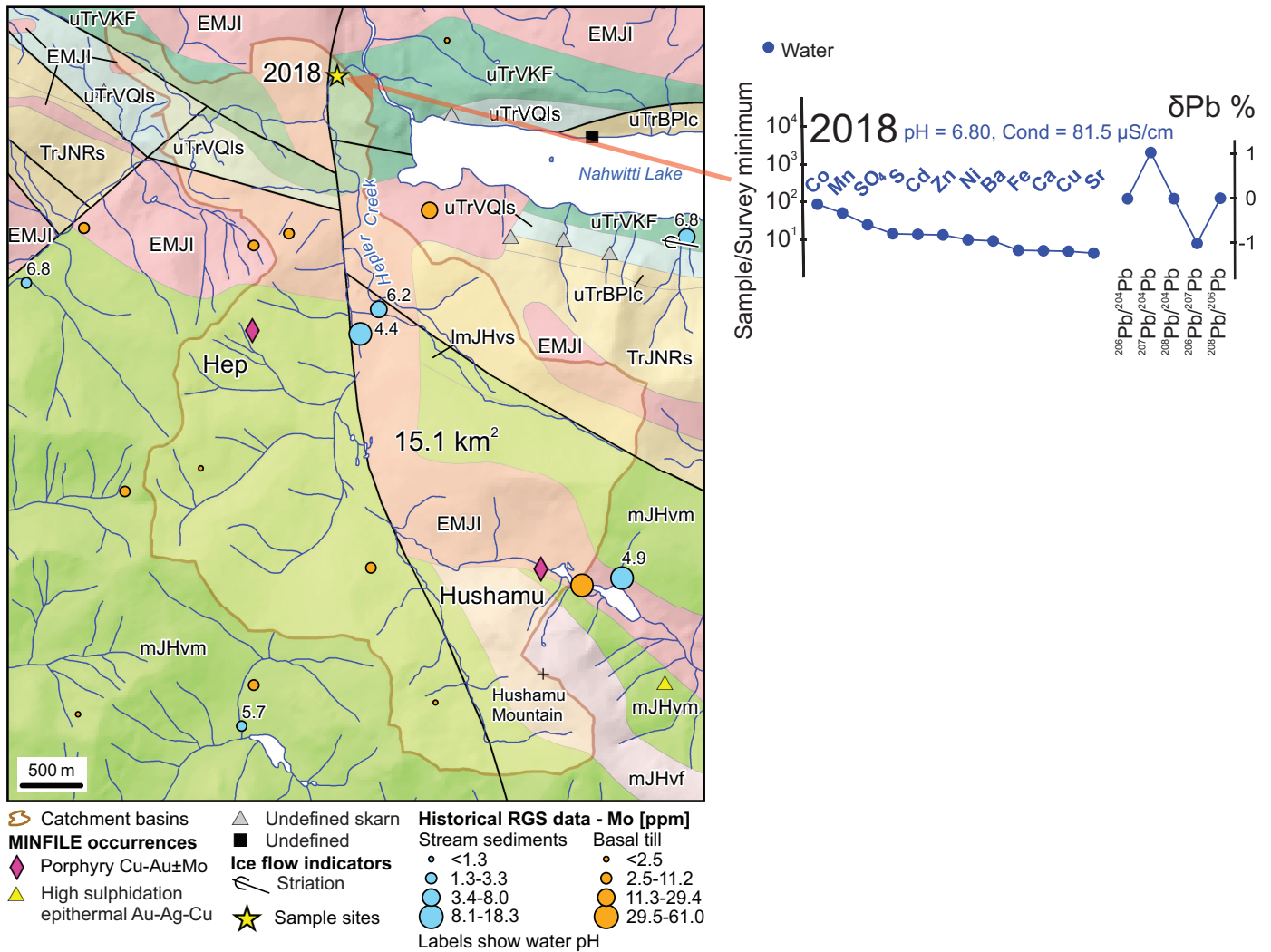


**Fig. 14.** Hepler Creek basin, northern Vancouver Island, leaders of ranked element contrast relative to survey minimum and  $\delta^{206}\text{Pb}/^{204}\text{Pb}$ ,  $\delta^{207}\text{Pb}/^{204}\text{Pb}$ ,  $\delta^{208}\text{Pb}/^{204}\text{Pb}$ ,  $\delta^{206}\text{Pb}/^{207}\text{Pb}$ , and  $\delta^{208}\text{Pb}/^{206}\text{Pb}$  pattern (in %) for water sample.  $\delta\text{Pb}$  (%) values calculated as follows:  $\delta^{20i}\text{Pb}/^{20j}\text{Pb}$  (%) =  $100 \cdot (^{20i}\text{Pb}/^{20j}\text{Pb}_{\text{sample}} - ^{20i}\text{Pb}/^{20j}\text{Pb}_{\text{galena}}) / ^{20i}\text{Pb}/^{20j}\text{Pb}_{\text{galena}}$ , where  $^{20i}\text{Pb}/^{20j}\text{Pb}_{\text{galena}}$  is the Pb isotopic composition of 2.5N HCl leachate of galena-bearing mineralization (sample 19ARU001; MINFILE galena 061). Ice-flow indicators after Clague et al. (1982), Kerr (1992), Meldrum and Bobrowsky (1994), Bobrowsky et al. (1995), Bobrowsky (1997), and Bobrowsky and Meldrum (1994a, b). Regional geochemical survey (RGS) data after Matysek and Day (1988), Gravel and Matysek (1989), Matysek et al. (1989), Kerr et al. (1992), Bobrowsky and Sibbick (1996), and Jackaman (2011, 2013a, b, 2014). Bedrock legend as in Figure 3.

geochemical field or background, which is defined as a geological space with variable element concentrations ( $C_i$ ) above zero in each point in space and time, or

$$C_i = f(x, y, z, T) > 0 \quad (\text{Eq. 3})$$

Because elements predominantly occur in a dispersed state rather than forming concentrations, much of the geochemical field has concentrations of ore elements close to their Clarke values (i.e., normal state), which only rarely deviate from this level, i.e., form geochemical anomalies (Solovov et al., 1990). Hence, the local geochemical background ( $C_b$ ) can be defined as the average (modal) concentration of an element ( $C_x$ ) in a homogeneous area away from apparent anomalies (Matveev,

2003). Background values of ore elements are lognormally distributed in a normal geochemical field so that 99.86% of background values are less than  $(C_x + 3s)$ , where  $s$  is standard deviation. Thus, the threshold of anomalous concentration ( $C_a$ ) for any single point in a geochemical field is

$$\log C_a = \log C_x + 3s_{\log}, \text{ or } C_a = C_x \cdot \varepsilon^3, \quad (\text{Eq. 4})$$

where  $C$  is the geometric average concentration of an element, and  $\varepsilon$  is standard multiplier

$$\varepsilon = \text{antilog } s_{\log} \quad (\text{Eq. 5})$$

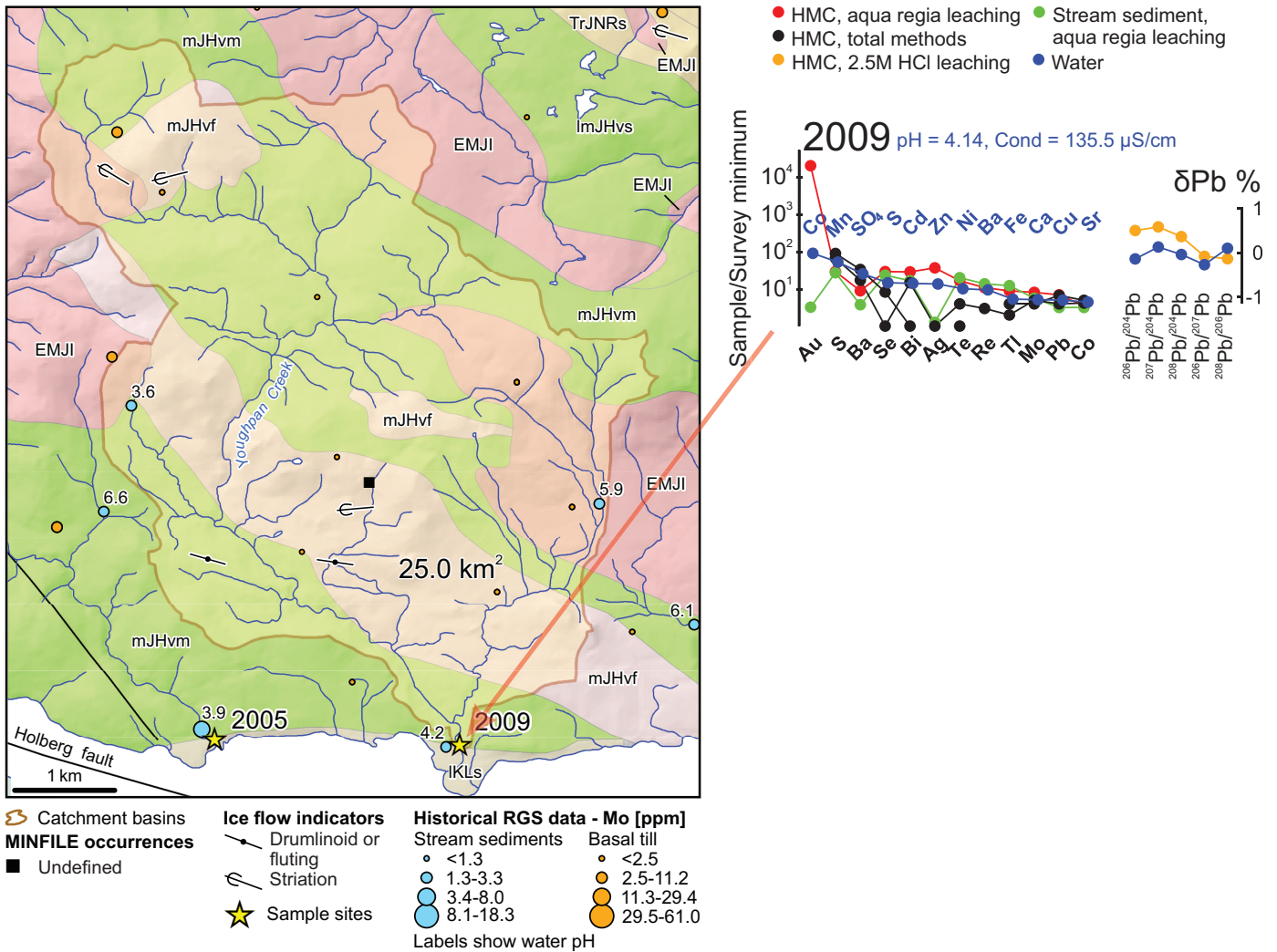


**Fig. 15.** Youghpan Creek basin, northern Vancouver Island, leaders of ranked element contrast relative to survey minimum and  $\delta^{206}\text{Pb}/^{204}\text{Pb}$ ,  $\delta^{207}\text{Pb}/^{204}\text{Pb}$ ,  $\delta^{208}\text{Pb}/^{204}\text{Pb}$ ,  $\delta^{206}\text{Pb}/^{207}\text{Pb}$ , and  $\delta^{208}\text{Pb}/^{206}\text{Pb}$  patterns (in %) for stream sediment, heavy mineral concentrate, and water samples. Water pH, conductivity, and analyte labels shown above patterns.  $\delta\text{Pb}$  (%) values calculated as follows:  $\delta^{20i}\text{Pb}/^{20j}\text{Pb}$  (%) =  $100 \cdot \frac{^{20i}\text{Pb}/^{20j}\text{Pb}_{\text{sample}} - ^{20i}\text{Pb}/^{20j}\text{Pb}_{\text{galena}}}{^{20i}\text{Pb}/^{20j}\text{Pb}_{\text{galena}}}$ , where  $^{20i}\text{Pb}/^{20j}\text{Pb}_{\text{galena}}$  is the Pb isotopic composition of 2.5N HCl leachate of galena-bearing mineralization (sample 19ARU001; MINFILE 092L 061). Ice-flow indicators from Clague et al. (1982), Kerr (1992), Meldrum and Bobrowsky (1994), Bobrowsky et al. (1995), Bobrowsky and Bobrowsky (1997), and Bobrowsky and Meldrum (1994a, b). Regional geochemical survey (RGS) data after Matysek and Day (1988), Gravel and Matysek (1989), Matysek et al. (1989), Kerr et al. (1992), Bobrowsky and Sibbick (1996), and Jackaman (2011, 2013a, b, 2014). Bedrock legend as in Figure 3.

For a group of proximal points in a geochemical field having elevated concentrations of an element, the anomaly threshold becomes

$$C_{a(m)} = C \cdot \varepsilon^{3/\sqrt{m}}, \quad (\text{Eq. 6})$$

where  $m = 2, 3, \dots, 9$  is the number of proximal points with concentrations  $C_x \geq C_{a(m)}$ , with  $m \leq 9$  for any number of points within the anomaly contour. The contrast of a geochemical anomaly ( $\gamma$ ) for lognormally distributed elements is the difference between the maximum concentration ( $C_{max}$ ) above background and its statistical noise (Matveev, 2003):

$$\gamma = (1/\log \varepsilon) \cdot \log (C_{max}/C_b). \quad (\text{Eq. 7})$$

## 6.2. Lithochemical dispersion in a drainage system

Because secondary dispersion halos and related dispersion streams have much larger surficial expression than their primary ore deposit sources, they are readily detectable by regional geochemical surveys. Hydrochemical dispersion of elements is generally subordinate relative to mechanical (i.e., lithochemical) dispersion in drainage systems (Matveev, 2003; Solovov, 1985; Solovov et al., 1990). Hence, ignoring the dispersion of metals dissolved in water, ideal lithochemical dispersion in a drainage system can be applied to interpret stream sediment and HMC geochemical surveys. The total volumetric productivity ( $P$ ) or quantity of metal above local

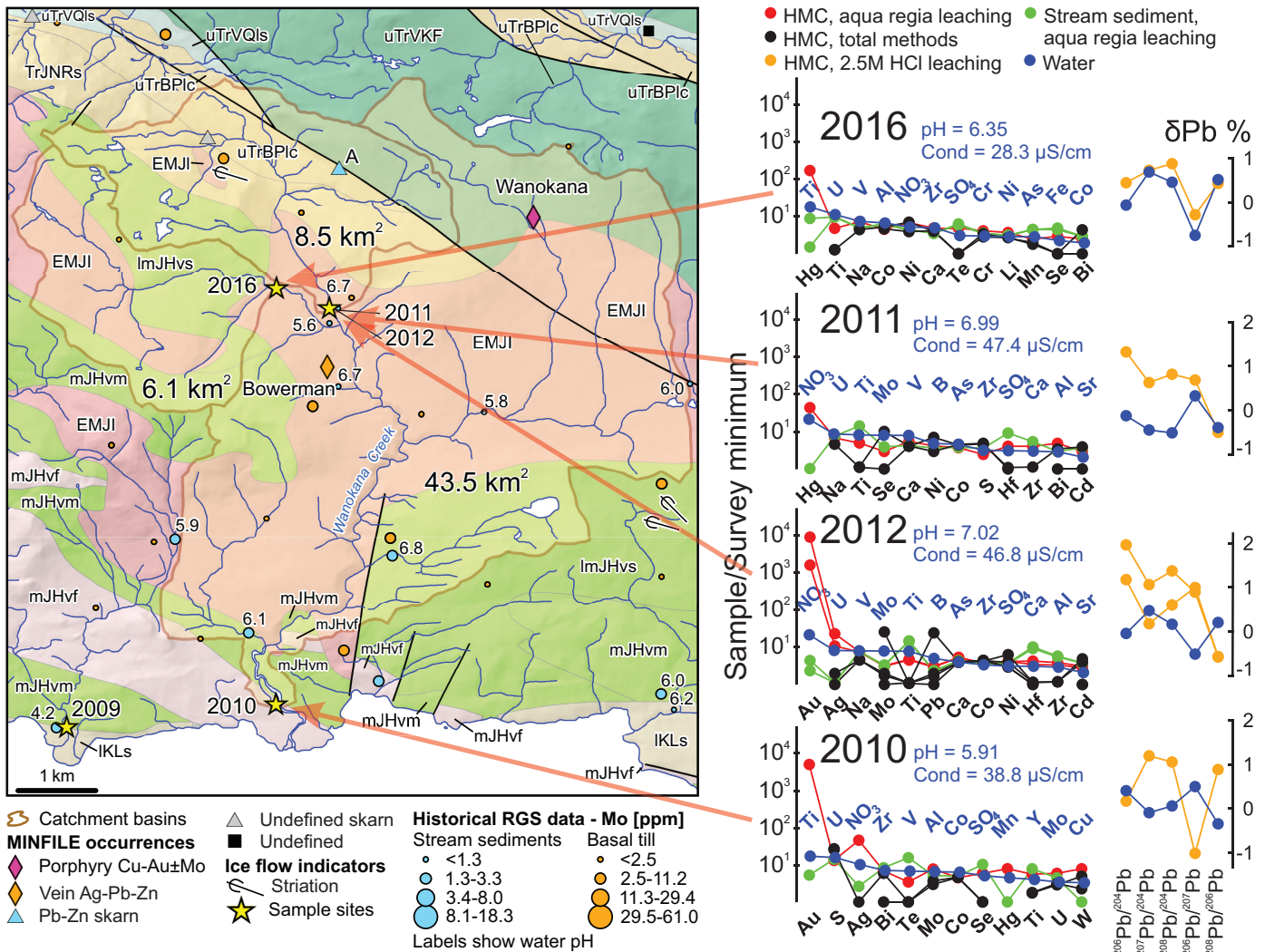


**Fig. 16.** Wanokana Creek basin, northern Vancouver Island, leaders of ranked element contrast relative to survey minimum and  $\delta^{206}\text{Pb}/^{204}\text{Pb}$ ,  $\delta^{207}\text{Pb}/^{204}\text{Pb}$ ,  $\delta^{208}\text{Pb}/^{204}\text{Pb}$ ,  $\delta^{206}\text{Pb}/^{207}\text{Pb}$ , and  $\delta^{208}\text{Pb}/^{206}\text{Pb}$  patterns (in %) for stream sediment, heavy mineral concentrate, and water samples. Water pH, conductivity, and analyte labels shown above patterns.  $\delta\text{Pb}$  (%) values calculated as follows:  $\delta^{20i}\text{Pb}/^{20j}\text{Pb}$  (%) =  $100 \cdot \frac{(^{20i}\text{Pb}/^{20j}\text{Pb})_{\text{sample}} - (^{20i}\text{Pb}/^{20j}\text{Pb})_{\text{galena}}}{(^{20i}\text{Pb}/^{20j}\text{Pb})_{\text{galena}}}$ , where  $(^{20i}\text{Pb}/^{20j}\text{Pb})_{\text{galena}}$  is the Pb isotopic composition of 2.5N HCl leachate of galena-bearing mineralization (sample 19ARU001; MINFILE 092L 061). Ice-flow indicators from Clague et al. (1982), Kerr (1992), Meldrum and Bobrowsky (1994), Bobrowsky et al. (1995), Bobrowsky (1997), and Bobrowsky and Meldrum (1994a, b). Regional geochemical survey (RGS) data after Matysek and Day (1988), Gravel and Matysek (1989), Matysek et al. (1989), Kerr et al. (1992), Bobrowsky and Sibbick (1996), and Jackaman (2011, 2013a, b, 2014). Bedrock legend as in Figure 3.

background (in tonnes of metal) for  $n$  streams draining the secondary dispersion halo of an ore deposit is

$$P = \frac{1}{k'k} \cdot \sum_{i=1}^n [S \cdot (C - C_b)] \cdot \frac{1}{40} \cdot H \quad (\text{Eq. 8})$$

where  $S$  is catchment area of stream basin at the sampling site (in  $\text{m}^2$ ),  $C$  is the anomalous concentration of element in the sample (in wt.%),  $C_b$  is the average local background concentration of an element (in wt.%),  $k' < > 1$  is the local proportionality coefficient between the productivity of the dispersion stream and that of the secondary dispersion halo,  $k < > 1$  is the residual productivity or proportionality coefficient between the quantity of an element in the secondary dispersion halo and that in the

ore body, and  $H$  is the calculation depth or probable depth of an ore zone based on geometric and geochemical resemblance of genetically similar deposits. The divider '40' converts  $\text{m}^2\%$  into tonnes (after Grigoryan et al., 1983; Solovov, 1985; Solovov et al., 1990; Matveev, 2003).

The values of  $k'$  depend on local hydrography and individual properties of elements such as their actual mechanical versus hydrochemical dispersion. The residual productivity ( $k$ ) also depends on individual properties of elements, morphology of an ore deposit, and local geochemical landscape which was defined by B.B. Polynov in 1956 as an area of uniform migration of elements between the lithosphere, hydrosphere, atmosphere, and biosphere (see Solovov, 1985). Generally,  $k$  value changes

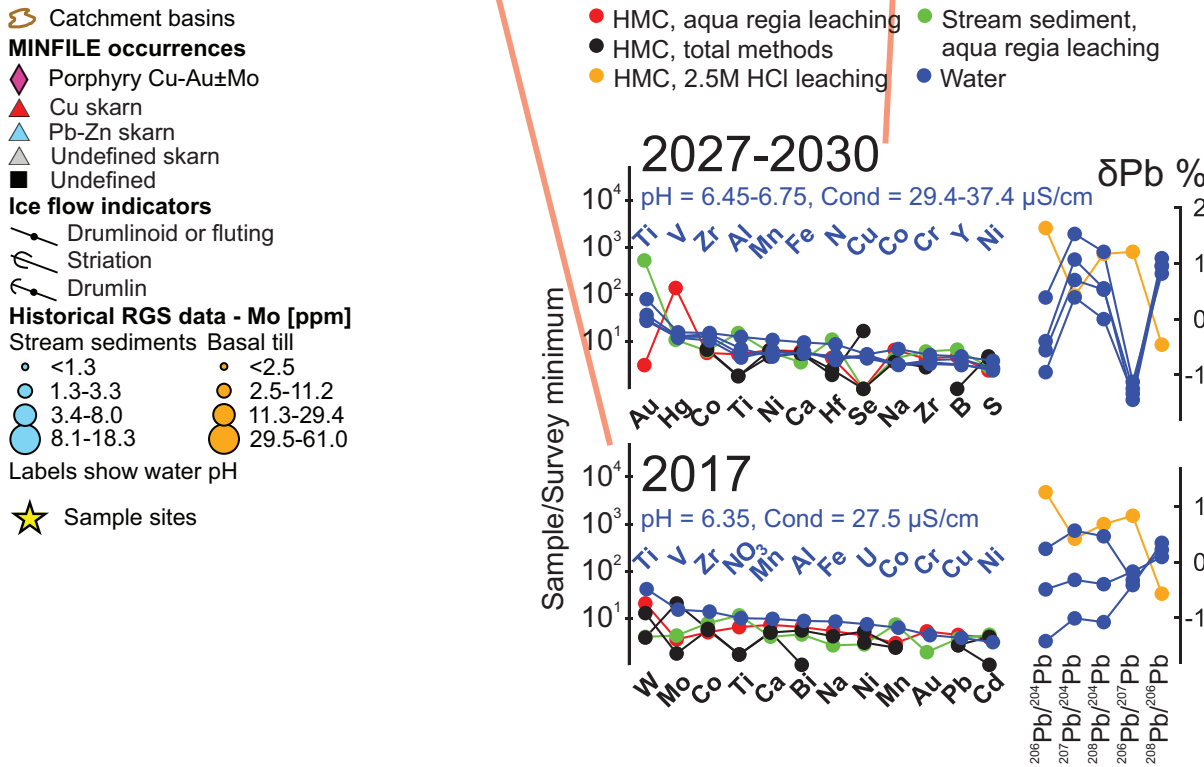
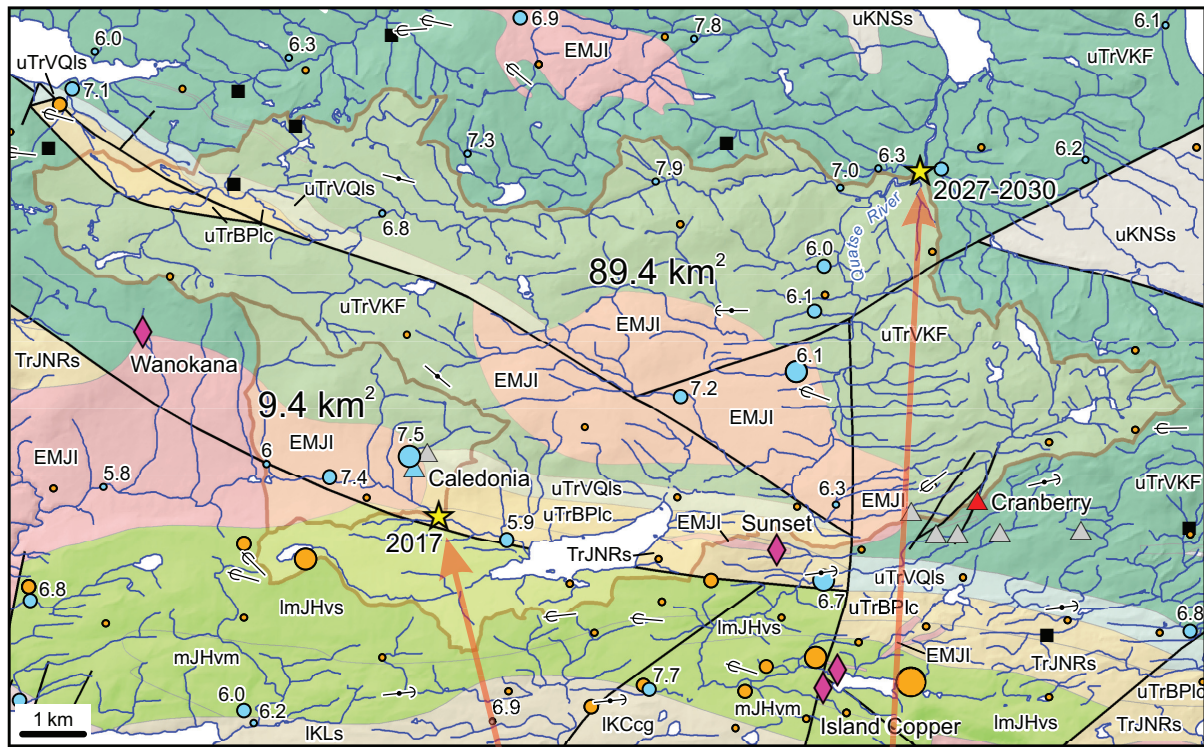


**Fig. 17.** Leaders of ranked element contrast relative to survey minimum and  $\delta^{206}\text{Pb}/^{204}\text{Pb}$ ,  $\delta^{207}\text{Pb}/^{204}\text{Pb}$ ,  $\delta^{208}\text{Pb}/^{204}\text{Pb}$ ,  $\delta^{206}\text{Pb}/^{207}\text{Pb}$ , and  $\delta^{208}\text{Pb}/^{206}\text{Pb}$  patterns (in %) for stream sediment, heavy mineral concentrate, and water samples from Quatse River basin, northern Vancouver Island. Water pH, conductivity, and analyte labels shown above patterns.  $\delta\text{Pb}$  (%) values calculated as follows:  $\delta^{20i}\text{Pb}/^{20j}\text{Pb}$  (%) =  $100 \cdot (\frac{^{20i}\text{Pb}/^{20j}\text{Pb}_{\text{sample}}}{^{20i}\text{Pb}/^{20j}\text{Pb}_{\text{galena}}} - \frac{^{20i}\text{Pb}/^{20j}\text{Pb}_{\text{galena}}}{^{20i}\text{Pb}/^{20j}\text{Pb}_{\text{galena}}})$  where  $^{20i}\text{Pb}/^{20j}\text{Pb}_{\text{galena}}$  is the Pb isotopic composition of 2.5N HCl leachate of galena-bearing mineralization (sample 19ARU001; MINFILE 092L 061). Ice flow indicators from Clague et al. (1982), Kerr (1992), Meldrum and Bobrowsky (1994), Bobrowsky et al. (1995), Bobrowsky (1997), and Bobrowsky and Meldrum (1994a, b). Regional geochemical survey (RGS) data after Matysek and Day (1988), Gravel and Matysek (1989), Matysek et al. (1989), Kerr et al. (1992), Bobrowsky and Sibbick (1996), and Jackaman (2011, 2013a, b, 2014). Bedrock legend as in Figure 3.



**Fig. 18.** Indicator minerals in panned sluice heavy mineral concentrates of alluvium from northern Vancouver Island. **a)** Euhedral magnetite,  $\text{Fe}^{2+}\text{Fe}^{3+}_2\text{O}_4$ , and spessartine,  $(\text{Mn}^{2+}, \text{Fe}^{2+})_3(\text{Al}, \text{Fe}^{3+})_2(\text{SiO}_4)_3$ , at the mouth of Hushamu Creek (sample 2005; 1-2 mm-size fraction). **b)** Almandine fragment,  $(\text{Fe}^{2+}, \text{Mn}^{2+})_3(\text{Al}, \text{Fe}^{3+})_2(\text{SiO}_4)_3$ , and euhedral spessartine near the mouth of Quatse River (sample 2027; 0.5-1.0 mm-size fraction).

with depth due to hypogene enrichment ( $k > 1$ ) or leaching ( $k < 1$ ) of ore elements. Based on numerous geochemical surveys in different geochemical landscapes,  $k$  values for most ore elements are close to unity for actively eroding mountainous areas (Matveev, 2003). For a detailed discussion of the theory and practice of geochemical exploration and quantitative interpretation of real dispersion streams using differential equations, the reader is referred to Grigoryan et al. (1983), Solovov (1985), Solovov et al. (1990), and Matveev (2003).

### 6.3. Prognostic geochemical resources based on dispersion streams

The objective of regional geochemical surveys investigating dispersion streams is to find large deposits with economic mineralization close to present erosional levels. Productivity defined above is a parametric and thus objective measure of

a geochemical anomaly, which is the basis for identifying prospective areas. Panning of alluvium is the oldest prospecting method for placer gold, diamonds, tin, tungsten, and other commodities. Kukanov et al. (1983), Petrenko et al. (1986), and Kaplenkov (2003, 2006, 2008) collected and analyzed panned HMC samples for many elements in eastern Chukotka and identified several prospective areas; their predictions ultimately led to the discovery of large base and precious metal deposits. We adopted a simplified approach for evaluating drainage lithochemical results in terms of volumetric productivity per element, which is calculated for each stream basin based on the data for near-mouth stream sediment and HMC samples. Assuming  $k' = k = 1$  and  $H = 1$  m, equation 8 above for productivity of lithochemical anomaly in a drainage system,  $P$  (in tonnes per 1 m depth), reduces to

$$P = S \cdot (C - C_b) / 40, \quad (\text{Eq. 9})$$

where  $S$  is the catchment area of stream basin at the sampling site (in  $\text{m}^2$ ),  $C$  is the above-background concentration of an element in the stream sediment, moss-mat sediment, or HMC sample (in wt.%), and  $C_b$  is the average background concentration of an element (in wt.%). Because our dataset is limited to a few samples, estimating background values as discussed above is not possible. Hence, background per element was calculated as the average of survey values within the range of 10 times the minimum value (e.g., 1.5-15). Although the background values may differ from those based on strict geochemical field theory, this simple approach is similar to the classical ranking for panning of gold ('nil-trace-counts-weight') proven by centuries of prospecting. Lithochemical dispersion in high-order streams also significantly differs from ideal dispersion stream, which adequately characterizes only first-order basins. In addition, elements concentrated in heavy minerals (e.g., Au, Pt, Sn, W, Zr, Nb, Ta, REE) will have  $k' > 1$ , whereas elements migrating in dispersion stream in solution or a non-mineral form, adsorbed on clays and other colloidal particles (e.g., Cu, Mo, Zn, Pb) will have  $k' < 1$  in HMC samples. Hence, prognostic geochemical figures based on ideal dispersion stream are intended only for evaluating the survey results and identifying the most prospective basins. Prognostic geochemical resources ( $P$ ) could be refined by determining local  $k'$  and  $k$  values for elements of interest, using realistic depth ( $H$ ) based on the expected geometric and geochemical resemblance to a known deposit, and solving the equation of real dispersion stream (Solovov, 1985; Solovov et al., 1990; Matveev, 2003). If the difference between predicted geochemical resources and observed resources in a partially eroded ore deposit is less than three, they are considered satisfactory (Grigoryan et al., 1983). Well-known geochemical zoning of ore systems (Emmons, 1924) also allows estimating the level of erosion for a predicted ore deposit using multiplicative ratios of highly mobile (e.g., Ag-Hg-Sb) to less mobile (e.g., W-Sn-Bi) ore and indicator elements (Grigoryan et al., 1983; Solovov, 1985; Solovov et al., 1990; Matveev, 2003).

Table 1 lists calculated background values and volumetric productivities (in tonnes per 1 m depth) of the main ore and pathfinder elements for each stream basin based on the stream and moss-mat sediment (<0.18 mm fraction) and HMC (<1 mm fraction) geochemistry. HMC results for ‘partial’ values (aqua regia digestion–ICP-ES/MS) and ‘total’ values (fusion–ICP-ES/MS, XRF, and INAA) are given separately. Values for stream and moss-mat sediment samples (bulk sediment) are also ‘partial’. Discrepancies between the sample media and different analytical methods reflect different roles of lithochemical (mechanical) and hydrochemical forms of dispersion for individual elements, different mineralogy, and geochemical landscapes even in the northern Vancouver Island study area. Bulk stream and moss-mat sediment samples (<0.18 mm-size, sieved fraction) confidently detect Cu, Mo, Re, Te, Se, Bi, and In, but generally have poor contrast for heavy metals such as Au, Ag, W, and REE, missing even placer Au at Loss Creek. HMC samples (<1 mm-size, ‘grey’ fraction) greatly enhance the contrast for Mo, Zn, Pb, Au, Ag, W, Sn, Li, Cs, Ge, Be, Y, Sc and REE, with ‘total’ values yielding greater anomaly contrast for elements hosted in refractory minerals.

Manganese-rich garnet is abundant in the HMC samples at Loss Creek (Fig. 7a). The garnet is the main host of Y, Sc, and heavy rare earth elements (HREE), with their productivities ( $n \cdot 10^3$ – $n \cdot 10^4$  tonnes/m) indicating a large deposit of these metals, according to Krasnikov’s classification of mineral deposits by size (Matveev, 2003). Given that placer garnet is readily concentrated from alluvium, it warrants a metallurgical feasibility study as a potential ore for economic recovery of Y, Sc, and HREE. In addition to Sc, Y, and HREE, Loss Creek basin shows significant prognostic resources ranking from middle- to large-size deposits for Au (confirms placer gold occurrence), Mn (3.1 million tonnes/m), Zn, Li, Cr, Ni, W, Ga, Se, Co, Ge, B, and Cd (Table 1).

As noted above, stream-sediment and HMC samples confirm epithermal Au-Ag-Cu and blind porphyry Cu-Mo-Au deposits at Hushamu. HMC samples greatly enhance the anomaly contrast for Au, Ag, Ba, Sn, Tl, Pb, Zn, and V even many km downstream from the deposit at the Hushamu Creek mouth, where stream-sediment samples did not detect anomalous Au and Ag (Table 1). Productivities of Cu, Mo, Re, Te, Se, Bi, and In based on stream-sediment samples are generally consistent with those based on HMC samples, reflecting predominantly mechanical dispersion of these elements in the drainage system. Volumetric productivities per 1 m depth based on stream-sediment and HMC samples generally confirm the 43-101 resources (Indicated + Inferred) of 131 tonnes Au, 179 tonnes Re, 37619 tonnes Mo, and 1.09 million tonnes Cu for the Hushamu deposit (Tahija et al., 2017). As discussed above, the predicted resources may overestimate Au and other heavy metals concentrated in HMC samples and underestimate metals readily soluble in acidic waters such as Cu and Zn. The subdued Cu geochemical anomaly at Hushamu reflects blind hypogene porphyry Cu-Mo-Au mineralization covered by a

thick silica-clay leached cap (Panteleyev and Koyanagi, 1993, 1994; Panteleyev et al., 1995; Tahija et al., 2017). In contrast, the HMC samples confidently detect the epithermal Au-Ag-Cu mineralization and the above-ore primary halo (Ba-Zn-Pb-Sb-Se-Tl) of the deeper porphyry copper system, which generate prominent secondary dispersion in the Hushamu basin. Hence, HMC geochemistry detects even blind porphyry mineralization despite an extensive leached cap and hydrochemical dispersion of metals in highly acidic waters.

Our results also predict significant resources of Ag, Au, Ba, V, Re, Mo, Zn, Pb, Te, Se, Tl, Bi, Sn, In, Zr, and Ga for the Youghpan Creek basin (Table 1). These findings are important because mineral occurrences of these metals are not known in that basin. Prognostic resources for the Wanokana basin confirm known occurrences of porphyry Cu (MINFILE 092L 272), Ag-Pb-Zn±Au vein (MINFILE 092L 131), and Zn-Pb-Cu-Ag±Au skarn (MINFILE 092L 393 and 272) styles of mineralization in that basin. In addition, near-mouth samples predict significant resources of LREE, HREE, Y, Sn, W, Li, and Cs (Table 1). The elevated REE (especially LREE) and Y are accompanied by anomalous (tonnes/m) Mn (38653), Ba (22396), V (20505), Zr (17013), P (14440), Sr (3572), Hf (1227), Nb (497), Ga (301), Ta (42), Th (65), and U (76). An anomalous LREE-Ba-V-Zr-Hf-P-Sr-Nb-Ta-Th-U association suggests carbonatite or alkaline rock-hosted rare-metal mineralization yet to be discovered. This is hardly surprising given the Nb, REE, Y, Zr, Th, U, and fluorite mineralization related to Jurassic to Paleogene peralkaline and carbonatite magmatism in Alaska (e.g., Warner, 1989; Gunter et al., 1993; Thompson, 1997). Nixon et al. (2020) report Late Neogene magmatism (Klaskish Plutonic Suite) associated with porphyry Cu-Mo±Au mineralization immediately south of the Holberg fault on northern Vancouver Island. This young magmatic suite follows along the northeast-trending Brooks Peninsula fault zone, which coincides with the southern limit of Neogene volcanism in the region and marks an extensional regime in the Queen Charlotte basin (Lewis et al., 1997). Hence, the LREE-Ba-V-Zr-Hf-P-Sr-Nb-Ta-Th-U anomaly (Table 1) indicates peralkaline or carbonatite magmatism controlled by major high-angle structures such as Holberg fault and related to the Neogene or older event(s), overprinting the Bonanza magmatic arc on northern Vancouver Island.

The HMC geochemistry from Caledonia Creek indicates significant upstream LREE, Mo, W, Mn, Zr, Ba, Sr, and Hf anomalies. Elevated Pb and Zn also confirm Zn-Pb-Cu skarn mineralization such as the Caledonia developed prospect (MINFILE 092L 061). The geochemistry of a stream-sediment sample near the mouth of Quatse River returned anomalous Au, Ag, Zn, Y, Sc, REE (mainly HREE), Zr, Sr, P, V, Hf, B, and Ga, which indicate rare-metal mineralization in this watershed. However, analysis of the HMC sample at this site does not indicate above-background concentrations of Au, Ag, Zn, and Sc, but shows anomalous Se and W. Both sample media indicate anomalous Cu, Y and REE, reflecting Island Copper

Table 1. Geochemical background and productivity of elements (in tonnes per 1 m depth) in stream basins.

| Element  | Ag    | Au     | Cu  | Mo   | Zn    | Pb  | Co  | Ni   | Re     | Te    | Hg    | Sb   | Se   | Tl    | Bi    | W    | Sn   | In    | Li    | Cs   | Ge   | Be   | Y     | Sc   | ΣHREE | ΣLREE |    |  |  |
|--|-------|--------|-----|------|-------|-----|-----|------|--------|-------|-------|------|------|-------|-------|------|------|-------|-------|------|------|------|-------|------|-------|-------|----|--|--|
| <b>Background (ppm)</b>  |       |        |     |      |       |     |     |      |        |       |       |      |      |       |       |      |      |       |       |      |      |      |       |      |       |       |    |  |  |
| Bulk sediment  | 0.093 | 0.0025 | 43  | 1.3  | 50    | 6.7 | 14  | 18   | 0.0024 | 0.064 | 0.074 | 0.19 | 0.59 | 0.058 | 0.080 | 0.16 | 0.60 | 0.040 | 7.1   | 0.65 | 0.12 | 0.26 | 7.1   | 6.2  | 5.2   | 30    | 30 |  |  |
| HMC 'partial'  | 0.036 | 0.0016 | 38  | 0.85 | 64    | 5.0 | 11  | 20   | 0.0023 | 0.043 | 0.021 | 0.22 | 0.28 | 0.057 | 0.081 | 0.24 | 0.77 | 0.057 | 7.4   | 0.43 | 0.20 | 0.24 | 10    | 7.4  | 7.5   | 30    | 30 |  |  |
| HMC 'total'  | 0.18  | 0.0016 | 41  | 0.85 | 109   | 3.7 | 20  | 38   | 0.025  | 0.37  | NA    | 0.68 | 3.2  | 0.25  | 0.11  | 0.96 | 2.1  | 0.093 | 8.4   | 0.73 | 3.3  | 1.2  | 20    | 47   | 18    | 82    | 82 |  |  |
| <b>Productivity (tonnes/m)</b>   |       |        |     |      |       |     |     |      |        |       |       |      |      |       |       |      |      |       |       |      |      |      |       |      |       |       |    |  |  |
| <i>Loss Creek, near mouth (sample sites 1002 and 1007); catchment area = 68.0 km<sup>2</sup></i> |       |        |     |      |       |     |     |      |        |       |       |      |      |       |       |      |      |       |       |      |      |      |       |      |       |       |    |  |  |
| Bulk sediment  |       |        |     |      |       |     |     | 2740 |        |       |       |      | 9    | 2     | 41    |      |      |       | 1529  | 81   |      |      |       |      |       |       |    |  |  |
| HMC 'partial'  | 85    | 1025   |     |      | 974   | 951 |     |      |        |       | 1336  |      |      |       |       | 34   |      |       | 500   |      | 34   |      | 8549  | 678  | 4369  |       |    |  |  |
| HMC 'total'  | 78    | 833    | 181 | 8    | 28724 | 621 | 871 | 2182 | 1      | NA    | 1532  |      |      |       |       | 2568 | 99   |       | 14377 |      | 753  | 57   | 86132 | 5553 | 41516 | 2873  |    |  |  |
| <i>Hushamu Creek</i>   |       |        |     |      |       |     |     |      |        |       |       |      |      |       |       |      |      |       |       |      |      |      |       |      |       |       |    |  |  |
| <i>Headwater (sample site 2007); catchment area = 3.82 km<sup>2</sup></i>                        |       |        |     |      |       |     |     |      |        |       |       |      |      |       |       |      |      |       |       |      |      |      |       |      |       |       |    |  |  |
| Bulk sediment  | 0.2   | 0.7    | 430 | 61   | 119   |     |     | 0.1  | 4      | 0.1   | 0.1   | 69   | 0.3  | 9     |       |      | 6    | 1     |       |      |      |      | 40    |      | 40    | 102   |    |  |  |
| HMC 'partial'  |       | 0.1    | 144 | 65   | 87    |     |     | 0.1  | 4      |       | 0.2   | 48   | 0.6  | 10    |       |      | 9    | 1     |       |      |      |      |       |      |       |       |    |  |  |
| HMC 'total'  | 0.2   | NA     | 147 | 65   | 213   |     |     | 2    | NA     | 1     | 120   | 7    | 10   |       |       |      | 75   | 2     | 6     |      |      | 14   |       | 6    | 6     | 15    |    |  |  |
| <i>Middle course (sample site 2006); catchment area = 12.2 km<sup>2</sup></i>                    |       |        |     |      |       |     |     |      |        |       |       |      |      |       |       |      |      |       |       |      |      |      |       |      |       |       |    |  |  |
| Bulk sediment  | 4     | 0.2    | 131 | 109  | 19    | 129 |     | 0.4  | 28     | 0.1   | 6     | 333  | 1    | 17    |       |      | 9    | 1     |       |      |      |      |       |      |       |       |    |  |  |
| HMC 'partial'  | 3     | 2      | 224 | 149  | 270   | 182 | 52  | 0.3  | 34     | 9     | 10    | 278  | 1    | 47    |       |      | 7    | 1     |       |      |      |      |       |      |       |       |    |  |  |
| HMC 'total'  | 0.8   | NA     | 130 | 159  | 733   | 214 |     | 0.3  | 25     | NA    | 16    | 40   | 2    | 49    |       |      | 35   | 1     | 17    | 27   |      | 5    |       | 7    |       |       |    |  |  |
| <i>Near mouth (sample site 2005); catchment area = 20.5 km<sup>2</sup></i>                       |       |        |     |      |       |     |     |      |        |       |       |      |      |       |       |      |      |       |       |      |      |      |       |      |       |       |    |  |  |
| Bulk sediment  | 3     | 0.1    | 428 | 129  | 99    |     |     | 0.2  | 24     | 0.2   | 3     | 316  | 0.1  | 17    |       |      | 8    | 0.8   |       |      |      | 1    | 51    | 12   | 27    |       |    |  |  |
| HMC 'partial'  | 24    | 315    | 325 | 161  | 1146  | 180 |     | 0.3  | 18     | 1     | 4     | 190  | 0.1  | 18    |       |      | 4    | 0.2   |       |      |      | 6    |       |      | 2     | 60    |    |  |  |
| HMC 'total'  | NA    | 304    | 151 | 677  | 247   |     |     | 0.2  | 12     | NA    | 6     | 569  | 8    | 16    |       |      | 23   | 0.3   | 6     |      |      | 31   |       | 35   | 2     |       |    |  |  |
| <i>Tributary (sample site 2008); catchment area = 1.86 km<sup>2</sup></i>                        |       |        |     |      |       |     |     |      |        |       |       |      |      |       |       |      |      |       |       |      |      |      |       |      |       |       |    |  |  |
| Bulk sediment  |       |        | 3   |      |       |     |     |      | 0.4    | 0.2   |       | 9    | 0.1  | 0.3   |       |      |      |       | 7     | 1    |      | 0.2  | 0.3   |      | 2     | 23    |    |  |  |
| HMC 'partial'  |       |        | 4   | 40   | 8     |     |     | 0.5  |        |       | 3     |      | 0.5  |       |       |      |      |       | 25    | 2    |      | 0.8  |       |      |       |       |    |  |  |
| HMC 'total'  | NA    |        | 29  | 236  | 5     |     |     | NA   | 15     | 0.7   | 0.3   | 0.1  |      |       |       |      |      | 26    | 4     |      |      |      |       |      |       |       |    |  |  |

Table 1. Continued.

| Element   | Ag   | Au  | Cu   | Mo    | Zn   | Pb  | Co   | Ni   | Re  | Te  | Hg | Sb   | Se  | Tl  | Bi  | W   | Sn  | In  | Li  | Cs | Ge | Be  | Y   | Sc  | $\Sigma$ HREE | $\Sigma$ LREE |     |     |
|---|------|-----|------|-------|------|-----|------|------|-----|-----|----|------|-----|-----|-----|-----|-----|-----|-----|----|----|-----|-----|-----|---------------|---------------|-----|-----|
| <b><i>Youghpan Creek, near mouth (sample site 2009); catchment area = 25.0 km<sup>2</sup></i></b> |      |     |      |       |      |     |      |      |     |     |    |      |     |     |     |     |     |     |     |    |    |     |     |     |               |               |     |     |
| Bulk sediment   |      |     | 89   |       | 18   |     |      |      | 0.7 | 22  | 4  | 263  | 12  | 16  |     |     | 6   | 0.6 |     |    |    |     |     | 41  | 8             |               | 91  |     |
| HMC 'partial'   | 31   | 558 |      | 142   | 6716 | 211 | 25   |      | 0.5 | 19  | 9  | 170  | 8   | 32  |     |     | 2   | 2   |     |    |    |     | 23  |     |               |               | 20  |     |
| HMC 'total'   | NA   | NA  | 197  | 17231 | 314  |     |      | 0.3  | 27  | NA  | 20 | 219  | 9   | 30  |     |     | 51  | 0.4 |     |    |    | 2   |     |     | 0.6           |               |     |     |
| <b><i>Wanokana Creek</i></b>  |      |     |      |       |      |     |      |      |     |     |    |      |     |     |     |     |     |     |     |    |    |     |     |     |               |               |     |     |
| <b><i>Headwater (sample sites 2011 and 2012); catchment area = 8.47 km<sup>2</sup></i></b>        |      |     |      |       |      |     |      |      |     |     |    |      |     |     |     |     |     |     |     |    |    |     |     |     |               |               |     |     |
| Bulk sediment   | 1    |     | 5    | 158   |      |     | 34   |      | 0.1 | 5   |    |      |     |     |     |     |     |     |     |    | 2  | 2   | 32  | 5   | 13            |               | 79  |     |
| HMC 'partial'   | 3    | 34  |      | 7     | 36   |     | 25   | 46   | 6   |     |    | 0.6  |     |     |     |     |     |     | 1   |    |    |     |     |     | 2             |               | 36  |     |
| HMC 'total'   | NA   | NA  | 90   | 60    | 48   |     |      | NA   | NA  | 33  |    |      |     |     |     |     |     |     | 3   |    |    |     |     |     |               |               | 0.5 |     |
| <b><i>Near mouth (sample site 2010); catchment area = 43.5 km<sup>2</sup></i></b>                 |      |     |      |       |      |     |      |      |     |     |    |      |     |     |     |     |     |     |     |    |    |     |     |     |               |               |     |     |
| Bulk sediment   | 4    | 0.2 | 134  |       |      | 202 |      | 0.2  | 28  |     |    | 164  | 10  |     |     |     |     |     | 10  |    |    | 16  | 109 |     | 55            |               | 455 |     |
| HMC 'partial'   | 69   | 239 |      | 232   |      | 403 |      | 0.1  | 3   | 13  | 34 | 6    | 61  | 68  |     |     |     |     | 13  |    | 7  | 380 |     | 310 |               | 2825          |     |     |
| HMC 'total'   | NA   | NA  | 234  | 1707  | 13   |     |      | NA   | NA  | 24  |    | 14   | 118 | 155 | 0.7 | 171 | 27  |     | 4   |    | 4  | 602 |     | 167 |               | 2969          |     |     |
| <b><i>Tributary (sample site 2016); catchment area = 6.10 km<sup>2</sup></i></b>                  |      |     |      |       |      |     |      |      |     |     |    |      |     |     |     |     |     |     |     |    |    |     |     |     |               |               |     |     |
| Bulk sediment   |      |     | 5    |       | 93   | 89  |      | 1    | 5   | 6   |    |      |     |     |     |     | 11  | 2   |     |    |    |     | 0.7 |     |               |               |     |     |
| HMC 'partial'   |      |     | 5    |       | 60   | 247 |      | 1    | 50  | 0.3 |    |      |     |     |     |     | 48  | 3   |     |    |    | 0.9 |     | 0.1 |               |               | 80  |     |
| HMC 'total'   | NA   | NA  | 7    | 125   | 10   | 2   | 175  | NA   | NA  | 6   |    |      |     |     | 1   |     | 0.1 | 39  | 2   |    |    |     |     |     |               |               | 14  |     |
| <b><i>Caledonia Creek (sample site 2017); catchment area = 9.35 km<sup>2</sup></i></b>            |      |     |      |       |      |     |      |      |     |     |    |      |     |     |     |     |     |     |     |    |    |     |     |     |               |               |     |     |
| Bulk sediment   | 0.34 |     | 17   | 323   | 32   | 254 |      |      | 0.2 | 0.3 |    | 0.2  | 6   | 2   |     |     |     |     | 0.3 |    |    | 1   |     |     |               |               |     |     |
| HMC 'partial'   |      |     | 11   | 177   | 5    | 122 | 51   | 0.5  |     |     | 1  | 44   | 0.7 | 1   |     |     |     |     |     |    |    | 1   |     |     | 0.8           |               |     | 94  |
| HMC 'total'   | NA   | NA  | 242  | 192   | 32   | 68  |      | NA   | NA  | 8   |    | 3    | 85  | 0.2 |     |     |     |     |     |    |    |     |     |     |               |               |     | 390 |
| <b><i>Quatse River, near mouth (sample site 2027); catchment area = 89.4 km<sup>2</sup></i></b>   |      |     |      |       |      |     |      |      |     |     |    |      |     |     |     |     |     |     |     |    |    |     |     |     |               |               |     |     |
| Bulk sediment   | 10   | 104 | 5838 |       | 2150 |     | 1532 | 3312 |     | 166 | 60 |      |     |     |     |     |     |     |     |    |    |     |     | 293 | 659           | 146           |     | 97  |
| HMC 'partial'   |      |     | 6428 |       |      |     | 1834 | 3418 |     | 595 | 13 |      |     |     |     | 81  |     |     |     |    |    |     |     |     |               | 125           | 43  | 71  |
| HMC 'total'   | NA   | NA  | 5013 | 11    |      |     | 1803 | 3241 |     | NA  | 94 | 2438 |     |     | 87  |     | 2   |     |     |    |    |     | 199 |     | 76            |               |     | 60  |

**Table 1.** Continued.

Notes: Bulk sediment is <0.18 mm-size, sieved fraction of bulk stream and moss mat-sediment; HMC is heavy mineral concentrate (<1 mm-size, sieved fraction) recovered from <2 mm-size fraction of bulk alluvium (11-16 kg). 'Partial' values based on aqua regia digestion - inductively coupled plasma emission spectrometry (ICP-ES) combined with inductively coupled plasma mass spectrometry (ICP-MS); 'total' values based on lithium borate and sodium peroxide fusion - ICP-ES/MS combined with X-ray fluorescence, and thermal instrumental neutron activation analysis (INAA).  $\sum\text{HREE} = \text{Gd} + \text{Tb} + \text{Dy} + \text{Ho} + \text{Er} + \text{Tm} + \text{Yb} + \text{Lu}$ ;  $\sum\text{LREE} = \text{La} + \text{Ce} + \text{Pr} + \text{Nd} + \text{Sm} + \text{Eu}$ . Background is the average of concentration values within the range of 10 times the minimum concentration value per element.

The above-background productivity of element dispersion in a stream system, P (in tonnes per 1 m depth), is calculated as  $P = S(C - C_b)/40$ , where S is catchment area at sampling site (in m<sup>2</sup>), C is concentration of element above local background value in sample (in wt%), C<sub>b</sub> is the local background concentration of element as defined above (in wt%). Divider 40 converts m<sup>2</sup>% into tonnes (after Grigoryan et al., 1983; Solovov, 1985; Solovov et al., 1990; Matveev, 2003). See discussion in text for details.

'NA' = not analyzed; blank values indicate background level concentration of element.

In addition, HMC samples at Loss Creek yield (tonnes/m): 306653 Mn, 38542 Cr, 1640 Ga, 661 B, 613 Cd, 594 Nb, 235 Hf, 207 Th, and 76 Ta, plus 3511 Ba based on bulk sediment analyses. HMC samples at Hushamu Creek yield up to (tonnes/m): 22350 Ba, 4964 V, 4584 Zr, 4050 P, 3063 Mn, 1055 Sr, 408 Hf, 228 B, 35 Nb, 24 Ga, and 13 U; bulk sediments have mostly blank or much lower values for these elements. HMC sample at Youghpan Creek yields (tonnes/m): 329965 Ba, 25339 Mn, 29366 V, 8299 P, 5928 Sr, 5528 Zr, 651 Hf, 117 Ga, and 10 U; bulk sediment sample has much lower values for Ba, Sr, Zr, Hf, and P, and blank for others. HMC samples at Wanokana Creek yield up to (tonnes/m): 38653 Mn, 22396 Ba, 20505 V, 19394 P, 17013 Zr, 3572 Sr, 1227 Hf, 497 Nb, 301 Ga, 76 U, 65 Th, 42 Ta, and 1.8 Cd; bulk sediment samples indicate up to (tonnes/m): 125 Th, 3.4 Cd, and 8.6 B, but much lower or blank values for others. HMC sample at Caledonia Creek yields (tonnes/m): 13334 Mn, 4545 Zr, 1857 Ba, 1364 Sr, 274 Hf, 30 Ga, 22 Nb, 10 B, and 2 Cd; bulk sediment sample yields (tonnes/m): 17195 Mn, 85 V, 34 Ga, 5 Cd, but much lower or blank values for others. HMC sample at Quatse River yields (tonnes/m): 68716 Zr, 19745 Sr, 18501 P, 13488 V, 2868 Hf, 546 B, 238 Ga, 12 Cd; bulk sediment sample yields (tonnes/m): 42828 Mn, 3143 Cr, 1132 B, but much lower or blank values for others.

suite porphyry Cu-Mo occurrences (Perelló et al., 1995) and perhaps garnet as a source of elevated HREE-Y-Sc in the catchment of Quatse River.

#### 6.4. Hydrochemical dispersion

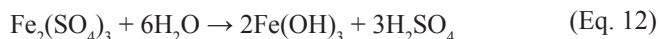
Stream waters draining altered volcanic rocks of the Bonanza Group hosting epithermal Au-Ag-Cu mineralization on northern Vancouver Island exemplify natural acid drainage with pH as low as 2.0, conductivity up to 2400  $\mu\text{S}/\text{cm}$ , TDS up to 1190 mg/L, and  $\text{SO}_4^{2-}$  up to 1300 mg/L (Koyanagi and Panteleyev, 1993, 1994; Sibbick and Laurus, 1995a; Panteleyev et al., 1996b). Waters draining massive sulphide deposits elsewhere have pH values as low as 1.0 and  $\text{SO}_4^{2-}$  concentration up to 123 g/L (Matveev, 2003). Sulphide minerals are unstable in the hypergene environment and readily oxidize. Free sulphuric acid is generated by the oxidation of pyrite, which is the most common sulphide mineral in the altered rocks (Panteleyev and Koyanagi, 1993, 1994; Panteleyev et al., 1995; Tahija et al., 2017)



In the presence of free oxygen, ferrous iron sulphate is unstable and oxidizes to ferric iron sulphate according to



Hydrolysis of  $\text{Fe}_2(\text{SO}_4)_3$  in weakly acidic waters liberates sulphuric acid



Ferric iron hydroxide precipitates from solution and forms stable limonite  $\text{Fe}_2\text{O}_3 \cdot n\text{H}_2\text{O}$  (Fig. 19). Both ferric iron sulphate  $\text{Fe}_2(\text{SO}_4)_3$  and sulphuric acid oxidize and facilitate dissolution of other sulphides, the oxidation of which in turn generates sulphuric acid (Matveev, 2003). Cation-deficient, altered volcanic rocks cannot neutralize acidic waters, which results in natural  $\text{H}_2\text{SO}_4$  drainage at Hushamu. Sulphates of ore metals formed by oxidation of hypogene sulphides are soluble in acidic waters, which favour hydrochemical dispersion of most metals, including Fe, Al, Cu, Zn, Cd, Ni, Fe, Mn, and Pb. However, most metals precipitate from solution as hydroxides at a pH of about 5.5 (Grigoryan et al., 1983; Solovov, 1990).

The solubility of iron in the presence of  $\text{Cu}^{2+}$  (0.005-0.011 mg/L) is a function of dissolved oxygen activity at different pH, such as for waters of the Hushamu and Youghpan creeks (Fig. 20). Precipitation of  $\text{Fe}^{2+}$  and  $\text{Cu}^{2+}$  cations begins in weakly acidic waters forming  $\text{CuFeO}_2$ , which is predominant in neutral water. A plot of the copper-iron-sulphur system versus pH and dissolved oxygen activity for waters from Hushamu and Youghpan creeks (Fig. 21) provides further insight into hypergene processes and mineralogy of the secondary dispersal halo at Hushamu. Assuming oxygen activity constrained by  $\text{SO}_4^{2-}/\text{HS}^-$  equilibrium, these waters are in equilibrium with



**Fig. 19.** Brown limonite ( $\text{Fe}_2\text{O}_3 \cdot n\text{H}_2\text{O}$ ) precipitate in highly acidic Hushamu Creek, which drains an epithermal Au-Ag-Cu and a blind porphyry Cu-Mo-Au system.

covellite, chalcocite, bornite, elemental sulphur,  $\text{Fe}^{2+}$  and  $\text{SO}_4^{2-}$  ions at pH values between 3.8 and 5.9. The observed mineralogy of the clay-quartz leached cap and oxidation zone of hypogene ore at Hushamu (Panteleyev, 1992; Panteleyev and Koyanagi, 1993, 1994; Panteleyev et al., 1995; Tahija et al., 2017) confirms the equilibrium assemblage modelled here based on the stream water chemistry.

In contrast, weakly acidic to neutral waters of Loss, Wanokana, and Caledonia creeks and Quatse River are less favourable for hydrochemical dispersion of most elements. Metals form soluble bicarbonates and complexes with organic acids in such waters. Most metals precipitate as hydroxides, carbonate minerals and other salts from neutral and alkaline waters, except for anion-forming Si, Al, Ge, As, V, U, and Mo, and carbonate complexes of Cu, Sc, Y, and Zr, which are soluble in these waters (Grigoryan et al., 1983; Solovov, 1990).

#### 6.5. Lead isotopes as tracers of dispersion in streams

Unlike concentrations of elements, Pb isotopic ratios fingerprint distinct sources making them more efficient tracers of ore fluids and dispersion processes. The application of Pb isotopes in surficial sediments is a well-established method in mineral exploration (e.g., Gulson, 1986; Bell and Franklin, 1993; Bell and Murton, 1995; Simonetti et al., 1996; Hussein et al., 2003; Rukhlov and Ferbey, 2015). Rukhlov and Ferbey (2015) first tested a simplified method of using Pb isotopic ratios measured by ICP-MS in the 2.5N HCl leachate of the <0.063 mm fraction of till samples for mineral exploration of Jurassic VMS deposits in the Canadian Cordillera. The method is based on the Pb isotopic contrast generated between a Pb-rich, U-Th-poor ore (e.g., galena having Th/Pb and U/Pb  $\sim 0$ ) and Pb-poor, U-Th-rich host rocks (e.g., intermediate-felsic rocks having high Th/Pb and U/Pb) due to the in situ decay of U and Th isotopes, thereby increasing the  $^{206}\text{Pb}/^{204}\text{Pb}$ ,  $^{207}\text{Pb}/^{204}\text{Pb}$  and  $^{208}\text{Pb}/^{204}\text{Pb}$  with time in the country rocks but not

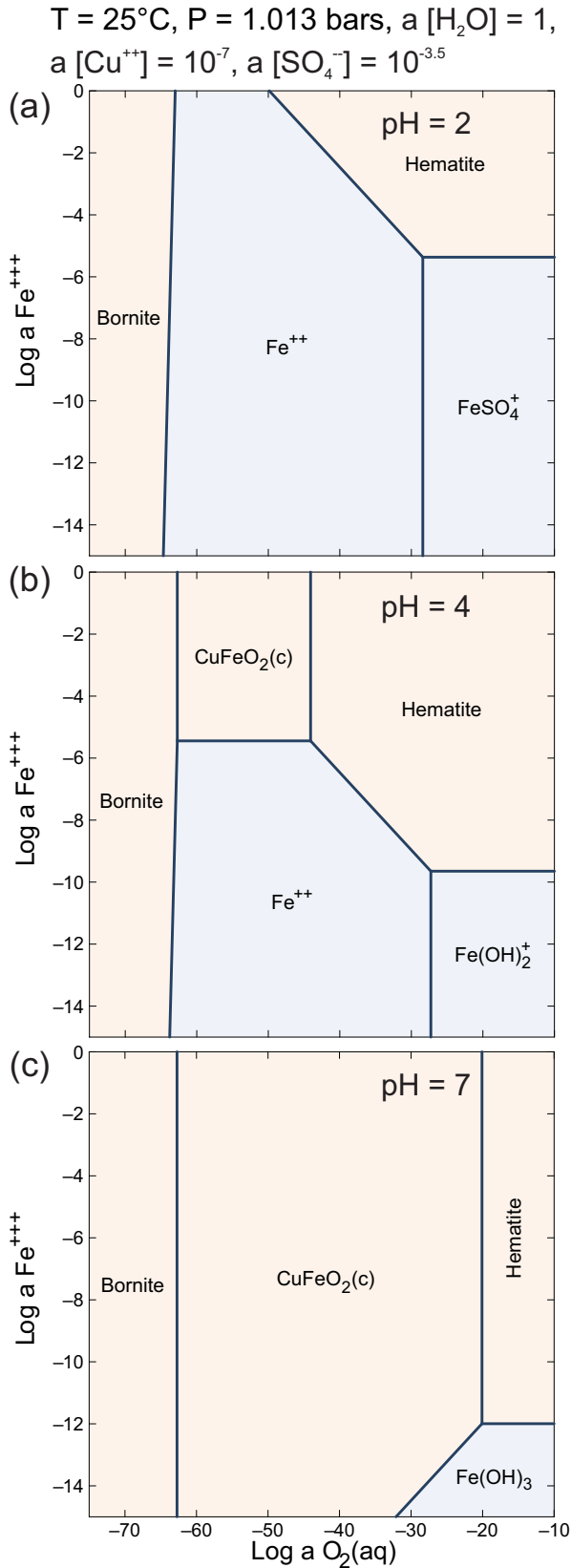


**Fig. 20.** Solubility of Fe<sup>3+</sup> and mineral stability fields versus Log a O<sub>2</sub>(aq) for water from Hushamu and Youghpan creeks at T = 25°C, P = 1.013 bars, a [Cu<sup>2+</sup>] = 10<sup>-7</sup>, a [H<sub>2</sub>O] = 1, a [SO<sub>4</sub><sup>2-</sup>] = 10<sup>-3.5</sup>, and fixed pH: (a) pH = 2; (b) pH = 4; and (c) pH = 7.

in the ore. The isotopic contrast could also be a primary feature of mineralization. The weak acid extraction targeting labile Pb, as opposed to the total digestion of sample, enhances the isotopic contrast. Mixing between the isotopically distinct end members such as the unradiogenic Pb in ore and the radiogenic Pb in host rock occurs during lithochemical (mechanical), hydrochemical, and biochemical dispersion and is the basis for using Pb isotopes in mineral exploration.

Lead isotopic compositions of stream waters and 2.5N HCl leachates of stream and moss-mat sediment (<0.18 mm fraction), HMC (<1 mm fraction), and mineralized rock samples from Vancouver Island along with tills and a VMS ore from Rukhlov and Ferbey (2015), and Vancouver Island galenas from Godwin et al. (1988) form a linear array on <sup>206</sup>Pb/<sup>207</sup>Pb vs. <sup>208</sup>Pb/<sup>206</sup>Pb diagram (Fig. 22). The array also extends a linear trend defined by the analyses of honey from Vancouver area and environs, which have higher <sup>208</sup>Pb/<sup>206</sup>Pb and lower <sup>206</sup>Pb/<sup>207</sup>Pb values (Smith et al., 2019). Analyzed for the first time, stream waters show a wide range of Pb isotopic compositions and overlap that of stream sediments, HMCs, and the ores. The hyperbolic trends defined by tills, VMS ore, and country rock on the Pb concentration versus Pb isotopic ratio diagrams reflect mechanical mixing between the isotopically distinct VMS ore and country rocks during glacial dispersion (Figs. 22c and d; Rukhlov and Ferbey, 2015). Most of the data from this study also follow the same mixing trend. Stream waters and honey have much lower Pb contents and plot outside of the mixing trend (note the logarithmic scale for x-axis in Figs. 22c and d).

We recast Pb isotopic ratios as δ values (in %) relative to a local ore isotopic composition, which in the case of a Pb-rich ore will have the minimum <sup>206</sup>Pb/<sup>204</sup>Pb, <sup>207</sup>Pb/<sup>204</sup>Pb, and <sup>208</sup>Pb/<sup>204</sup>Pb ratios:

$$\text{(Eq. 13)}$$

$$\delta^{20i\text{Pb}/20j\text{Pb}} (\%) = 10^2 \cdot \frac{(20i\text{Pb}/20j\text{Pb})_{\text{sample}} - 20i\text{Pb}/20j\text{Pb}_{\text{ore}}}{20i\text{Pb}/20j\text{Pb}_{\text{ore}}}$$

where <sup>20i</sup>Pb/<sup>20j</sup>Pb<sub>sample</sub> is Pb isotopic ratio in sample, and <sup>20i</sup>Pb/<sup>20j</sup>Pb<sub>ore</sub> is the Pb isotopic ratio of galena-bearing ore at Caledonia developed prospect (MINFILE 092L 061). Hence, the Pb isotopic composition of a sample that is identical to the reference ore translates into a δPb (%) value of zero. Samples having less radiogenic Pb isotopic compositions will have negative δPb (%) values, and those with more radiogenic Pb ratios such as country rocks will have positive δPb (%) values. A simple linear plot of δPb (%) values calculated for <sup>206</sup>Pb/<sup>204</sup>Pb, <sup>207</sup>Pb/<sup>204</sup>Pb, <sup>208</sup>Pb/<sup>204</sup>Pb, <sup>206</sup>Pb/<sup>207</sup>Pb, and <sup>208</sup>Pb/<sup>206</sup>Pb ratios thus defines the Pb isotopic signature of a sample, which fingerprints mixing between the isotopically distinct end members such as Pb-rich ore and country rocks. As discussed above, both lithochemical and hydrochemical dispersion streams from porphyry Cu-Mo±Au and epithermal Au-Ag-Cu deposits in Hushamu and Youghpan creek basins have distinct δPb (%) isotopic signatures close to zero, which approximates the Pb isotopic composition of Caledonia Zn-Pb-Cu-Ag skarn (MINFILE 092L 061). Our results demonstrate the efficiency

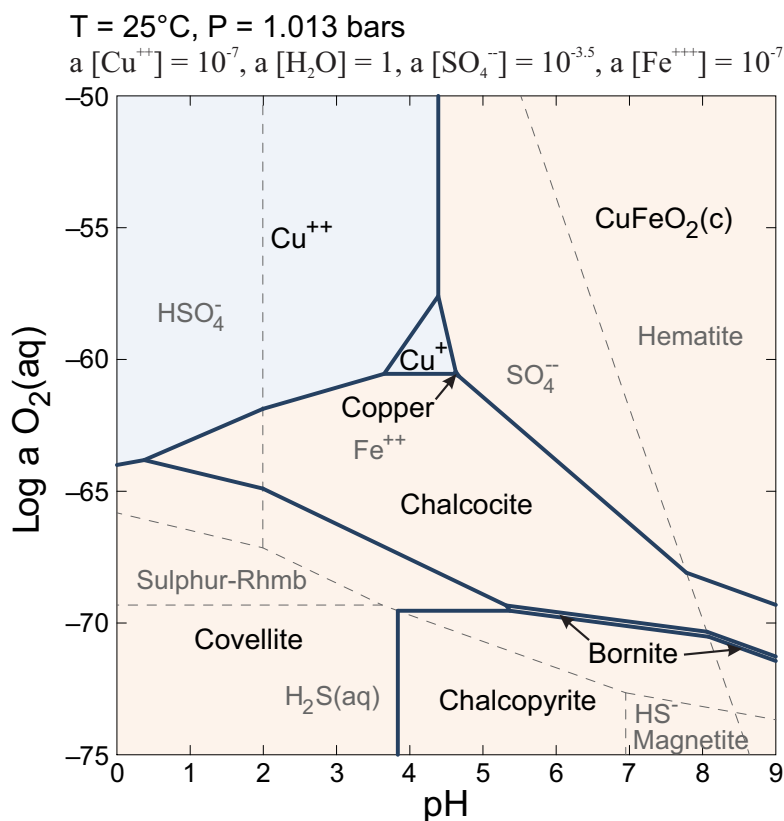


**Fig. 21.** Copper-iron-sulphur system versus pH and Log  $a_{\text{O}_2(\text{aq})}$  for water from Hushamu and Youghpan creeks at  $T = 25^\circ\text{C}$ ,  $P = 1.013$  bars,  $a[\text{Cu}^{2+}] = 10^{-7}$ ,  $a[\text{H}_2\text{O}] = 1$ ,  $a[\text{SO}_4^{2-}] = 10^{-3.5}$ , and  $a[\text{Fe}^{3+}] = 10^{-7}$ . Broken lines are boundaries for iron and sulphur species:  $\text{Fe}^{2+}$ , magnetite ( $\text{Fe}^{2+}\text{Fe}_2^{3+}\text{O}_4$ ), hematite ( $\text{Fe}_2\text{O}_3$ ),  $\text{HSO}_4^-$ ,  $\text{SO}_4^{2-}$ , elemental sulphur (sulphur-rhmb),  $\text{H}_2\text{S}(\text{aq})$ , and  $\text{HS}^-$ .

of Pb isotopic tracing in mineral exploration and environmental applications (e.g., Smith et al., 2019). Affordable HR-ICP-MS analysis of stream waters and 2.5N HCl leachates of sediments and rocks provides enough precision to resolve the natural Pb isotopic variability.

## 7. Conclusions

We have tested stream water, stream and moss-captured sediment, and alluvial HMC samples collected from several drainages on Vancouver Island and analyzed by different methods for a wide range of elements and Pb isotopic compositions. Panned sluice HMC samples (<1 mm-size, 'grey' fraction) of bulk alluvium greatly enhanced the geochemical anomaly contrast, even at mouth of high-order streams, many km downstream from known mineralization. In contrast, less representative, low-volume, bulk stream and moss-captured sediment samples (<0.18 mm fraction) commonly failed to detect even proximal mineralization. Water chemistry provides important information on hydrochemical dispersion of elements in the streams and constrains equilibrium ore mineral assemblages. Lead isotopic ratios in stream water and 2.5N HCl leachates of bedload sediments and HMC measured by inexpensive ICP-MS are sufficiently precise to fingerprint isotopically distinct end-members such as Pb-bearing ore, country rocks, and anthropogenic pollution in the dispersion

system. Quantified geochemical resources based on dispersion streams in terms of volumetric productivity (in tonnes per 1 m depth) are parametric and thus an objective measure of the geochemical anomaly.

We propose a three-fold drainage geochemical survey program that consists of reconnaissance, exploration, and detailed stages. The objective of the reconnaissance stage is to identify prospective areas based on collecting one near-mouth HMC sample (200-400 g) per stream (3<sup>rd</sup> or higher order) at 1:200,000 to 1:500,000 scale. 'Grey' HMC samples, recovered by panning or sluicing 10-20 kg of the <2 mm fraction of bulk alluvium in the field, should retain sulphides and other indicator minerals such as garnet as opposed to hard-panned 'black sand' with a specific gravity >5 g/cm<sup>3</sup>. HMC samples must be analyzed for as many elements as possible and with the lowest minimum detection limits per analyte to recognize subtle geochemical anomalies and non-traditional types of economic deposits. Ranking analytical results normalized to minimum values per element reveals contrast leaders of a dispersion stream, which identify the type of ore deposit in the catchment basin. Multiplicative ratios of highly mobile (e.g., Ag-Hg-Sb) to less mobile (e.g., W-Sn-Bi) ore and indicator elements indicate level of erosion for the predicted ore system. Mineralogical analysis of anomalous HMC samples not only identifies commodities such as gold, diamonds, and other

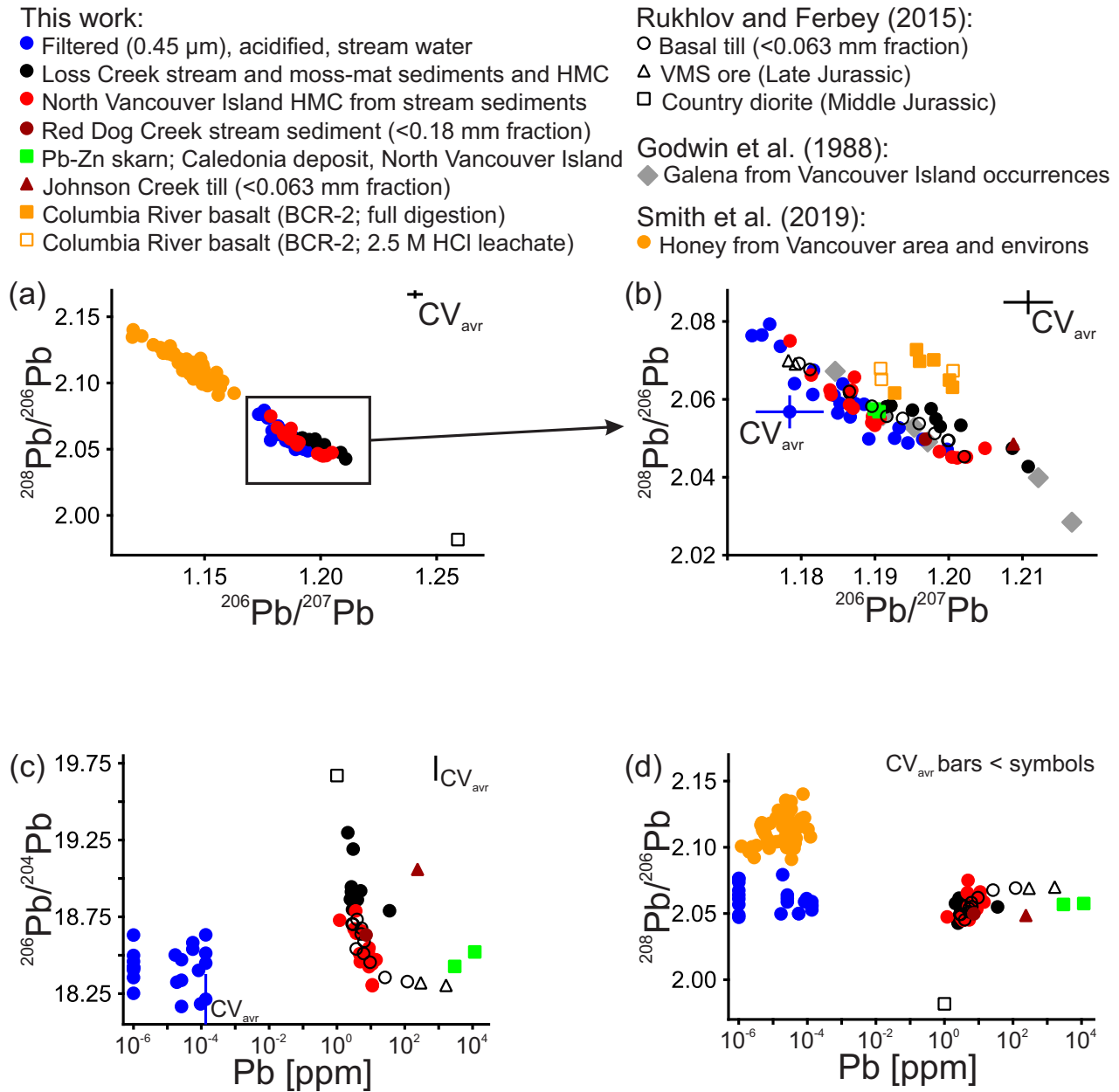


**Fig. 22.** **a)** and inset **b)**  $^{206}\text{Pb}/^{207}\text{Pb}$  vs.  $^{208}\text{Pb}/^{206}\text{Pb}$  plots for stream waters and 2.5N HCl leachates of stream sediment, moss-mat sediment, heavy mineral concentrate (HMC), rock, and reference samples analyzed in this study. **c)** Pb [ppm] vs.  $^{206}\text{Pb}/^{204}\text{Pb}$ . **d)** Pb [ppm] vs.  $^{208}\text{Pb}/^{206}\text{Pb}$ . Compiled data from Godwin et al. (1988), Rukhlov and Ferbey (2015), and Smith et al. (2019). Uncertainties in terms of average coefficient of variation ( $\text{CV}_{\text{avr}}$ ) based on at least 6 duplicate pairs (after Abzalov, 2008).

indicator minerals, but also provides additional control of the geochemical data. In the second stage, one near-mouth HMC sample is taken from each tributary of the prospective basin and the adjacent watersheds identified during reconnaissance. The purpose of this stage is to identify the area for the final, detailed study of the ore field, deposit, or ore body. Depending on physiography and geochemical landscape, geochemical methods at this stage may include lithochemical, hydrochemical, atmochemical (e.g., soil and above-ground  $\text{SO}_2$ ,  $\text{CO}_2$ ,  $\text{O}_2$ ,  $\text{CH}_4$ ,  $\text{H}_2\text{S}$ , and Hg vapour surveys), and biochemical surveys of

the secondary and primary dispersion halos, accompanied by geophysical surveys, detailed mapping, and excavation.

#### Acknowledgments

We thank Stephen Cook (Independent Consultant), Wayne Jackaman (Noble Exploration Services Ltd.), and Gene Dodd (Billiken Gold Ltd.) for discussions of drainage sampling procedures and equipment. Wayne Jackaman also helped R.E.L. and A.R. in the field in April. We acknowledge Don Harrison (Senior Inspector of Mines Permitting, British

Columbia Ministry of Energy, Mines and Petroleum Resources) for approving our use of a sluice in the field. Bruce Northcote (British Columbia Geological Survey), John McClintock (Northisle Copper & Gold Inc.), and Western Forest Products Inc. are thanked for discussions about access in the northern Vancouver Island area. Commercial laboratories are thanked for quality and timely analyses. We thank Jeffrey R. Chiarenzelli (St. Lawrence University) and Lawrence B. Aspler (British Columbia Geological Survey) for thorough reviews and constructive comments.

### References cited

- Abzalov, M.Z., 2008. Quality control of assay data: A review of procedures for measuring and monitoring precision and accuracy. *Exploration and Mining Geology*, 17, 1-14.
- Archibald, D.A., and Nixon, G.T., 1995.  $^{40}\text{Ar}/^{39}\text{Ar}$  geochronometry of igneous rocks in the Quatsino-Port McNeill map area, northern Vancouver Island. In: *Geological Fieldwork 1994*, British Columbia Ministry of Energy, Mines, and Petroleum Resources, British Columbia Geological Survey Paper 1995-1, pp. 49-59.
- Arne, D., and Brown, O., 2015. Catchment analysis applied to the interpretation of new stream sediment data, northern Vancouver Island (NTS 102I and 92L). *Geoscience BC Report 2015-04*, 41 p.
- Bell, K., and Franklin, J.M., 1993. Application of lead isotopes to mineral exploration in glaciated terrains. *Geology* 21, 1143-1146.
- Bell, K., and Murton, J.B., 1995. A new indicator of glacial dispersal: lead isotopes. *Quaternary Science Reviews* 14, 275-287.
- Bobrowsky, P.T., 1997. Surficial geology of northern Vancouver Island area (NTS 92L/5, 6, 11, 12). British Columbia Ministry of Employment and Investment, British Columbia Geological Survey Open File 1997-08, scale 1:100,000.
- Bobrowsky, P.T., and Meldrum, D.G., 1994a. Surficial geology of the Port McNeill area (NTS 92L/11). British Columbia Ministry of Energy, Mines and Petroleum Resources, British Columbia Geological Survey Open File 1994-04, scale 1:50,000.
- Bobrowsky, P.T., and Meldrum, D., 1994b. Preliminary drift exploration studies, northern Vancouver Island (92L/6, 92L/11). In: *Geological Fieldwork 1993*, British Columbia Ministry of Energy, Mines and Petroleum Resources, British Columbia Geological Survey Paper 1994-1, pp. 87-99.
- Bobrowsky, P.T., and Sibbick, S.J., 1996. Till geochemistry of northern Vancouver Island area (NTS 92L/5, 6W, 11W, 12). British Columbia Ministry of Energy, Mines and Petroleum Resources, British Columbia Geological Survey Open File 1996-07, 25 p.
- Bobrowsky, P.T., Best, M., Dunn, C.E., Huntley, D.H., Lowe, C., Roberts, M.C., Seemann, D.A., and Sibbick, S.J., 1995. Integrated drift exploration studies on northern Vancouver Island. In: *Geological Fieldwork 1994*, British Columbia Ministry of Energy, Mines and Petroleum Resources, British Columbia Geological Survey Paper 1995-1, pp. 23-33.
- Clague, J.J., Fulton, R.J., and Ryder, J.M., 1982. Surficial geology, Vancouver Island and adjacent mainland, British Columbia, map. Geological Survey of Canada, Open File 837, scale 1:1,000,000.
- Dawson, G.M., 1887a. Geological map of the northern part of Vancouver Island and adjacent coasts, British Columbia. Geological Survey of Canada, Multicoloured Geological Map 247, scale 1:506,880.
- Dawson, G.M., 1887b. Report on a geological examination of the northern part of Vancouver Island and adjacent coasts. Geological Survey of Canada, Annual Report 1886, Part B, 129 p.
- DeBari, S.M., Anderson, R.G., and Mortensen, J.K., 1999. Correlation amongst lower to upper crustal components in an island arc: the Jurassic Bonanza arc, Vancouver Island, Canada. *Canadian Journal of Earth Sciences*, 36, 1371-1413.
- Emmons, W.H., 1924. Primary downward changes in ore deposits. *Transactions of the American Institute of Mining Engineers* LXX, 964-997.
- Gabrielse, H., Monger, J.W.H., Wheeler, J.O., and Yorath, C.J., 1991. Morphogeological belts, tectonic assemblages, and terranes. In: Gabrielse, H. and Yorath, C.J., (Eds.), *Geology of the Cordilleran Orogen in Canada*, Geological Survey of Canada, *Geology of Canada*, vol. 4, pp. 15-59 (also *Geological Society of America, The Geology of North America*, v. G-2).
- Godwin, C.I., Gabites, J.E., and Andrew, A., 1988. Lead table: a galena lead isotope database for the Canadian Cordillera, with a guide to its use by explorationists. British Columbia Ministry of Energy, Mines and Petroleum Resources, British Columbia Geological Survey Paper 1988-4, 187 p.
- Gravel, J.L., and Matysek, P.F., 1989. 1988 regional geochemical survey, northern Vancouver Island and adjacent mainland (092E, 092K, 092L, 102I). In: *Geological Fieldwork 1988*, British Columbia Ministry of Energy, Mines and Petroleum Resources, British Columbia Geological Survey Paper 1989-1, pp. 585-591.
- Grigoryan, S.V., Solovov, A.P., and Kuvin, M.F., 1983. Инструкция по геохимическим методам поисков рудных месторождений. М-во геологии СССР. - М.: Недра [Manual on Geochemical Methods of Exploration for Ore Deposits. USSR Ministry of Geology. Nedra, Moscow], 191 p.
- Gulson, B.L., 1986. Lead Isotopes in Mineral Exploration. *Developments in Economic Geology* 23, Elsevier, Amsterdam, 245 p.
- Gunter, M.E., Johnson, N.E., Knowles, C.R., and Solie, D.N., 1993. Optical, x-ray, and chemical analyses of four eudialytes from Alaska. *Mineralogical Magazine* 57, 743-744.
- Hammack, J.L., Nixon, G.T., Koyanagi, V.M., Payie, G.J., Panteleyev, A., Massey, N.W.D., Hamilton, J.V., and Haggart, J.W., 1994. Preliminary geology of the Quatsino - Port McNeill area, northern Vancouver Island (NTS 92L/12, 11W). British Columbia Ministry of Energy, Mines and Petroleum Resources, British Columbia Geological Survey Open File 1994-26, scale 1:50,000.
- Hammack, J.L., Nixon, G.T., Payie, G.J., Snyder, L.D., Haggart, J.W., Massey, N.W.D., and Barron, D., 1995. Preliminary geology of the Quatsino - Cape Scott area, northern Vancouver Island (NTS 92L/12W; 102I/8, 9). British Columbia Ministry of Energy, Mines and Petroleum Resources, British Columbia Geological Survey Open File 1995-09, scale 1:50,000.
- Hawkes, H.E., 1976. The downstream dilution of stream sediment anomalies. *Journal of Geochemical Exploration* 6, 345-358.
- Holland, S.S., 1976. Landforms of British Columbia. British Columbia Ministry of Energy, Mines and Petroleum Resources, British Columbia Geological Survey Bulletin 48, 138 p.
- Hussein, A.A., Lochner, C., and Bell, K., 2003. Application of Pb isotopes to mineral exploration in the Halfmile Lake area, Bathurst, New Brunswick. In: *Massive Sulfide Deposits of the Bathurst Mining Camp, New Brunswick, and Northern Maine*, W.D. Goodfellow, S.R. McCutcheon and J.M. Peter (Eds.), *Economic Geology Monographs* 11, pp. 679-688.
- Jackaman, W., 2011. Regional stream sediment and water geochemical data, Vancouver Island, British Columbia (NTS 92B, C, E, F, G, K, L & 102I). *Geoscience BC Report 2011-04*, 5 p.
- Jackaman, W., 2013a. Regional stream sediment and water geochemical data, northern Vancouver Island, British Columbia. *Geoscience BC Report 2013-11*, 7 p.
- Jackaman, W., 2013b. Northern Vancouver Island till sample reanalysis (ICP-MS). *Geoscience BC Report 2013-12*, 8 p.
- Jackaman, W., 2014. Regional stream sediment geochemical data, sample reanalysis (INAA), northern Vancouver Island, British Columbia. *Geoscience BC Report 2014-03*, 4 p.
- Jeffrey, W.G., 1962. Preliminary geological map, Alice Lake-Benson Lake. British Columbia Department of Mines and Petroleum

- Resources, British Columbia Geological Survey Preliminary Map 1962, scale 1:63,360.
- Kaplenkov, G.N., 2003. Шлихогеохимический метод поисков: новые аспекты применения и значение. - Материалы VI Международной конференции «Новые идеи в науках о Земле», 8 апреля 2003 г., под редакцией А.М. Кузнецова. Московский государственный геологоразведочный университет имени Серго Орджоникидзе (МГРИ-МГГРУ), Москва [Heavy mineral concentrate geochemical exploration method: new application aspects and significance. In: New Ideas in the Earth Sciences, Kuznetsov, A.M., (Ed.), Proceedings of the VI International Conference, April 8, 2003, Moscow State Geological Exploration University (MGRI-MGGRU), Moscow], p. 48.
- Kaplenkov, G.N., 2006. Проспекторская геология. - Государственное Управление Ресурсами, Министерство природных ресурсов Российской Федерации, № 5, Москва [Prospecting geology. In: State Resource Management, Ministry of Natural Resources of Russian Federation, 5, Moscow], pp. 38-48.
- Kaplenkov, G.N., 2008. Опытные геолого-проспекторские поиски. - Тезисы научно-практической конференции «Прогноз, поиски, оценка рудных и нерудных месторождений-достижения и перспективы», 20-21 мая 2008 г. Федеральное агентство по недропользованию (Роснедра), Российское геологическое общество (Росгео), Российская Академия естественных наук (РАЕН), Международная Академия минеральных ресурсов, Центральный научно-исследовательский геологоразведочный институт цветных и благородных металлов (ЦНИГРИ), Москва. [Orientation geological prospecting. In: Forecast, Exploration, and Evaluation of Ore and Non-Metallic Deposits - Achievements and Prospects, Abstracts of the Applied Science Conference, May 20-21, 2008, Federal Agency for Subsoil Management, the Russian Geological Society, the Russian Academy of Natural Sciences, the International Academy of Mineral Resources, and Central Research Institute of Geological Prospecting for Base and Precious Metals, Moscow], p. 114.
- Kerr, D.E., 1992. Surficial geology of the Quatsino area, NTS 092L/12. British Columbia Ministry of Energy, Mines and Petroleum Resources, British Columbia Geological Survey Open File 1992-06, scale 1: 50,000.
- Kerr, D.E., Sibbick, S.J., and Jackaman, W., 1992. Till geochemistry of the Quatsino map area (NTS 92L/12). British Columbia Ministry of Energy, Mines and Petroleum Resources, British Columbia Geological Survey Open File 1992-21, 14 p.
- Koyanagi, V.M., and Panteleyev, A., 1993. Natural acid-drainage in the Mount McIntosh - Pernbenon Hills area, northern Vancouver Island (92L/12). In: Geological Fieldwork 1992, British Columbia Ministry of Energy, Mines and Petroleum Resources, British Columbia Geological Survey Paper 1993-1, pp. 445-450.
- Koyanagi, V.M., and Panteleyev, A., 1994. Natural acid rock-drainage in the Red Dog - Hushamu - Pemberton Hills area, northern Vancouver Island. In: Geological Fieldwork 1993, British Columbia Ministry of Energy, Mines and Petroleum Resources, British Columbia Geological Survey Paper 1994-1, pp. 119-125.
- Kukanov, A.B., Kaplenkov, G.N., et al., 1980. Отчет о региональной групповой геологической съемке масштаба 1:50000 в верховьях р.Тнеквеема, листы Q-60-57-АБ и ВГ, Q-60-58-АБ и Q-60-69-АБ и ВГ, Тэркэнейвеемский отряд, 1976-1980 гг., Восточно-Чукотская геологоразведочная экспедиция, № 2628, Эгвекинот [Report on regional geological mapping in the Tnekveem River headwaters, map sheets Q-60-57-AB and VG, Q-60-58-AB, and Q-60-69-AB and VG, Terkeneyveem party, 1976-1980. East Chukotka Exploration Expedition, No. 2628, Egvekinot], scale 1:50,000.
- Lett, R.E., 2008. A multi-media analysis of stream geochemistry on Vancouver Island, British Columbia: Implications for mineral exploration. British Columbia Ministry of Energy and Mines, British Columbia Geological Survey, GeoFile 2008-08, 92 p.
- Lett, R., and Rukhlov, A.S., 2017. A review of analytical methods for regional geochemical survey (RGS) programs in the Canadian Cordillera. In: Ferbey, T., Plouffe, A., and Hickin, A.S., (Eds.), Indicator Minerals in Till and Stream Sediments of the Canadian Cordillera. Geological Association of Canada Special Paper Volume 50, and Mineralogical Association of Canada Topics in Mineral Sciences Volume 47, pp. 53-108.
- Lewis, T.J., Lowe, C., and Hamilton, T.S., 1997. Continental signature of a ridge-trench-triple junction: northern Vancouver Island. Journal of Geophysical Research 102, 7767-7781.
- Massey, N.W.D., and Melville, D.M., 1991. Quatsino sound project. In: Geological Fieldwork, British Columbia Ministry of Energy, Mines and Petroleum Resources, British Columbia Geological Survey Paper 1991-1, pp. 85-88.
- Matveev, A.A., 2003. Геохимические поиски месторождений полезных ископаемых (краткий курс лекций). - М.: Изд-во Московского университета [Geochemical Exploration of Ore Deposits, Lecture Course Notes. Moscow State University Press, Moscow], 110 p.
- Matysek, P.F., and Day, S.J., 1988. Geochemical orientation surveys: northern Vancouver Island fieldwork and preliminary results. In: Geological Fieldwork 1987, British Columbia Ministry of Energy, Mines and Petroleum Resources, British Columbia Geological Survey Paper 1988-1, pp. 493-502.
- Matysek, P.F., Gravel, J.L., and Jackaman, W., 1989. British Columbia regional geochemical survey, Alert Bay and Cape Scott (NTS 92L and 102I). Geological Survey of Canada, Open File 2040, and British Columbia Ministry of Energy, Mines and Petroleum Resources, British Columbia Geological Survey, Regional Geochemical Survey (RGS) 23, 154 p.
- Meldrum, D.G., and Bobrowsky, P.T., 1994. Drift exploration potential of the Port McNeill area (NTS 92L/11). British Columbia Ministry of Energy, Mines and Petroleum Resources, British Columbia Geological Survey Open File 1994-11, scale 1:50,000.
- Monger, J.W.H., 2014. Seeking the suture: The Coast-Cascade conundrum: Geoscience Canada, 41, 379-398.
- Monger, J.W.H., and Hutchison, W.W., 1971. Metamorphic map of the Canadian cordillera. Geological Survey of Canada, Paper 70-33, 71 p.
- Muller, J.E., 1977. Geology of Vancouver Island. Geological Association of Canada, Mineralogical Association of Canada, Joint Annual Meeting 1977, Field Trip 7, April 21-24, Guidebook, 54 p.
- Muller, J.E., 1980. Geology-Victoria map area, Vancouver Island and Gulf islands, British Columbia. Geological Survey of Canada, Open File 701, scale 1:100,000.
- Muller, J.E., 1982. Geology of Nitinat Lake map area. Geological Survey of Canada, Open File 821, scale 1:125,000.
- Muller, J.E., and Roddick, J.A., 1983. Geology, Alert Bay-Cape Scott, British Columbia. Geological Survey of Canada, Map 1552A, scale 1:250,000.
- Muller, J.E., Northcote, K.E., and Carlisle, D., 1974. Geology and mineral deposits of Alert - Cape Scott map-area (92L-102I), Vancouver Island, British Columbia. Geological Survey of Canada, Paper 74-8, includes Map 4-1974, scale 1:250,000.
- Nelson, J.L., Colpron, M., and Israel, S., 2013. The Cordillera of British Columbia, Yukon and Alaska: tectonics and metallogeny. In: Colpron, M., Bissig, T., Rusk, B.G., and Thompson, F.H., (Eds.), Tectonics, Metallogeny, and Discovery: The North American Cordillera and Similar Accretionary Settings. Society of Economic Geologists, Inc. Special Publication 17, pp. 53-109.
- Nixon, G.T., and Orr, A.J., 2007. Recent revisions to the Early Mesozoic stratigraphy of northern Vancouver Island and metallogenic implications. British Columbia Ministry of Energy, Mines and Petroleum Resources, British Columbia Geological Survey Paper 2007-1, pp. 163-178.
- Nixon, G.T., Hammack, J.L., Koyanagi, V.M., Payie, G.J.,

- Panteleyev, A., Massey, N.W.D., Hamilton, J.V., and Haggart, J.W., 1994. Preliminary geology of the Quatsino-Port McNeill map areas, northern Vancouver Island. In: Geological Fieldwork 1993, British Columbia Ministry of Energy, Mines, and Petroleum Resources, British Columbia Geological Survey Paper 1994-1, pp. 63-85.
- Nixon, G.T., Hammack, J.L., Koyanagi, V.M., Payie, G.J., Haggart, J.W., Orchard, M.J., Tozer, T., Archibald, D.A., Friedman, R.M., Palfy, J., and Cordey, F., 2000. Geology of the Quatsino-Port MacNeill area, northern Vancouver Island (draft). British Columbia Ministry of Energy, Mines, and Petroleum Resources, British Columbia Geological Survey Geoscience Map 2000-6, scale 1:50,000.
- Nixon, G.T., Hammack, J.L., Payie, G.J., Snyder, L.D., Archibald, D.A., and Barron, D.J., 1995. Quatsino-San Josef map area, northern Vancouver Island: Geological overview. In: Geological Fieldwork 1994, British Columbia Ministry of Energy, Mines, and Petroleum Resources, British Columbia Geological Survey Paper 1995-1, pp. 9-21.
- Nixon, G.T., Hammack, J.L., Payie, G.J., Snyder, L.D., Koyanagi, V.M., Hamilton, J.V., Panteleyev, A., Massey, N.W.D., Haggart, J.W., and Archibald, D.A., 1997. Geology of northern Vancouver Island: preliminary compilation (NTS 92L/5, 6, 11, 12; 102I/8, 9). British Columbia Ministry of Energy, Mines and Petroleum Resources, British Columbia Geological Survey Open File 1997-13, scale 1:100,000.
- Nixon, G.T., Hammack, J.L., Koyanagi, V.M., Payie, G.J., Haggart, J.W., Orchard, M.J., Tozer, T., Archibald, D.A., Friedman, R.M., Palfy, J., and Cordey, F., 2006a. Geology of the Quatsino - Port McNeill area, northern Vancouver Island (NTS 92L/11, 12E). British Columbia Ministry of Energy, Mines and Petroleum Resources, British Columbia Geological Survey Geoscience Map 2006-02, scale 1:50,000.
- Nixon, G.T., Hammack, J.L., Koyanagi, V.M., Payie, G.J., Snyder, L.D., Panteleyev, A., Massey, N.W.D., Archibald, D.A., Haggart, J.W., Orchard, M.J., Friedman, R.M., Tozer, T., Tipper, H.W., Poulton, T.P., Palfy, J., Cordey, F., and Barron, D.J., 2006b. Geology of the Holberg - Winter Harbour Area, Northern Vancouver Island (NTS 92L/12W, 102I/8, 9). British Columbia Ministry of Energy, Mines and Petroleum Resources, British Columbia Geological Survey Geoscience Map 2006-03, scale 1:50,000.
- Nixon, G.T., Larocque, J., Pals, A., Styan, J., Greene, A.R., and Scoates, J.S., 2008. High-Mg lavas in the Karmutsen flood basalts, northern Vancouver Island (NTS 092L): stratigraphic setting and metallogenic significance. British Columbia Ministry of Energy, Mines and Petroleum Resources, British Columbia Geological Survey Paper 2008-1, pp. 175-190.
- Nixon, G.T., Hammack, J.L., Koyanagi, V.M., Payie, G.J., Orr, A.J., Haggart, J.W., Orchard, M.J., Tozer, E.T., Friedman, R.M., Archibald, D.A., Palfy, J., and Cordey, F., 2011a. Geology, geochronology, litho-geochemistry and metamorphism of the Quatsino-Port McNeill area, northern Vancouver Island (NTS 92L/11, and parts of 92L/05, 12 and 13). British Columbia Ministry of Energy and Mines, British Columbia Geological Survey Geoscience Map 2011-02, scale 1:50,000.
- Nixon, G.T., Hammack, J.L., Koyanagi, V.M., Snyder, L.D., Payie, G.J., Panteleyev, A., Massey, N.W.D., Hamilton, J.V., Orr, A.J., Friedman, R.M., Archibald, D.A., Haggart, J.W., Orchard, M.J., Tozer, E.T., Tipper, H.W., Poulton, T.P., Palfy, J., and Cordey, F., 2011b. Geology, geochronology, litho-geochemistry and metamorphism of the Holberg-Winter harbour area, northern Vancouver Island (parts of NTS 92L/05, 12, 13; 102I/08, 09 and 16). British Columbia Ministry of Energy and Mines, British Columbia Geological Survey Geoscience Map 2011-01, scale 1:50,000.
- Nixon, G.T., Friedman, R.M., and Creaser, R.A., 2020. Late Neogene porphyry Cu-Mo(±Au-Ag) mineralization in British Columbia: the Klaskish Plutonic Suite, northern Vancouver Island. In: Geological Fieldwork 2019, British Columbia Ministry of Energy, Mines and Petroleum Resources, British Columbia Geological Survey Paper 2020-1 (this volume).
- Northcote, K.E., 1969. Geology of the Port Hardy-Coal Harbour area. In: British Columbia Department of Mines Annual Report on Lode Metals, 1968, pp. 84-87.
- Northcote, K.E., 1971. Rupert Inlet-Cape Scott map area. In: Geology, Exploration and Mining in B.C. 1970, British Columbia Ministry of Energy, Mines and Petroleum Resources, pp. 254-258.
- Northcote, K.E., and Muller, J.E., 1972. Volcanism, plutonism, and mineralization: Vancouver Island. Canadian Institute of Mining, Metallurgy and Petroleum, Bulletin 65, 49-57.
- Panteleyev, A., 1992. Copper-gold-silver deposits transitional between subvolcanic porphyry and epithermal environments. In: Geological Fieldwork 1991, British Columbia Ministry of Energy, Mines and Petroleum Resources, British Columbia Geological Survey Paper 1992-1, pp. 231-234.
- Panteleyev, A. and Koyanagi, V.M., 1993. Advanced argillic alteration in Bonanza volcanic rocks, northern Vancouver Island - transitions between porphyry copper and epithermal environments. In: Geological Fieldwork 1992, British Columbia Ministry of Energy, Mines and Petroleum Resources, British Columbia Geological Survey Paper 1993-1, pp. 287-298.
- Panteleyev, A., and Koyanagi, V.M., 1994. Advanced argillic alteration in Bonanza volcanic rocks, northern Vancouver Island - lithologic and permeability controls. In: Geological Fieldwork 1993, British Columbia Ministry of Energy, Mines and Petroleum Resources, British Columbia Geological Survey Paper 1994-1, pp. 101-110.
- Panteleyev, A., Reynolds, P.H., and Koyanagi, V.M., 1995.  $^{40}\text{Ar}/^{39}\text{Ar}$  ages of hydrothermal minerals in acid sulphate-altered Bonanza volcanics, northern Vancouver Island. In: Geological Fieldwork 1994, British Columbia Ministry of Energy, Mines and Petroleum Resources, British Columbia Geological Survey Paper 1996-1, pp. 61-65.
- Panteleyev, A., Bobrowsky, P.T., Nixon, G.T., and Sibbick, S.J., 1996a. Northern Vancouver Island integrated project. In: Geological Fieldwork 1995, British Columbia Ministry of Energy, Mines and Petroleum Resources, British Columbia Geological Survey Paper 1996-1, pp. 57-59.
- Panteleyev, A., Sibbick, S.J., and Koyanagi, V.M., 1996b. Natural acid rock-drainage in northern Vancouver Island - its place in geoenvironmental ore deposits models. In: Geological Fieldwork 1995, British Columbia Ministry of Energy, Mines and Petroleum Resources, British Columbia Geological Survey Paper 1996-1, pp. 61-66.
- Perelló, J., Fleming, J.A., O'Kane, K.P., Burt, P.D., Clarke, G.A., Himes, M.D., and Reeves, A.T., 1995. Porphyry copper-gold-molybdenum deposits in the Island Copper cluster, northern Vancouver Island, British Columbia. In: Schroeter, T.G., (Ed.), Porphyry Deposits of the Northwest Cordillera of North America, Canadian Institute of Mining, Metallurgy and Petroleum, Special Volume 46, pp. 214-238.
- Petrenko, E.E., Kozlov, G.P., and Kaplenkov, G.N., 1986. Отчет о региональной групповой геологической съемке масштаба 1:50000 на левобережье среднего течения р. Амгуэмы, листы Q-1-13-Г, Q-1-14-ВГ, Q-1-15-В, Q-1-25-БГ, Q-1-26-АБ и Q-1-27-АБ, Маравамский отряд, 1981-1986 гг., Восточно-Чукотская геологоразведочная экспедиция, № 2827, Эгвекино [Report on regional geological mapping on left bank of the middle course of Amguema River, map sheets Q-1-13-G, Q-1-14-VG, Q-1-15-V, Q-1-25-BG, Q-1-26-AB and Q-1-27-AB, Maravaam party, 1981-1986. East Chukotka Exploration Expedition, No. 2827, Egvekinot], scale 1:50,000.

- Read, P.B., Woodsworth, G.J., Greenwood, H.J., Ghent, E.D., and Evenchick, C.A., 1991. Metamorphic map of the Canadian Cordillera. Geological Survey of Canada, Map 1714A, scale 1:2,000,000.
- Rose, A.W., Hawkes, H.E., and Webb, J.S., 1979. Geochemistry in Mineral Exploration. London Academic Press, London, United Kingdom, 657 p.
- Rukhlov, A.S., and Ferbey, T., 2015. Applications of lead isotopes in till for mineral exploration: a simplified method using ICP-MS. British Columbia Ministry of Energy and Mines, British Columbia Geological Survey, Paper 2015-2, 93 p.
- Rukhlov, A.S., and Gorham, J., 2007. Commerce Resources Corp. 2006 diamond drilling and exploration at the Blue River Property, north of Blue River, British Columbia. British Columbia Ministry of Energy, Mines and Petroleum Resources, British Columbia Geological Survey, Assessment Report 29024, 41 p., 16 appendices.
- Rukhlov, A.S., Mao, M., and Rippon, C., 2018. Rapid identification of sand-size mineral grains using portable XRF: A new method for indicator mineral surveys. In: Geological Fieldwork 2017, British Columbia Ministry of Energy, Mines and Petroleum Resources, British Columbia Geological Survey Paper 2018-1, pp. 167-182.
- Rukhlov, A.S., Fortin, G., Kaplenkov, G.N., Lett, R.E., Lai, V.W.-M., and Weis, D., 2019. Supplementary data for multi-media geochemical and Pb isotopic evaluation of modern drainages on Vancouver Island. British Columbia Ministry of Energy, Mines and Petroleum Resources, British Columbia Geological Survey GeoFile 2019-14, 1 p.
- Safronov, N.I., 1971. Основы геохимических методов поисков рудных месторождений. - Л.: Недра [Fundamentals of Geochemical Methods of Exploration for Ore Deposits, Nedra, Leningrad], 216 p.
- Sibbick, S.J., 1994. Preliminary report on the application of catchment basin analysis to regional geochemical survey data, northern Vancouver Island (NTS 92L/03,04,05 and 06). In: Geological Fieldwork 1993, British Columbia Ministry of Energy, Mines and Petroleum Resources, British Columbia Geological Survey Paper 1994-1, pp. 111-117.
- Sibbick, S.J., and Laurus, K.A., 1995a. Investigation of a natural acid rock drainage and an anomalous mercury-bearing stream, northern Vancouver Island. In: Geological Fieldwork 1994, British Columbia Ministry of Energy, Mines and Petroleum Resources, British Columbia Geological Survey Paper 1995-1, pp. 67-70.
- Sibbick, S.J., and Laurus, K.A., 1995b. Integrated geological and geochemical map for the prediction of intrusion-related mineralization, northern Vancouver Island. British Columbia Ministry of Energy, Mines and Petroleum Resources, British Columbia Geological Survey Open File 1995-12, scale 1:250,000.
- Simonetti, A., Bell, K., and Hall, G.E.M., 1996. Pb isotopic ratios and elemental abundances for selective leachates from near-surface till: implications for mineral exploration. Applied Geochemistry 11, 721-734.
- Smith, K.E., Weis, D., Amini, M., Shiel, A.E., Lai, V.W.-M., and Gordon, K., 2019. Honey as a biomonitor for a changing world. Nature Sustainability 2, 223-232.
- Solovov, A.P., 1985. Геохимические методы поисков месторождений полезных ископаемых: Учебник для вузов. - М.: Недра [Methods of Geochemical Exploration for Ore Deposits: Textbook. Nedra, Moscow], 294 p.
- Solovov, A.P., Arhipov, A.Ya., Bugrov, V.A., Vorobiev, D.M., Gershman, D.M., Grigoryan, C.V., Kvyatkovsky, E.M., Matveev, A.A., Milyaev, C.A., Nikolaev, V.A., Perelman, A.I., Shvarov, Yu.V., Yufa, B.A., and Yaroshevsky, A.A., 1990. Справочник по геохимическим поискам полезных ископаемых. - М.: Недра [Handbook on Geochemical Exploration of Ore Deposits. Nedra, Moscow], 335 p.
- Tahija, L., Roth, D., Game, B., Shouldice, T., Burt, P., Nilsson, J., and Wickland, B., 2017. North Island copper and gold project, preliminary economic assessment, NI 43-101 Technical Report, 174 p.
- Thompson, T.B., 1997. Uranium, thorium, and rare metal deposits of Alaska. In: Mineral Deposits of Alaska, Goldfarb, R.J. and Miller, L.D., (Eds.), Economic Geology Monograph 9, pp. 466-482.
- Warner, J.D., 1989. Columbium-, rare-earth element-, and thorium-bearing veins near Salmon Bay, southeastern Alaska. United States Bureau of Mines, Open File Report 6-89, 25 p.
- Weis, D., Kieffer, B., Maerschalk, C., Barling, J., De Jong, J., Williams, G., Hanano, D., Pretorius, W., Mattielli, N., Scoates, J.S., Goolaerts, A., Friedman, R., and Mahoney, J.B., 2006. High-precision isotopic characterization of USGS reference materials by TIMS and MC-ICP-MS. Geochemistry, Geophysics, Geosystems 7 (8), Q08006, doi:10.1029/2006GC001283.